Geoscience Frontiers 5 (2014) 303–350

Contents lists available at ScienceDirect

China University of Geosciences (Beijing)

Geoscience Frontiers

journal homepage: www.elsevier.com/locate/gsf

Focus paper

# Plate tectonics in the late Paleozoic

Mathew Domeier [a,*], Trond H. Torsvik [a,b,c]

[a] Center for Earth Evolution and Dynamics (CEED), University of Oslo, NO-0316 Oslo, Norway
[b] Geodynamics, NGU, N-7491 Trondheim, Norway
[c] School of Geosciences, University of Witwatersrand, Wits 2050, South Africa

ARTICLE INFO

*Article history:*
Received 21 November 2013
Received in revised form
13 January 2014
Accepted 15 January 2014
Available online 28 January 2014

*Keywords:*
Late Paleozoic
Paleogeography
Plate tectonics
Plate kinematics
Paleomagnetism

ABSTRACT

As the chronicle of plate motions through time, paleogeography is fundamental to our understanding of plate tectonics and its role in shaping the geology of the present-day. To properly appreciate the history of tectonics—and its influence on the deep Earth and climate—it is imperative to seek an accurate and global model of paleogeography. However, owing to the incessant loss of oceanic lithosphere through subduction, the paleogeographic reconstruction of 'full-plates' (including oceanic lithosphere) becomes increasingly challenging with age. Prior to 150 Ma ~60% of the lithosphere is missing and reconstructions are developed without explicit regard for oceanic lithosphere or plate tectonic principles; in effect, reflecting the earlier mobilistic paradigm of continental drift. Although these 'continental' reconstructions have been immensely useful, the next-generation of mantle models requires global plate kinematic descriptions with full-plate reconstructions. Moreover, in disregarding (or only loosely applying) plate tectonic rules, continental reconstructions fail to take advantage of a wealth of additional information in the form of practical constraints. Following a series of new developments, both in geodynamic theory and analytical tools, it is now feasible to construct full-plate models that lend themselves to testing by the wider Earth-science community. Such a model is presented here for the late Paleozoic (410–250 Ma) together with a review of the underlying data. Although we expect this model to be particularly useful for numerical mantle modeling, we hope that it will also serve as a general framework for understanding late Paleozoic tectonics, one on which future improvements can be built and further tested.



## 1. Introduction

Since its origin in the nascent mobilistic concept of continental drift, as first put forth by Wegener (1912), paleogeography has come to be fundamental to our understanding and interpretation of geology and geophysics. But though Wegener had presented a late Paleozoic reconstruction (relative to Europe and Africa) a century ago, it wasn't until the plate tectonic revolution of the 1960s that the wider Earth-science community came to appreciate and adopt a mobilistic paradigm—and with it, the obvious significance of paleogeography. Ironically, since the development and acceptance of plate tectonics, work on pre-Cretaceous paleogeography has been almost exclusively conducted under the framework of the now-superseded theory of continental drift. Of course, paleogeographers have not rejected plate tectonics in favor of its archetype, but nonetheless, general considerations of plate boundaries and oceanic lithosphere are largely absent from pre-Cretaceous models. The reason for that is simple: due to the incessant destruction of oceanic lithosphere by subduction, information pertaining to the oceanic component of plates is progressively lost with time. Moving backward, at 150 Ma ~60% of the lithosphere is missing (Torsvik et al., 2010b), thus making a global 'full-plate' reconstruction exceedingly challenging prior to that time.

However, with the advent of powerful new geodynamic concepts (Torsvik et al., 2008b) and analytical tools (www.gplates.org), in addition to ever-growing libraries of paleogeographic data, it is now feasible to make significant progress on that front, which, in

* Corresponding author.
*E-mail address:* mathew.domeier@fys.uio.no (M. Domeier).

Peer-review under responsibility of China University of Geosciences (Beijing)

Production and hosting by Elsevier

1674-9871/$ – see front matter © 2014, China University of Geosciences (Beijing) and Peking University. Production and hosting by Elsevier B.V. All rights reserved.
http://dx.doi.org/10.1016/j.gsf.2014.01.002

effect, 'pushes' plate tectonics backward into early Mesozoic and Paleozoic time. The rationale for such effort is broad: not only will 'full-plate' reconstructions yield myriad testable scenarios, predictions, insights and novel questions, they are also necessary for the execution of next-generation numerical models (Bower et al., 2013; Bull et al., submitted for publication). Moreover, as it is certain that plate tectonics was operating in the early Mesozoic and Paleozoic, it is natural that we should strive to make models that conform to this framework.

Stampfli and Borel (2002) and Stampfli et al. (2013) first attempted to apply plate tectonic principles to the early Mesozoic and Paleozoic, producing a 'full-plate' (hereafter just 'plate') model with a careful accounting of plate kinematics and consideration of geodynamic forces. Unfortunately, the critical underpinning, industry-confidential details of their model are not accessible, and so it is impractical to test or improve. Seton et al. (2012) later paved the way with newly available and freely accessible tools, and released the details of a global plate model that extends back to the earliest Jurassic (200 Ma). Following their lead, we present here a global plate model that spans late Paleozoic time (410–250 Ma). Importantly, our model is constrained both by observational data and by plate tectonic principles, and includes explicitly prescribed plate boundaries and oceanic lithosphere that are rigorously managed throughout the modeled interval. Although we have endeavored to make this model conform to the existing observational record and thus expect that it will be useful as an input, reference and predictive tool, we also hope that it will prove suitably amenable to modification so as to act as an infrastructure for further improvements.

## 2. Methodology

### 2.1. Fundamental data and models

The foundation of our plate model is the continental reconstruction model of Torsvik et al. (submitted for publication), which itself is founded upon a global paleomagnetic dataset (Torsvik et al., 2012), a catalog of LIP and kimberlite distributions (Torsvik et al., 2008b, 2010a) and a wealth of qualitative to semi-quantitative geological and paleontological data. A further discussion of those data and their specific paleogeographic implications for our plate model follows in Section 4.

Paleomagnetism represents our single most valuable paleogeographical tool for times prior to the Cretaceous, but it can only be used to constrain latitude (longitude is indeterminate) and Paleozoic paleomagnetic records are only available from the continents. Furthermore, their quantity and quality are highly variable in both space and time, and thus are our constraints on paleolatitude. Unfortunately, some of the greatest deficiencies in the Phanerozoic dataset are found in our interval of interest. For example, only one paleomagnetic pole is available from Laurussia for 390–340 Ma, Siberia only has one reliable entry for the Devonian and Carboniferous and South China has no Carboniferous data. Where data are absent, interpolation is used to make a naïve estimate according to a smoothly varying spherical spline, but that approach is obviously limited—as always, more data are needed. Enticingly, a plate model loaded with other forms of data may be able to offer novel constraints on paleolatitude; we will revisit this idea in Section 5.2.

Concerning paleolongitude, Torsvik et al. (2008b, 2010a,b) showed that LIP and kimberlite occurrences of the last 320 Myr—when reconstructed to their original positions in a mantle reference frame—coincided with the margins of the large low shear wave velocity provinces (LLSVPs) in the lowermost mantle. Following the assumption that the LLSVPs have remained stable from the earliest Paleozoic, as they demonstrably have since the Mesozoic, we can construct models with provisional paleolongitude, when and where LIPs and kimberlites are found. However, reconstructions of this kind must be prepared in a mantle reference frame and therefore must first be corrected for true polar wander (TPW) (Torsvik et al., submitted for publication). In the late Paleozoic there were six known LIP eruptions and approximately 35 kimberlite emplacements, the latter mostly in Siberia and northern Laurussia.

Although paleontology only acts as a qualitative to semi-quantitative paleogeographical tool, it can prove invaluable in constraining paleolatitude or relative paleolongitude, particularly when other forms of data are ambiguous (i.e. indeterminate hemisphere or multiple LLSVP margins) or lacking. Such fossil data do not feature strongly in our following discussion, but they have played a prominent role in the continental reconstruction model which was our starting framework. Many specific reconstructions within this model are underpinned by observations of paleobiogeographical provinciality and/or temperature-sensitive biota, and much of that data has been reviewed in a series of papers by Cocks and Torsvik (2005, 2007, 2011, 2013) and Torsvik and Cocks (2004, 2009, 2011, 2013).

A variety of geological data were likewise used in the continental reconstruction model, some of which we review below. Our focus here is on those data which communicate information about plate interactions and dynamics, so readers looking, for example, for a treatment on the climate-sensitive facies data should refer to the papers cited above. Broadly, the compiled and presented geologic data include spatio-temporal details of regionally important episodes of magmatism, metamorphism and orogenesis, as well as key stratigraphic and structural relationships. They have been organized spatially, according to qualitatively defined margins, to facilitate the construction of simplified plate boundaries.

### 2.2. Construction of plate model

Using *GPlates* software (www.gplates.org), we have constructed a network of plate boundaries by drawing both from the relative motions described by the continental reconstruction model and from our interpretations of the compiled geological data (Section 3). From the geological data, observations of arc magmatism, HP/UHP metamorphism, ophiolite obduction, etc. can be used to infer the location, duration and polarity of a convergent margin, whereas rift-related sedimentation, volcanism, etc. may herald the development of a divergent one. Likewise, structural studies can communicate the style of a collisional event or the sense of motion along a transform boundary. By employing basic plate tectonic principles, the kinematic data extracted from the continental reconstruction model can be used to infer the character—and occasionally the location—of plate boundaries within the geographic domain of the continents. For example, in a purely divergent system, an Euler pole describing the relative motion between two continents would also describe the spreading between them. By assuming that the axis of the embryonic ridge approximates the trace of a great-circle passing through the Euler pole, and that spreading is symmetrical, the location and orientation of the plate margin can be tracked. It is similarly straightforward to predict the orientation of transform faults, since they follow the trace of a small circle about the Euler pole describing the relative motion of the bounding plates. In a global kinematic model, even geometrical considerations as simple as the conservation of area can provide great insight into the former positions and relationships of plate boundaries.

In practice, construction of the plate boundary network is an iterative process, as boundaries must not only meet the constraints imposed by a given time, but also evolve with kinematic continuity

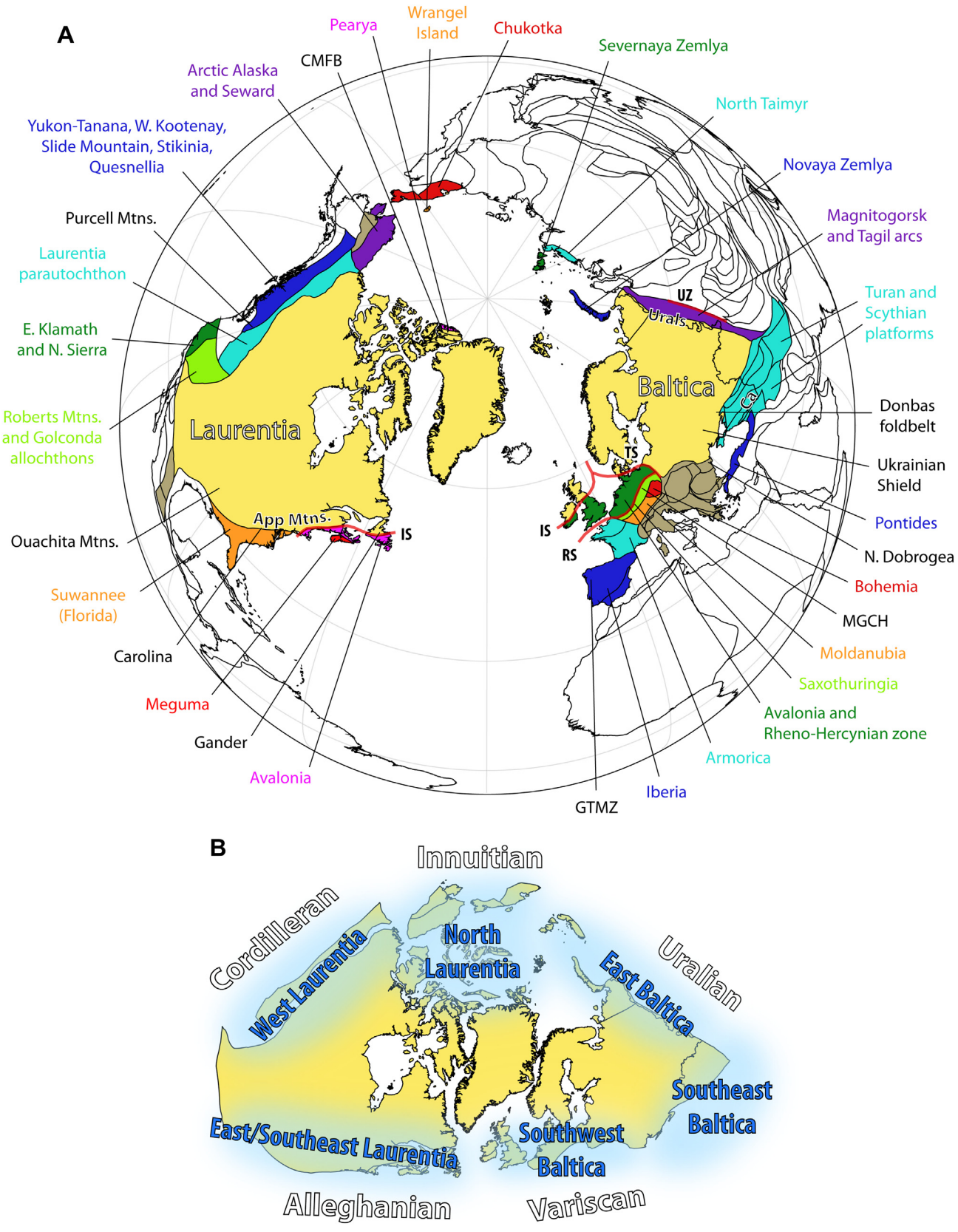


**Figure 1.** (A) Modern map showing the present-day location of the cratons that constituted Laurussia (yellow), the various terranes that were accreted to, rifted from, or remobilized along its margins in late Paleozoic time (various bright colors), and other features discussed in Section 3.1. Brown areas are late Paleozoic terranes not explicitly discussed. *Abbreviations*: App, Appalachian; Ca, Caucasus; CMFB, Clements Markham fold belt; GTMZ, Galicia-Trás-os-Montes zone; IS, Iapetus suture; MGCH, mid-German crystalline high; RS, Rheic suture; TS, Thor suture; UZ, East Uralian/Trans-Uralian zone. (B) Schematic early Devonian reconstruction of Laurussia showing its margins and orogenic systems as we define and discuss them in Section 3.1.

**Table 1**
Summarized interpretations of plate kinematics along continental margins. * denotes collision/orogenic events.

| Margin (sub-domain) | Onset (Ma) | Termination (Ma) | Type | Polarity |
|---|---|---|---|---|
| **Laurussia** | | | | |
| ***East Laurentia (Appalachian margin)*** | | | | |
| (North Appalachians) | 420 | 370? | Convergent | West-dipping |
| (South Appalachians) | 420 | 370? | Passive? | ? |
| | 370? | 320 | Transform | Dextral |
| | *Collision with northwest Gondwana at 320 Ma | | | |
| ***South Laurentia (Ouachita margin)*** | | | | |
| | Cambrian | 320 | Passive | – |
| | *Collision with northwest Gondwana at 320 Ma | | | |
| ***West Laurentia (Cordillera margin)*** | | | | |
| | Neoproterozoic | 390 | Passive | – |
| | 390 | 370 | Convergent | East dipping |
| | 370 | 350 | Divergent | – |
| | 350 | 250 | Passive | – |
| | *Accretion of peri-Laurentian arcs at 250 Ma | | | |
| *Peri-Laurentian arc, east margin (facing Laurentia)* | | | | |
| | 370 | 350 | Divergent | – |
| | 350 | 270 | Passive | – |
| | 270 | 250 | Convergent | West dipping |
| | *Accretion to Laurentia at 250 Ma | | | |
| *Peri-Laurentian arc, west margin (facing Panthalassa)* | | | | |
| | 370 | 270 | Convergent | East dipping |
| | 270 | 250 | Transform? | ? |
| ***North Laurentia (Innuitian)*** | | | | |
| | 420 | 400 | Transform | Sinistral |
| | *Accretion of Pearya and Arctic Alaska-Chukotka at 420–400 Ma | | | |
| | *Ellesmerian orogeny at 370–360 Ma | | | |
| *Arctic Alaska-Chukotka terrane, south margin (facing Panthalassa)* | | | | |
| | 420 | 400 | ? | ? |
| | 390 | 370 | Convergent | North dipping |
| | 370 | 350 | Divergent | – |
| | 350 | Jurassic | Passive | – |
| ***East Baltica (Uralian)*** | | | | |
| | Early Paleozoic | 380 | Passive | – |
| | *Accretion of Magnitogorsk arc at 380 Ma | | | |
| | 380 | 345? | Passive | – |
| | *Accretion of Tagil arc at 345(?) Ma | | | |
| | 345 | 310 | Passive | – |
| | *Collision with Kazakhstania at 310 Ma | | | |
| *Magnitogorsk arc, west side (facing Baltica)* | | | | |
| | 415 | 380 | Convergent | East dipping |
| | *Accretion to Baltica at 380 Ma | | | |
| *Tagil arc, west side (facing Baltica)* | | | | |
| | Ordovician | 345? | Convergent | East dipping |
| | *Accretion to Baltica at 345(?) Ma | | | |
| ***Southeast Baltica (Scythian and Turan Platforms)*** | | | | |
| | Mid-Paleozoic? | Triassic | Convergent? | North dipping? |
| ***Southwest Baltica*** | | | | |
| (Southern British Isles) | Silurian | 390? | Convergent? | North dipping? |
| (Rheno-Hercynian zone) | 420? | 390? | Divergent? | – |
| | *Accretion of Variscan terranes at 370–340 Ma | | | |
| | 370 | 320 | Transform | Dextral |
| *Variscan terrane assemblage, north side (facing Baltica)* | | | | |
| (North margin, intraoceanic) | Silurian | 340? | Convergent | South dipping? |
| (North margin, internal) | 370 | 350 | Convergent | South dipping |
| | *Accretion to Baltica at 370–340 Ma | | | |
| **Gondwana** | | | | |
| ***Northwest Gondwana (west of Taurides)*** | | | | |
| *Variscan terrane assemblage, south side (facing Paleotethys)* | | | | |
| | 420? | 410? | Divergent | – |
| | 410? | 370 | Passive | – |
| | 370 | 320? | Convergent | North dipping |
| *North Gondwana margin (facing Paleotethys)* | | | | |
| | 420? | 410? | Divergent | – |
| | 410? | 370 | Passive | – |
| | 370 | 320 | Transform to convergent | Dextral, east dipping |
| | *Collision with southern Laurussia at 320 Ma | | | |
| *Mixtexca-Oaxacan terrane, west margin* | | | | |
| | 320 | 270 | Convergent | East dipping |
| ***Northeast Gondwana (Taurides and east)*** | | | | |
| *Cimmerian terrane, north margin (facing Paleotethys)* | | | | |
| | 420? | 410? | Divergent | – |
| | 410? | Triassic | Passive | – |

**Table 1** (*continued*)

| Margin (sub-domain) | Onset (Ma) | Termination (Ma) | Type | Polarity |
|---|---|---|---|---|
| *Cimmerian terrane, south margin (facing Neotethys)* | | | | |
| | 295 | 275 | Divergent | – |
| | 275 | Mesozoic | Passive | – |
| *North Gondwana margin (facing Neotethys)* | | | | |
| | 295 | 275 | Divergent | – |
| | 275 | Mesozoic | Passive | – |
| ***Southeast Gondwana*** | | | | |
| | 390? | 380? | Convergent? | West dipping? |
| | *Accretion of Gamilaroi-Calliope arc at 380 Ma | | | |
| | 380 | 300 | Convergent | West dipping |
| | 300 | 270 | Passive to transform | Dextral? |
| | 270 | 250 | Convergent | West dipping |
| | *Accretion of Gympie-Brook Street terrane at 250 Ma | | | |
| *Gamilaroi-Calliope arc, east side (facing Panthalassa)* | | | | |
| | Silurian | 380 | Convergent | West dipping |
| | *Accretion to southeast Gondwana at 380 Ma | | | |
| *Gympie-Brook Street terrane, east side (facing Panthalassa)* | | | | |
| | 300 | 250 | Convergent | West dipping |
| | *Accretion to southeast Gondwana at 250 Ma | | | |
| ***South Gondwana*** | | | | |
| | 420? | 300? | Convergent | North dipping |
| | 300? | 270? | Passive to transform? | Dextral? |
| | 270 | 250 | Convergent | North dipping |
| | *Accretion of Gympie-Brook Street terrane at 250 Ma | | | |
| ***West Gondwana*** | | | | |
| | 420 | 390 | Convergent | East dipping? |
| | *Accretion of Chilenia at 390 Ma | | | |
| | 390 | 340 | Passive | – |
| | 340 | Mesozoic | Convergent | East dipping |
| *North Patagonia, south margin (facing South Patagonia)* | | | | |
| | 420? | 390? | Convergent | Northeast dipping |
| | 390 | 340 | Passive | – |
| | 340 | 310 | Convergent | Northeast dipping |
| | *Accretion of South Patagonia at 310 Ma | | | |
| *South Patagonia, north margin (facing North Patagonia)* | | | | |
| | 420 | 310 | Passive | – |
| | *Collision with North Patagonia at 310 Ma | | | |
| *South Patagonia, southwest margin (facing Panthalassa)* | | | | |
| | 420? | 390? | ? | ? |
| | 390 | Mesozoic | Convergent | Northeast dipping |
| **Siberia and Amuria** | | | | |
| ***East Siberia (proto-Verkhoyansk margin)*** | | | | |
| | Cambrian | 385 | Passive | – |
| | 380 | 360 | Divergent? | – |
| | 360 | Mesozoic | Passive | – |
| ***Northwest Siberia (Uralian margin and West Siberian Basin)*** | | | | |
| | Cambrian | 320 | Passive | – |
| | *Accretion of northern Taimyr at 320 Ma | | | |
| ***Southwest Siberia*** | | | | |
| | 420 | 340 | Convergent | East dipping |
| | 340 | 270? | Transform | ? |
| | *Oblique collision with Kazakhstan at 360–310(?) Ma | | | |
| ***Southeast Siberia and Amuria*** | | | | |
| *Siberia and Mongolian terranes north of Mongol Okhostsk suture* | | | | |
| | Silurian | 360 | Passive | – |
| | 360 | Triassic | Convergent | North dipping |
| *Amuria, north margin (facing the Mongol Okhostsk Ocean)* | | | | |
| | Silurian | 330 | Passive | – |
| | 330 | Triassic | Convergent | South dipping |
| *Amuria, south margin (facing Panthalassa/Paleoasian Ocean)* | | | | |
| | Early Paleozoic | 250? | Convergent | North dipping |
| | *Collision with North China at 250(?) Ma | | | |
| **Kazakhstania** | | | | |
| ***Internal' Kazakhstania*** | | | | |
| | 420 | 310 | Convergent | West dipping |
| | *Oroclinal bending at 380(?)–310 Ma | | | |
| ***External' Kazakhstania*** | | | | |
| (Zharma-Saur) | 380 | 320 | Convergent | South dipping |
| | *Oblique collision with Siberia at 360–310(?) Ma | | | |
| (Uralian) | 420 | 380 | Convergent | East dipping |
| | 380 | 360? | Passive? | – |
| | 360? | 310 | Convergent | East dipping |

(*continued on next page*)

**Table 1** (*continued*)

| Margin (sub-domain) | Onset (Ma) | Termination (Ma) | Type | Polarity |
|---|---|---|---|---|
| | *Collision with Baltica at 310 Ma | | | |
| (Krygyzstan Tian Shan) | 420 | 380 | Convergent | North dipping |
| | 380 | 320? | Passive? | – |
| | 320? | 310 | Convergent | North dipping |
| | *Collision with Tarim at 310 Ma | | | |
| (Chinese Tian Shan) | 310 | 250 | Transform | ? |
| | 420 | 310 | Convergent | North dipping |
| | *Collision with Tarim at 310 Ma | | | |
| | 310 | 250 | Transform | ? |
| **North China and Tarim** | | | | |
| ***Northern North China*** | | | | |
| | 420 | 400 | ? | ? |
| | 400 | 360? | Convergent | South dipping |
| | 360? | 330 | Passive? | – |
| | 330 | 250 | Convergent | South dipping |
| | *Collision with Amuria at 250 Ma | | | |
| ***Beishan*** | | | | |
| | 420 | 250 | Convergent | South dipping |
| | *Collision with Amuria at 250 Ma | | | |
| ***Northern Tarim*** | | | | |
| | Neoproterozoic | 310 | Passive | – |
| | *Collision with Kazakhstania at 310 Ma | | | |
| ***Southern Tarim and Qaidam*** | | | | |
| | 420? | Mesozoic | Convergent | North dipping |
| ***Southern North China*** | | | | |
| | 420 | 330 | Convergent | North dipping |
| | *Accretion of South Qinling at 330–320(?) Ma | | | |
| (Southern South Qinling) | 320 | Triassic | Convergent | North dipping |
| **South China and Japan** | | | | |
| ***Northwestern South China*** | | | | |
| | 420? | Triassic | Passive | – |
| ***Southeastern South China*** | | | | |
| | 420 | 410 | Divergent | – |
| | 410 | 250 | Passive | – |
| ***Southwestern South China*** | | | | |
| | 410 | 390 | Divergent | – |
| | 390 | 250 | Passive | – |
| ***Proto-Japan*** | | | | |
| | Early Paleozoic | Mesozoic | Convergent | West dipping |
| **Annamia** | | | | |
| ***Northeastern Annamia*** | | | | |
| | 410 | 390 | Divergent | – |
| | 380 | 280 | Passive | – |
| | 280 | Triassic | Convergent | Southwest dipping |
| ***West Annamia*** | | | | |
| (Sukhothai) | 390 | 380 | Divergent | – |
| | 380 | 300 | Passive | – |
| | 300 | Triassic | Convergent | East dipping |

to fit the observations of other times. When solutions are not unique we have adopted the simplest one which satisfies the existing constraints. Thus, equipped with the continental reconstruction model and a network of inferred plate boundaries, we have built plates with continuously closing polygons (Gurnis et al., 2012), from which emerges a plate model with global coverage that is continuous in both space and time (Appendix 1). Although the boundaries were implemented at an arbitrary time-stepping of 1 Myr, the temporal resolution of the plate model can be scaled according to the needs of the user; the same applies to spatial scaling.

## 3. Geological observations

### 3.1. Laurussia (Laurentia, Baltica and Avalonia)

#### 3.1.1. East/Southeast Laurentia (Alleghanian-Ouachita margin)

The collision between Laurentia and Balonia (Baltica + Avalonia) that resulted in the closure of the Iapetus Ocean, the Caledonide orogeny and the formation of Laurussia (Fig. 1) began in the Silurian, but protracted orogenesis along the proto-Appalachian margin continued into the Devonian. Following the locally-defined Silurian Salinic orogeny, the northern proto-Appalachians were affected by polyphase deformation and high-grade metamorphism associated with the late Silurian–early Devonian Acadian orogeny (van Staal et al., 2009). The accretion of Avalonia to Laurentia remains the conventional explanation for that event—and the one we provisionally adopt—but the apparent delay between Caledonide and Acadian orogenesis is surprising and the principal reason for alternative interpretations (e.g. Murphy and Keppie, 2005). The occurrence of 423–416 Ma arc magmatism along the trailing edge of the Gander terrane (inboard of Avalonia; Fig. 1) and 420–416 Ma subduction-related HP-LT metamorphism east of that arc provide evidence of late Silurian–early Devonian convergence between Avalonia and Laurentia, specifically by westward-dipping subduction (beneath Laurentia; Table 1) (van Staal et al., 2009). Another constraint on collision timing and the polarity of subduction is provided by the appearance of latest Silurian (~421 Ma) foredeep basin sediments on the northern margin of Avalonia. A complementary retroarc basin sequence is found in Laurentia, and during the early Devonian that foreland basin migrated westward with the Acadian

deformation front and the locus of regional magmatism (van Staal et al., 2009). Termination of Acadian deformation was diachronous in the northern proto-Appalachians, ending in the early Devonian in Newfoundland but continuing until the middle–late Devonian in Quebec (van Staal et al., 2009). Resumption of magmatism and deformation in the middle–late Devonian to earliest Carboniferous (early Mississippian) is termed the Neo-Acadian orogeny and is typically attributed to the collision of the most-outboard Meguma terrane with the trailing edge of Avalonia (Fig. 1). However, the tectonic narrative of that event is still vague.

Evidence of contemporaneous Acadian orogenesis in the southern proto-Appalachians is absent. Following middle Ordovician to Silurian plutonism and the collision of the Carolina terrane, Devonian plutonism along the margin was diminutive and deformation was restricted to shear zones in the Carolina zone and Blue Ridge province (Murphy and Keppie, 2005). Although a thick clastic wedge developed in the north of the southern proto-Appalachians in the middle Devonian, the sediment was likely sourced from the orogen to the northeast. In the late Devonian–earliest Carboniferous, the eastern Iapetus and peri-Gondwanan terranes of the southern proto-Appalachians were affected by intense ductile deformation and high-grade metamorphism. Like its counterpart to the north, that "Neo-Acadian" orogenic event is poorly understood, although Hibbard et al. (2010) conjectured that it resulted from collision of the Suwannee (Florida) terrane (Fig. 1).

Devonian to Carboniferous closure of the Rheic Ocean culminated in collision between Laurussia and Gondwana, construction of the Alleghanian orogen and the formation of the supercontinent Pangea. The polarity of Rheic Ocean subduction between Laurussia and Gondwana has long been ambiguous, perhaps in part because convergence and collision were oblique and the margins were strongly overprinted by later strike-slip motion. Structural clues from southern Laurentia have been used to argue that Laurentia was the lower plate during its collision with Gondwana (Thomas, 2004; Cook and Vasudevan, 2006; Nance and Linnemann, 2008), but continuity of the Appalachian margin with the active margin of southern Baltica (discussed below) alternatively implies that it was the upper plate prior to collision (Table 1) (Pe-Piper et al., 2010). The Devonian–Carboniferous tectono-magmatic activity in the Meguma terrane might also relate to Rheic subduction beneath Laurentia (van Staal et al., 2009). The Carboniferous of the northern Appalachians was typified by terrestrial to marine clastic sedimentation in narrow, NE-trending, fault-bound basins which developed under a regime of dextral strike-slip motion (Hatcher, 2010; Hibbard et al., 2010). A notable basin inversion occurred in the Canadian Maritimes in the late Mississippian–early Pennsylvanian and was accompanied by a change in sediment provenance to include distal sources from the west (Hibbard et al., 2010). In the southern Appalachians, onset of the Alleghanian orogeny was marked by the onset of shortening and the development of a clastic wedge in the middle Mississippian (~335–330 Ma) (Hibbard et al., 2010). Sedimentation in the northern part of that clastic wedge was interrupted by an episode of uplift and erosion in the early Pennsylvanian (~315 Ma), after which deposition resumed, and locally continued into the earliest Permian. As in the north, Alleghanian deformation in the southern Appalachian hinterland was accompanied by dextral motion on northeast-trending shear zones (Nance and Linnemann, 2008). To the east, in the outboard Iapetus and peri-Gondwanan terranes of Laurentia, granitoid plutonism occurred from the middle Mississippian to the mid-Permian (Hibbard et al., 2010). The tectonic origins of those rocks are debated, but they probably formed by crustal anatexis in response to both orogenic crustal thickening and post-orogenic extension (Mueller et al., in press).

In southern Laurentia, the Ouachita margin appears to have remained a passive platform in the Cambrian to Mississippian (Table 1) (Bradley, 2008). Middle–late Mississippian pyroclastic detritus and tuffs have been interpreted to herald the arrival of Gondwana, and with it, the late Mississippian to Pennsylvanian Ouachita orogeny (Mueller et al., in press). Orogenesis was characterized there by the construction of a thick, northward-encroaching clastic wedge, and by north-verging thrust sheets (Thomas, 2004; Nance and Linnemann, 2008).

#### 3.1.2. West Laurentia (Cordilleran margin)

Following Neoproterozoic rifting, the Cordilleran margin of Laurentia remained passive until the middle–late Devonian, when arc-related magmatism appeared in the eastern Klamath and northern Sierra terranes of the southern Cordillera and in the Yukon-Tanana and western Kootenay terranes of the northern Cordillera (Table 1; Fig. 1) (Bradley, 2008; Colpron and Nelson, 2011). In the south, that nascent arc magmatism was followed by the late Devonian–early Mississippian Antler orogeny, in which oceanic strata (Roberts Mountains allochthon) was thrust onto the lower–middle Paleozoic miogeocline and attendant foreland basin deposits advanced eastward upon the former platform (Dickinson, 2009). In the north, a local middle Devonian episode of shortening affected the Purcell Mountains, but was quickly supplanted by an extensional regime that began in the late Devonian (Colpron and Nelson, 2009). Extension inboard of the Yukon-Tanana terrane was highlighted by late Devonian–early Mississippian bimodal volcanism and the cessation of arc-related magmatism all along the parautochthon at about 354 Ma. In contrast, arc-magmatism intensified within the Yukon-Tanana terrane during the early Mississippian, suggesting that continuing subduction to the west of the Yukon-Tanana terrane may have driven back-arc extension to its east (Table 1) (Colpron and Nelson, 2009). Continued extension gave rise to a marginal basin (the Slide Mountain Ocean), now preserved as Devonian–Permian basinal strata in the Slide Mountain terrane and Golconda allochthon (Fig. 1).

By the middle Permian the subduction polarity appears to have inverted according to the occurrence of blueschists and ecologites (~269–267 Ma) on the eastern margin of the Yukon-Tanana terrane (Colpron and Nelson, 2009; Beranek and Mortensen, 2011). Middle to late Permian calc-alkaline intrusions and inferred forearc conglomerates containing blueschist and eclogite clasts are consistent with subduction along that margin (Beranek and Mortensen, 2011). The inception of west-dipping subduction beneath the peri-Laurentian arc instigated collapse of the Slide Mountain Ocean, culminating in east-vergent thrusting of the back-arc basinal strata (Golconda allochthon) onto the Laurentian platform and accretion of the peri-Laurentian arcs during the late Permian–early Triassic Sonoma orogeny (Table 1) (Dickinson, 2009). Further to the north, closure of the back-arc basin was marked by the correlative Klondike orogeny, which is defined by deformation and greenschist to amphibolite facies metamorphism in the Yukon-Tanana terrane (Beranek and Mortensen, 2011). Early to middle Triassic foreland basin deposits to the east were sealed together with the accreted terranes by a late Triassic overlap assemblage (Colpron and Nelson, 2009; Beranek and Mortensen, 2011).

#### 3.1.3. North Laurentia (Innuitian margin)

The Arctic margin of Laurentia appears to have been passive throughout the lower Paleozoic, finally being interrupted in the mid-Paleozoic by the arrival of exotic terranes with reportedly Baltic affinities (Lane, 2007; Beranek et al., 2010; Miller et al., 2011). In the east, the collision of the Pearya terrane under a

regime of sinistral transpression generated the Clements Markham fold belt and the Boothia Uplift (Fig. 1) (Beranek et al., 2010). The timing of collision is inferred to be late Silurian–early Devonian according to the occurrence of coarse late Silurian clastic rocks in central Ellesmere Island, a late Silurian–early Devonian unconformity in the Clements Markham fold belt and by a ~390 Ma post-tectonic pluton that intrudes the Pearya terrane (Colpron and Nelson, 2009). In the west, the Romanzof orogeny of the Arctic Alaska-Chukotka terrane is similarly thought to mark the timing of terrane docking against the arctic margin of Laurentia (Table 1). There deformation is confined to the east end of the terrane and was characterized by intense folding and E/NE-directed thrusting (Lane, 2007). Stratigraphic observations and cross-cutting late Devonian post-tectonic plutons place the age of deformation in the early Devonian (Lane, 2007). In the middle to late Devonian, magmatic rocks were emplaced in the Brooks Range of Arctic Alaska, the Seward Peninsula, and in Chukotka and Wrangel Island (Fig. 1). Middle Devonian arc-related magmatic rocks in Arctic Alaska (Ambler arc) and the Seward Peninsula seem to indicate the operation of a north-dipping subduction zone beneath the terrane then (Table 1) (Nokleberg et al., 2000; Colpron and Nelson, 2009; Beranek et al., 2010). However, late Devonian bimodal magmatism along that margin has been interpreted to reflect incipient rifting related to the nascent development of the Devonian–Jurassic Angayucham oceanic basin (Moore et al., 1994; Nokleberg et al., 2000; Amato et al., 2009). Indeed, a regional pre-Mississippian unconformity in the Arctic Alaska-Chukotka terrane is overlain by a thick, south-facing passive margin sequence of Mississippian to Jurassic age (Lane, 2007; Amato et al., 2009; Miller et al., 2010). The late Devonian inception and growth of that back-arc basin is similar to that observed along the Cordilleran margin to the south, and their evolution may thus have been in common.

In the late Devonian–early Mississippian, the arctic margin from northern Yukon to northern Greenland was affected by the enigmatic Ellesmerian orogeny, which produced a wide foreland fold belt and blanketed the region in a thick clastic wedge (Beranek et al., 2010). Structural and sedimentological observations indicate that both tectonic and sediment transport was south-directed, implying that orogenesis was caused by a collision to the north (Lane, 2007). Yet, the identity and present location of that northern terrane—often called "Crockerland"—remain unknown. On the basis of detrital zircon signatures in the relict clastic wedge, however, it has been inferred that Crockerland has a Baltic origin in common with the Pearya and Arctic Alaska-Chukotka terranes (Anfinson et al., 2012).

### 3.1.4. East Baltica (Uralian margin)

Late Cambrian to early Ordovician rifting along eastern Baltica established a passive margin that lasted until the Magnitogorsk island arc collided with the South Urals in the middle–late Devonian (Table 1; Fig. 1) (Bradley, 2008). The timing of that accretion is constrained by: an eastward shift in the locus of island arc magmatism in the Givetian, Frasnian UHP metamorphism of Baltica-derived crust and the Frasnian-Famennian deposition of westward-younging foreland basin sediments west of the arc (Brown et al., 2011). Together with the pre-late Devonian passive margin of Baltica, that indicates that subduction of the intervening ocean must have been eastward-directed, beneath the island arc. The oldest rocks of the Magnitogorsk island arc suggest that intraoceanic subduction commenced in the early Devonian, and consumption of the ocean basin continued until the middle–late Devonian collision (Brown et al., 2011).

To the north, in the Middle and North Urals, the late Ordovician to Devonian Tagil island arc is preserved in a structural position similar to the Magnitogorsk arc (i.e. the Magnitogorsk-Tagil Zone) and is also inferred to have formed above an east-dipping subduction zone, but the timing of its collision with Baltica is less well-defined. Broadly, Puchkov (2009a) and Brown et al. (2011) have determined that its accretion was underway in the early Carboniferous (Table 1). Yet further north, in the Polar Urals, Ordovician to Devonian passive margin sediments are found juxtaposed with Silurian–Devonian island arc volcanic rocks to the east. Together with reports of ophiolitic material and late Devonian–early Carboniferous HP metamorphic rocks to the west of the arc rocks, the observations there reveal a tectonic setting comparable to that in the south (Puchkov, 2009b; Görz and Hielscher, 2010).

After a brief interval of tectonic quiescence following the arc-continent collisions, the principal event of the Uralian orogeny—the closure of the Uralian Ocean and the collision and consolidation of Baltica, Siberia and Kazakhstania—began in the late Carboniferous and continued into the earliest Mesozoic. In Baltica that was recognized by the development of a westward-thickening foreland basin and an associated north-south trending, west-verging fold and thrust belt. The latter deformed late Carboniferous to early Triassic syn-orogenic sediments of the former (Brown et al., 2006). To the east, in the intensely deformed and metamorphosed East Uralian zone and the neighboring Trans-Uralian zone in the South and Middle Urals, early and late Carboniferous subduction-related granitoids are identified as magmatic arcs that formed on the western margin of Kazakhstania due to east-directed subduction of the Uralian Ocean (Bea et al., 2002). After continental collision in the late Carboniferous, the East Uralian zone acted as a major corridor of strike-slip motion that persisted into the early Mesozoic, and it was extensively intruded by Permian granites (Bea et al., 2002; Brown et al., 2008; Puchkov, 2009b).

The possible northward continuation of the Uralian orogen from the Polar Urals to Severnaya Zemlya, along a sinuous orogenic front that runs through Pai Khoi, Novaya Zemlya and Taimyr, is contentious (Fig. 1). In common with the Uralian margin to the south, Novaya Zemlya exhibits a Paleozoic succession of platform and shelf sediments deposited above a Cambro–Ordovician unconformity and a west-vergent fold and thrust belt that deforms the Paleozoic sequence (Pease and Scott, 2009; Görz and Hielscher, 2010). However, unlike the Uralian orogen elsewhere, the deformation in Novaya Zemlya appears to be predominantly Triassic–early Jurassic in age, and clear indications of a Devonian–Carboniferous island arc are lacking. In Taimyr, lower Paleozoic to mid-Carboniferous continental shelf and slope deposits (in South and Central Taimyr, respectively) of the Siberian platform are juxtaposed with deformed and metamorphosed Neoproterozoic to Cambrian turbidites (North Taimyr) along a major thrust zone (Gee et al., 2006; Görz and Hielscher, 2010). Yet, there too, contractional deformation developed mainly in the Mesozoic (Torsvik and Andersen, 2002; Buiter and Torsvik, 2007). However, notable late Paleozoic thrust faults and Carboniferous–Permian syn- to post-tectonic granitoids with volcanic arc geochemistry occur in North and Central Taimyr (Pease and Scott, 2009; Pease, 2011). Late Devonian–early Carboniferous folding and thrusting occurred in Severnaya Zemlya, but with an E to NE structural vergence, and allochthonous arcs or ophiolites of corresponding age have not been found (Gee et al., 2006; Lorenz et al., 2008). Thus, the relationship between the Uralian orogeny and the late Paleozoic and Mesozoic tectonism in Severnaya Zemlya and Taimyr is unclear. Nonetheless, the prevailing model supposes that Severnaya Zemlya, northern Taimyr and the northeastern Kara

Shelf together (the 'North Kara terrane' of Lorenz et al. (2008)) collided with Siberia in the late Paleozoic (Torsvik and Andersen, 2002).

*3.1.5. Southeast Baltica (Scythian and Turan platforms)*

The southeastern part of the East European craton includes the Ukrainian Shield and the Voronezh Massif, which are separated by the Dniepr-Donets Basin and the Donbas fold belt (the now-inverted Donbas Basin). The basins developed in the late Devonian–early Carboniferous during an interval of marked intracratonic rifting and attendant volcanism, the origins of which are puzzling (Stephenson et al., 2006). The craton is flanked to the south by the Scythian platform and to the southeast by the peri-Caspian Basin and the Turan platform (Fig. 1). Owing to the extensive sedimentary cover of those platforms, their pre-Mesozoic history is poorly known. Existing tectonic reconstructions of the region contrast strongly—despite often being based on the same sparse observations—and the interpretations drawn from the following discussion are thus provisional.

In the Greater Caucasus, which form the southern boundary of the Scythian platform, the first appearance of magmatism in the axial part of the range may have been coeval with Devonian to Carboniferous folding and metamorphism in the northern part of the range, but all are poorly characterized (Saintot et al., 2006). Devonian to Carboniferous igneous rocks are also recognized in Crimea and North Dobrogea, which may represent westward continuations of the Scythian platform, but those occurrences are similarly inadequately constrained (Saintot et al., 2006). A better documented phase of calc-alkaline volcanism and plutonism occurred in the Greater Caucasus in the late Carboniferous and early Permian, together with the generation of gneisses (Saintot et al., 2006). Contemporaneous late Carboniferous–early Permian magmatism also occurred to the north (in the Stavropol unit and Donbas fold belt), west (North Dobrogea) and south (in the Transcaucasus) (Alexandre et al., 2004; Natal'in and Şengör, 2005; Saintot et al., 2006). In the mid-Permian to Triassic the region was characterized by transtension to extension in the formation of continental basins and the extrusion of basalts in the Greater Caucasus and North Dobrogea (Saintot et al., 2006).

To the south, along the southern flank of the Greater Caucasus, a Devonian to Triassic sequence of fossiliferous flysch (Dizi Series) interspersed with Devonian magmatic rocks has been alternatively interpreted as an accretionary complex (Natal'in and Şengör, 2005) or a deep marine rift basin (Saintot et al., 2006). To the southwest, on the southern margin of the Black Sea, the Istanbul zone of the Pontides exhibits a thick sequence of early Carboniferous flysch with late Devonian–early Carboniferous (~390–335) detrital zircons inferred to be shed from an unknown magmatic arc (Okay et al., 2011). In the Sakarya zone of the Pontides, to the east and south of the Istanbul zone, granitoids were emplaced in the early Devonian and late Carboniferous, whereas early Carboniferous granitoids may have intruded the Strandja Massif west of the Istanbul zone (Okay et al., 2006, 2011). Unfortunately, the early to mid-Paleozoic affinity of the Pontides is not yet clearly established (the Istanbul zone in particular), so their relation to the Scythian domain is debated. Some authors (e.g. Okay et al., 2011) have correlated the Istanbul zone with Avalonia, which would imply propinquity to the Scythian platform already in the mid-Paleozoic. In any case, the Pontides must have been proximal to Baltica by the mid-to-late Carboniferous, when Variscan orogenesis folded Paleozoic rocks of the Istanbul zone and metamorphosed rocks of the Sakarya zone (Okay et al., 2006).

By means of gravity and magnetic survey data, Natal'in and Şengör (2005) identified a largely NW–SE oriented regional structural fabric in the Turan platform and inferred the presence of magmatic arc massifs paired with accretionary complexes and forearc basins. Rare outcrops and boreholes have yielded few radiometric ages, but the available data reveal that magmatism was active in the Carboniferous to early Mesozoic in the east (the Bukhara and Chardjou units) and in the Devonian to early Mesozoic in the central and western areas (Karakum, Mangyshlak, Tuarkyr and Karabogaz units); older (Silurian) granites are also reported from the Karabogaz unit (Garzanti and Gaetani, 2002; Natal'in and Şengör, 2005). Inferred mid-Paleozoic to early Mesozoic ophiolites, accretionary complexes and forearc sequences could indicate a long-lived subduction system spanning that interval, but the details are vague (Table 1). Existing evolutionary models for the complicated present-day mosaic range from terrane agglomeration (Garzanti and Gaetani, 2002) to the structural duplication of a single south-facing arc (Natal'in and Şengör, 2005).

*3.1.6. Southwest Baltica (Variscan margin)*

Prior to the Devonian, late Ordovician closure of the Tornquist Ocean resulted in collision between Baltica and Avalonia, leaving them juxtaposed along the Thor Suture (Fig. 1) (Torsvik and Rehnström, 2003). Following Caledonide orogenesis and extension, the first expression of Devonian tectonism in that region was the enigmatic "Acadian" (~400–390 Ma) deformation of the southern British Isles, which folded Cambrian to Silurian marine basinal sediments and left a mid-Devonian unconformity (Woodcock et al., 2007). A similar but perhaps slightly older event has been recognized in the neighboring Brabant Massif, but is poorly characterized. A satisfactory explanation for the "Acadian" event has yet to be reached, but Woodcock et al. (2007) suggested that it could have been due to northward subduction of the Rheic Ocean. They argued that evidence of that subduction is preserved in north-dipping reflectors in the lower crust of SW England and in the top-to-the-east thrust complexes of the Galicia-Trás-os-Montes zone of Iberia. The latter has commonly been recognized as a succession of parautochthonous (Gondwanan), ophiolitic (Rheic) and exotic continental (Laurussian) units that were progressively juxtaposed above a west-dipping subduction zone in the early to late Devonian (Arenas et al., 2007). Correspondingly, the upper (exotic) units of that thrust complex were affected by HP metamorphism at 400–390 Ma, coeval with the "Acadian" event (Arenas et al., in press). According to the age of the pre-Carboniferous ophiolities and a ~370 Ma HP metamorphic event, that entire sequence was subsequently accreted to Iberia in the late Devonian, during closure of a basin generally presumed to have been the Rheic Ocean. However, Arenas et al. (in press) reinterpreted the nature of the upper (exotic) units of that thrust stack, and argued that they rather represented the distal extended margin of Gondwana, and that both the 400–390 Ma and 370 Ma metamorphic events were due to repeated collisions between Laurussia and Gondwana.

The Rheic suture to the south of Avalonia demarcates the divide between Laurussia and the peri-Gondwanan Variscan terranes which accreted during the protracted late Devonian–Carboniferous Variscan orogeny (Fig. 1). Structural relics of that event can be seen to the south of Avalonia, in the Rheno-Hercynian zone: a belt of parauthocthonous and allochthonous nappes constituted by distal continental margin deposits, and perhaps elements from south of the Rheic Ocean, which were thrust northward onto the Laurussian margin in the late Devonian–Carboniferous (Franke, 2006; Shail and Leveridge, 2009). The dominance of north-vergent Variscan structures in the Rheno-Hercynian zone and south-dipping reflectors in its upper crust have been cited as evidence that Avalonia was part of the lower-plate during Rheic Ocean closure (Pharaoh et al., 2006; Woodcock et al., 2007). That is further supported by northward-migrating late Devonian–Carboniferous foreland basin deposits which were derived from orogenic highlands to the south

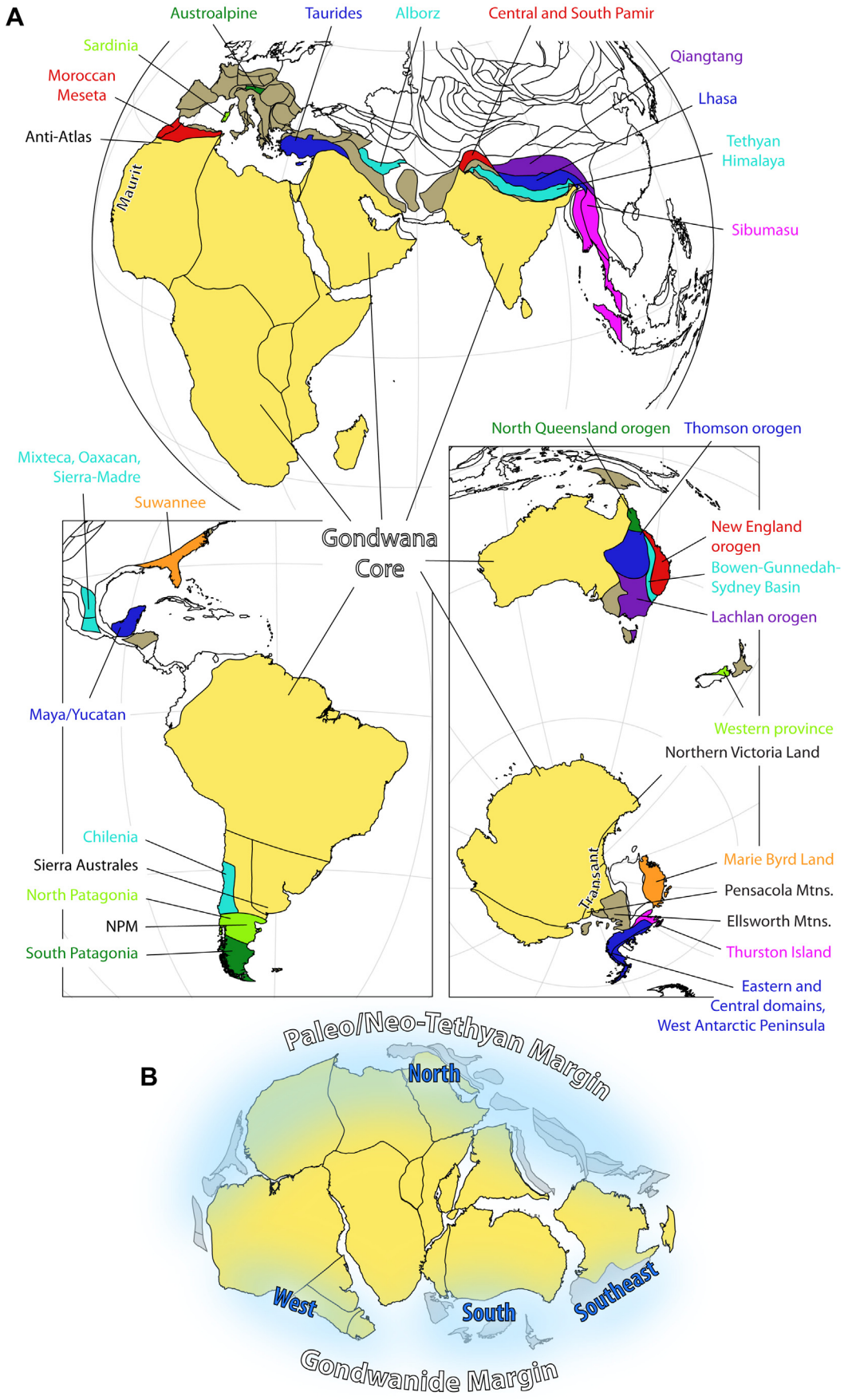
A
Austroalpine
Taurides
Alborz
Central and South Pamir
Sardinia
Moroccan Meseta
Anti-Atlas
Qiangtang
Lhasa
Tethyan Himalaya
Sibumasu
Maurit
North Queensland orogen
Thomson orogen
Mixteca, Oaxacan, Sierra-Madre
Suwannee
Gondwana Core
New England orogen
Bowen-Gunnedah-Sydney Basin
Lachlan orogen
Maya/Yucatan
Western province
Northern Victoria Land
Chilenia
Sierra Australes
North Patagonia
NPM
South Patagonia
Transant
Marie Byrd Land
Pensacola Mtns.
Ellsworth Mtns.
Thurston Island
Eastern and Central domains, West Antarctic Peninsula
B
Paleo/Neo-Tethyan Margin
North
West
South
Southeast
Gondwanide Margin

(mid-German crystalline high; see below) (Franke, 2006; Pharaoh et al., 2006). Prior to Variscan convergence, the Rheno-Hercynian zone underwent an early–middle Devonian phase of extension which resulted in regional subsidence, rift-related sedimentation, bimodal magmatism, and the exhumation of mantle peridotites now preserved in the Lizard ophiolite (Franke, 2006; Shail and Leveridge, 2009). As pointed out by Woodcock et al. (2007), the contradictory tectonic environments of the "Acadian" and Rheno-Hercynian zones during the early–middle Devonian might suggest that the latter was transported by strike-slip motion to its present position during/after "Acadian" deformation. Futhermore, the inferred subduction polarity of the early–middle Devonian "Acadian" zone is opposite to that of the late Devonian–Carboniferous Rheno-Hercynian zone, ostensibly necessitating a subduction inversion in the late Devonian. Thus the picture is dynamic, complex and far from resolved, but we cautiously proceed with this simplified narrative (Table 1).

The Variscan terranes to the south of the Rheic suture have been variously defined, but typically include: Bruno-Silesia, Saxothuringia, Bohemia, Moldanubia, North and South Armorica, and Iberia, the latter of which includes several distinct zones (Fig. 1). To the east, the Małopolska and Łysogóry blocks of Poland lie south of the Trans-European suture zone, but they were likely part of Baltica throughout the Paleozoic. The South Portuguese zone of SW Iberia is commonly affiliated with the Rheno-Hercynian zone and/or the Meguma terrane, implying that it lies to the north of the Rheic suture, but its lower Paleozoic position is unknown. The location of Bruno-Silesia in the lower Paleozoic is yet more ambiguous, with a range of postulated correlatives that lie on either side of the Rheic suture. The other terranes were more evidently peri-Gondwanan (Pharaoh et al., 2006).

In northern Saxothuringia, the mid-German crystalline high (MGCH) is interpreted to be a late Silurian–early Devonian intra-oceanic island arc formed above a south-dipping subduction zone, perhaps the first acting to close the Rheic Ocean (Franke, 2006). Faure et al. (2010) suggested that the MGCH may continue west into the Léon domain of North Armorica, with subduction-related rocks concealed offshore to the north (see also: Ballèvre et al., 2009). After an apparent lull in the mid-Devonian, arc-related plutonism recommenced in the MGCH in the late Devonian and continued into the mid-Carboniferous (Table 1). Devonian intraoceanic arc activity elsewhere in the Rheic has been inferred on the basis of possibly arc-related detritus in SW Iberia (Pereira et al., 2012) and from supra-subduction ophiolites in the Galicia-Trás-os-Montes zone (Arenas et al., 2007); although the latter is interpreted to reflect a north-dipping subduction zone. In the late Devonian–early Carboniferous arc magmatism also appeared in Bohemia, but there it represented a continental arc that was positioned above a south-dipping subduction zone (Schulmann et al., 2009; Žák et al., 2011).

Although the details remain far from clear, a spatially and temporally broad distribution of Devonian–Carboniferous (~420–340 Ma) HP/UHP metamorphic rocks across the Variscan terranes indicates that a complex set of convergent processes operated throughout that interval (Faryad, 2011; Faryad and Kachlík, 2013). In particular, the occurrence of HP/UHP metamorphic rocks and ophiolitic complexes within and between the various terranes (Bohemia, Moldanubia and South Armorica) indicates that additional, probably minor, oceanic basins existed among them—those were subducted as the terranes were telescoped in the Devonian–Carboniferous (e.g. Matte, 2001; Franke, 2006; Faure et al., 2008; Murphy et al., 2009; Schulmann et al., 2009; Faryad and Kachlík, 2013). Northward subduction of the Paleotethys Ocean to the south of the Variscan terranes has been conjectured from the occurrence of arc-related igneous rocks and forearc deposits in the southernmost Variscan units and from the incidence of marginal extension ascribed to slab rollback (Stampfli and Borel, 2002; Broska et al., 2013; von Raumer et al., 2013). According to those observations, Paleotethys subduction could have started in the late Devonian and continued into the Permian.

Continental collision in the early Carboniferous was highlighted by a ~340 Ma peak in HP/UHP metamorphism, ~355–335 Ma crustal thickening (nappe emplacement), and the intrusion of syntectonic plutons between ~355 and 340 Ma, followed by significant post-tectonic plutonism in Bohemia, Moldanubia, South Armorica, and Iberia (Franke, 2006; Schulmann et al., 2009). By the late Visean the prevailing regime of oblique convergence had evolved to one dominated by dextral translation, in turn giving rise to an extensive series of wrench faults, intra-continental rift basins and widespread volcanism that characterized late Carboniferous–early Permian post-Variscan Europe (Dostal et al., 2003; Wilson et al., 2004; McCann et al., 2006; Torsvik et al., 2008a).

### 3.2. Gondwana

#### 3.2.1. North Gondwana (Paleo/Neo-tethyan margin)

It is often assumed that the northern margin of Gondwana experienced a phase of broad and protracted extension in the early to mid-Paleozoic, which ultimately led to the opening of the Paleotethys Ocean and, correspondingly, to the rifting and subsequent drifting of the Variscan terranes (Table 1). Although widely embraced as a conceptual model, the evidence for that event remains poor in many regions. From subsidence patterns along the inferred margins of the Paleotethys, Stampfli (2000) concluded that the ocean opened diachronously in the Ordovician and Silurian. However, von Raumer and Stampfli (2008) revised that timing and placed the Paleotethys opening in the middle–late Devonian. On a smaller scale, well-preserved mid-Paleozoic sections occur in the Meseta and Anti-Atlas domains of Morocco, the Tauride domain of Turkey and the Alborz domain of Iran (Fig. 2), where Silurian—Devonian post-glacial black shales give way to carbonate rocks and basinal facies, and, more locally, mafic magmatic rocks and conglomerates (Wendt et al., 2005; Moix et al., 2008; Michard et al., 2010). Those sequences have been interpreted to reflect the progression from sluggish rifting to passive margin drowning, although they offer few specific temporal constraints. Late Silurian to early Devonian S-type granitoids (415–400 Ma) in the Maya Block (SE Mexico, Guatemala and Belize, Fig. 2; then situated to the north of the Amazonian Craton) might better constrain those extensional processes, but could alternatively be products of an active margin (Weber et al., 2012). Inferred rift-related igneous rocks of mid-Paleozoic age are also recognized in several areas of the conjugate (northern) margin of the Paleotethys (i.e. the south Variscan terranes), in Sardinia, Central Iberia and the Austroalpine basement (Fig. 2) (Gaggero et al., 2012; von Raumer et al., 2013), but there too the magmatic events were temporally protracted and the tectonic context of their emplacement is vague.

Once established, the south Paleotethyan margin in Turkey and Iran (and areas further east) remained passive throughout the late

**Figure 2.** (A) Modern map showing the present-day location of the Paleozoic core of Gondwana (yellow), the various terranes that were accreted to, rifted from, or remobilized along its margins in late Paleozoic time (various bright colors), and other features discussed in Section 3.2. Brown areas are late Paleozoic terranes not explicitly discussed. *Abbreviations*: Maurit, Mauritanides; NPM, North Patagonian Massif; Transant, Transantarctic. (B) Schematic early Devonian reconstruction of Gondwana showing its margins as we define and discuss them in Section 3.2.

Paleozoic (Table 1). In contrast, the Moroccan margin was affected by late Devonian to Carboniferous deformation, metamorphism and magmatism imposed by a dominantly transcurrent tectonic regime associated with Variscan orogenesis (Hoepffner et al., 2006). A notable phase of that episode was the occurrence of early Carboniferous HP metamorphism in the northern Mauritanide belt (Michard et al., 2010). By the late Carboniferous, deformation was most prominent in the Meseta, where there was NW–SE shortening and dextral wrenching along NE-trending fault systems. Devonian–Carboniferous polyphase deformation and metamorphism also occurred further west in the Mixteca-Oaxacan terrane of Mexico (Fig. 2), which was likely situated along the northwest margin of Amazonia throughout the Paleozoic (Nance et al., 2009). Keppie et al. (2008) and Keppie et al. (2012) interpreted a Devonian–early Carboniferous episode of HP metamorphism (and an inferred phase of coeval arc magmatism) to have been due to east-dipping subduction beneath the Mixteca-Oaxacan terrane. Exhumation and retrogression of the HP metamorphic rocks followed in the mid-Carboniferous, accompanied by migmatization and continued deformation (Keppie et al., 2008), perhaps in a transcurrent tectonic environment. Arc magmatism resumed in the Mixteca-Oaxacan terrane in the late Carboniferous to mid-Permian and, together with regional transtensional deformation, was probably produced by east-dipping, oblique subduction along the western margin of the terrane (Table 1) (Keppie et al., 2008; Kirsch et al., 2012). In the east, early Permian syn- to post-orogenic igneous rocks are recognized in the Suwannee terrane (Heatherington et al., 2010) and the Moroccan Meseta (Michard et al., 2010).

During the early Permian a second episode of margin-wide rifting occurred along north Gondwana, from Turkey through Tibet to northwest Australia, culminating in the detachment of the elongate Cimmerian terrane and the opening of the Neotethys Ocean (Table 1). Along the Arabian margin, the timing of that event is best known from the well-studied late Paleozoic–early Mesozoic stratigraphy of Oman. The rifting may have started as early as the late Carboniferous since indications of southwest-directed sediment and glacial ice transport imply the presence of an uplifted area to the northeast then (along the Arabian margin) (Blendinger et al., 1990; Lee, 1990; Al-Belushi et al., 1996). A subsequent inversion in the direction of sediment transport has been attributed to collapse of that crustal uplift (Al-Belushi et al., 1996). A concurrent change in sediment composition was equated to the detrital modes expected in an evolving rift system by Angiolini et al. (2003), who also identified a mid-Sakmarian unconformity as the temporal marker of incipient breakup ('breakup unconformity'). However, completion of the oceanization process was not evident until the middle Permian, when the abrupt appearance of pelagic carbonates and deep water radiolarian-bearing shale signaled the drowning of the rift shoulder (Stampfli et al., 1991; Angiolini et al., 2003; Baud et al., 2012). That timing is further supported by middle Permian pillow basalts and volcaniclastics in the Hawasina nappes of the coastal mountains of northeastern Oman. Although the origins of those rocks are debated (Stampfli et al., 1991; Pillevuit et al., 1997; Maury et al., 2003), it is widely agreed that they imply that rifting was underway by at least the middle Permian. Unambiguous evidence for late Paleozoic rifting of the conjugate margin of Iran is lacking, but the stratigraphic record reveals the development of a carbonate platform in the middle Permian, which is consistent with the tectonic framework established in Oman (Berberian and King, 1981; Stampfli et al., 1991; Alirezaei and Hassanzadeh, 2012).

Along the margin to the east, there is notable evidence of Carboniferous–early Permian extension in the Southeast Pamir, Qiangtang terrane and along the Tethyan Himalaya (Fig. 2). Much like in Oman, the late Paleozoic stratigraphy of the Southeast Pamir exhibits a late Carboniferous–early Permian syn-rift sequence of siliciclastics unconformably overlain by middle to late Permian carbonates and basinal facies, reflecting the development and drowning of a newly-created passive margin (Angiolini et al., 2003). Attendant early–middle Permian rift-related basalts are reported from northern Southeast Pamir and from the Rushan-Pshart zone which separates the Central and Southeast Pamir (Zhang et al., 2012b). Similarly, in the Qiangtang terrane, earliest Permian glacio-marine deposits, clastic rocks and inferred rift-related mafic magmatic rocks were replaced in Artinskian to Kungurian time by carbonates, turbidites and island arc type basalts (Zhang et al., 2012b, 2013b). Zhang et al. (2012b) concluded that marginal breakup initiated in the Sakmarian and progressed until final oceanization was achieved in the Kungurian—an evolution analogous to that seen in Oman. Further to the east, in the complicated and variably-defined Sibumasu terrane (Fig. 2), comparable late Paleozoic rift-related stratigraphic successions have been recognized in the Tengchong and Baoshan blocks, with the early Permian Woniusi basalts in the latter (Zhang et al., 2013b). To the south, widespread early Permian basaltic rocks (Selong Group basalts, Nar Tsum spilites, Bhote Kosi basalts) and associated syn- to post-rift sedimentary successions are found along the Tethyan Himalaya, reflecting extension along the conjugate (southern) margin of the emergent Neotethys (Garzanti et al., 1999; Zhu et al., 2010). Contemporaneous and voluminous flood basalt volcanism in the High Himalaya (Panjal Traps) has also been related to that regional rifting (Shellnutt et al., 2011), but is most likely the expression of a mantle plume.

### 3.2.2. Southeast Gondwana (Australian Gondwanide margin)

The late Paleozoic geologic record of eastern Australia chronicles a complex spatiotemporal interplay of convergent and extensional tectonism. Yet, in spite of the tangled details of its history, it is now broadly agreed that margin developed behind a long-lived, west-dipping subduction system, albeit with intermittent re-locations of the subduction zone itself (Glen, 2005, 2013; Champion et al., 2009). The alternating and often diachronous episodes of compression and tension that affected that margin have therefore been related to changes in plate boundary forces (Fergusson, 2010; but also see Gray and Foster, 2004). Drawing greatly from the excellent syntheses of Glen (2005) and Champion et al. (2009), we present a cursory review of those major tectonic cycles.

The Devonian opened to an extension-dominated regime characterized by basin development and sedimentation, and widespread felsic to bimodal magmatism in the Lachlan and Thomson orogens and northeast Tasmania (Fig. 2). Having followed a significant orogenic event in the Silurian, that extensional phase has often been associated with post-orogenic relaxation, but it could also have been driven by rollback of the subduction zone to the east. Dispersed occurrences of contractional to transcurrent deformation appeared in various areas during the poorly-defined ~420–400 Ma Bindian-Bowning orogeny, but only the southeast Lachlan orogen was markedly affected (Champion et al., 2009; Fergusson, 2010). The cause of that deformation is uncertain, but it could have been due to relative motion between subdomains of the Lachlan orogen (Willman et al., 2002). Otherwise, regional tension persisted until the ~390–380 Ma Tabberabberan orogeny, a major contractional phase that drove basin inversion in the Lachlan orogen and left Middle Devonian unconformities across much of eastern Australia (Glen, 2005; Champion et al., 2009). Explanations for that event include closure of a marginal basin (Melbourne Trough), final docking and amalgamation of the Lachlan orogen subdomains (as well as the union of western and northeastern Tasmania), and/or accretion of a late Silurian to middle Devonian intraoceanic arc (Gamilaroi-Calliope arc; Table 1)

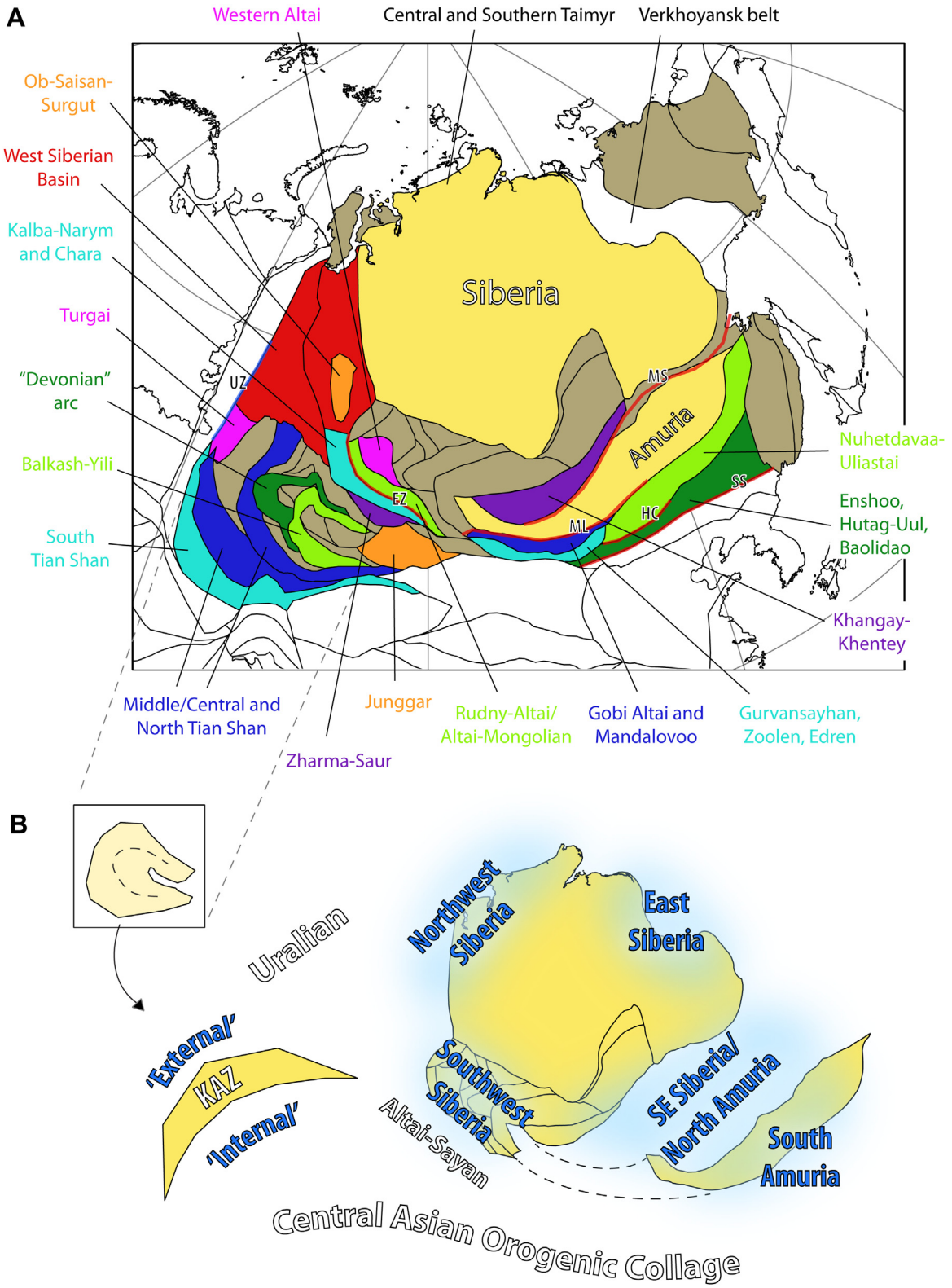


**Figure 3.** (A) Modern map showing the present-day location of the Siberian craton and the late Paleozoic core of Amuria (yellow), the various terranes that were accreted to, rifted from, or remobilized along their margins in late Paleozoic time (various bright colors), and other features discussed in Sections 3.3–3.4. Brown areas are late Paleozoic terranes not explicitly discussed. *Abbreviations*: EZ, Ertix shear zone; HC, Hegenshan complex; ML, main Mongolian lineament; MS, Mongol-Okhotsk suture; SS, Solonker suture; UZ, East Uralian/Trans-Uralian zone. (B) Schematic early Devonian reconstruction of Siberia, Amuria and retro-deformed Kazakhstania (the small inset schematically shows the present-day form of the orocline), showing their margins as we define and discuss them in Sections 3.3–3.4.

(Willman et al., 2002; Gray and Foster, 2004; Glen, 2005; Champion et al., 2009). Considering the composite nature of Tabberabberan deformation, it is possible that those processes acted together.

With the cessation of the Tabberabberan orogeny, regional stress inverted and basin formation, sedimentation and felsic to bimodal magmatism recommenced in the Lachlan, Thomson and North Queensland orogens from ~380 to 360 Ma. In the New England orogen to the east (Fig. 2), a forearc basin and accretionary wedge first appeared in the late Devonian–early Carboniferous, reflecting the nascent development of an active continental margin, presumably related to the accretion of the Gamilaroi-Calliope island arc (Champion et al., 2009; Glen, 2013). By the mid-Early Carboniferous, regional tension in the back-arc was again supplanted by an east-west shortening event (Kanimblan orogeny), and another chapter of thrusting and folding was added to the Lachlan and Thomson orogens (Glen, 2005; Champion et al., 2009). Continental arc magmatism in the New England orogen endured through the Kanimblan orogeny, and peaked in the late Carboniferous (~324–305 Ma), and so that transitory convergence was probably related to a changing balance in the marginal plate forces, rather than to collision. The subsequent termination of arc magmatism and forearc deposition in the latest Carboniferous has been interpreted to reflect an oceanward jump of the subduction zone to an intraoceanic complex offshore to the east (early Permian Gympie island arc; Table 1) (Champion et al., 2009). With that change came the introduction of regional tension and bimodal magmatism to the New England orogen, indicating that it occupied a backarc environment then. In the Lachlan and southern Thomson orogens, the mid-Carboniferous to early Permian interval was similarly characterized by the formation of back-arc and intracratonic basins, which ultimately led to the early Permian development of the NNW–SSE trending East Australian rift system (Bowen-Gunnedah-Sydney Basin; Fig. 2) (Glen, 2005, 2013; Champion et al., 2009). Thus, in the latest Carboniferous to late early Permian most of eastern Australia acted as a broad and actively extending backarc located behind a marginal island arc to the east.

During the late early to middle Permian the former forearc and accretionary wedge of the New England orogen were deformed into the Texas and Coffs Harbour oroclines, perhaps via dextral strike-slip motion (Champion et al., 2009). Shortly afterward the region returned to a regime of east-west contraction during the Hunter-Bowen orogeny, which spanned the late middle Permian to mid-Triassic. In the New England orogen that orogenic episode was associated with the development of a west-verging fold-thrust belt and conversion of the back-arc rift-system to a foreland basin (Glen, 2005, 2013; Champion et al., 2009). Collision of the Gympie island arc (~250 Ma) and resumption of the continental margin arc (~265–230 Ma) also occurred then, reflecting increased convergence between eastern Australia and the westward-subducting oceanic plate (Table 1) (Champion et al., 2009).

### 3.2.3. South Gondwana (Antarctic Gondwanide margin)

The Paleozoic margin of Gondwana that once lay outboard of the present-day Pacific margin of Antarctica was greatly excised in the late Paleozoic, and later fragmented and dispersed, with formerly-proximal elements now found scattered in southwest New Zealand, North Victoria Land and Marie Bryd Land (Fig. 2) (Adams, 2008). Since the latter two areas are remote and largely ice-covered, our knowledge of that margin is poor, and thus our account, which is largely dependent on inferred associations with eastern Australia, is tentative. A lack of Devonian–Carboniferous sedimentary sequences in those areas precludes the unequivocal recognition of subduction-accretion complexes, and leaves tectonic deductions to be drawn from the occurrence and nature of intrusive rocks (Tulloch et al., 2009). The earliest and most voluminous phase of late Paleozoic magmatism appeared in the Western province of the South Island of New Zealand at ~371–360 Ma, with the emplacement of the Karamea-Paringa paired S/I-type suite. The temporal association between the individual magmatic events, their geochemical characteristics and the rapidity of magma production point to a major extensional event in an intra-arc or back-arc environment (Tulloch et al., 2009; Scott et al., 2011). A similar setting has been inferred for the subsequent emplacement of the Ridge-Tobin paired S/I-type suite, which followed at ~355–342 Ma (Tulloch et al., 2009). Afterward, Carboniferous magmatism of the Western province was characterized by sporadic A-type granitic plutonism, as was the Median Batholith to the east (Mortimer et al., 1999b; Tulloch et al., 2009). Permian plutonic and volcanic rocks of various composition are known from the Brook Street terrane, an allocthonous terrane of the Eastern province of the South Island (Mortimer et al., 1999a). The Brook Street terrane has been recognized as a Permian intraoceanic arc and probably represents a continuation of the Gympie terrane from the New England orogen of Australia. Intervening elements of that arc system have also been recognized in New Caldedonia and the West Norfolk Ridge (Mortimer et al., 1999a; Spandler et al., 2005). Like the Gympie terrane, the Brook Street terrane is thought to have formed above a west-dipping subduction zone outboard of the Gondwanan margin (Nebel et al., 2007); its accretion in the Permo-Triassic must therefore have been preceded by the closure of a back-arc basin (Table 1).

Elsewhere among relics of that former margin, episodes of Devonian–Carboniferous calc-alkaline magmatism are seen in Marie Byrd Land, northern Victoria Land and the Eastern domain of the northern Antarctic Peninsula (Fig. 2) (Pankhurst et al., 1998; Boger, 2011). The late Devonian–early Carboniferous magmatic episodes in New Zealand appear to have broadly contemporaneous I-type granitoid counterparts in Marie Byrd Land (~375–350 Ma Ford Granodiorite and Fosdick Mountains complex) and northern Victoria Land (~370–350 Ma Admiralty Intrusives and Gallipoli Volcanics) (Pankhurst et al., 1998; Siddoway and Fanning, 2009). A subsidiary mid-Carboniferous phase of granitoid magmatism (~340–320 Ma) is also reported in Marie Byrd Land and northern Victoria Land, but is poorly defined. In the Eastern domain of the Antarctic Peninsula, early Devonian and mid-to-late Carboniferous igneous and metamorphic have been found in the Target Hill orthogneiss complex (Millar et al., 2002); Riley et al. (2012) have suggested that their occurrence may be locally-restricted, although late Carboniferous calc-alkaline orthogneisses have also been recognized on Thurston Island (Leat et al., 1993). More widespread metamorphic and magmatic activity affected the Antarctic Peninsula (Central and Eastern domains) during the mid-to-late Permian, and widespread but volumetrically minor Permian granitoid plutonism occurred in Marie Byrd Land which may have represented a magmatic arc (Pankhurst et al., 1998; Riley et al., 2012). In the foreland, the mid-to-late Permian was marked by the development of a fold and thrust belt in the Ellsworth and Pensacola Mountains, which was constructed in a regime of dextral transpression associated with the enigmatic Gondwanide orogeny (Curtis, 2001). Also at that time, foreland basin deposits in the Transantarctic Mountains recorded a major paleocurrent reversal and the appearance of magmatic arc detritus (Elliot and Fanning, 2008).

A parsimonious interpretation of that sparse data would be that the late Paleozoic history of that margin, like that of eastern Australia, was one of persistent convergence above a north-dipping subduction zone, with intermittent changes in regional stress due to adjustments in relative motion along the plate boundary (Table 1). We may also speculate, on account of the gross similarities with eastern Australia, that the absence of early Permian

magmatism outside of the Brook Street terrane may signify that subduction had jumped outboard to that intraoceanic arc system in the latest Carboniferous. Subsequent collapse of the intervening remnant basin could explain the mid-to-late Permian magmatism and convergence and accretion of the arc would coincide with the deformation observed in the foreland. Intriguingly, the backarc dextral transpression inferred for Gondwanide orogenesis there might be analogous with that responsible for the Texas and Coffs Harbour oroclines in Australia.

#### 3.2.4. West Gondwana (Proto-Andean margin)

The late Paleozoic history of Patagonia is controversial. The occurrence of late Carboniferous–early Permian NE–SW contractional structures with opposing vergence in the northern North Patagonian Massif and the southern margin of West Gondwana (Cerro de los Viejos, Sierra Australes fold and thrust belt; Fig. 2) presents a compelling argument for a late Paleozoic collision between Gondwana and an allocthonous Patagonia terrane (von Gosen, 2003; Ramos, 2008; Rapalini et al., 2010). However, late Paleozoic paleomagnetic data from the North Patagonian Massif correspond with those of Gondwana, implying that the landmasses were already proximal by the early Devonian (Rapalini, 2005). Furthermore, strong magmatic and isotopic correlatives can be drawn between the North Patagonian Massif and West Gondwana (Pampia block) back into the early Paleozoic (Martínez Dopico et al., 2011; Rapalini et al., 2013). To resolve that paradox, some models have treated Patagonia as a composite block comprised of a (para-) autochthonous northern block and an allochthonous southern block (Pankhurst et al., 2006; Ramos, 2008; Rapalini et al., 2010; Chernicoff et al., 2013). There are important differences between those models; for example, whether a minor ocean basin existed between the northern block and Gondwana and, if so, how it closed. But, there appears to be a common consensus that destruction of the ocean basin separating the northern and southern blocks was accomplished by late Paleozoic subduction beneath the former (i.e. north dipping subduction; Table 1). The most apparent plutonic rocks reflecting that subduction in the North Patagonian Massif are from the late early Carboniferous (~335–325), but relics of possibly subduction-related magmatism and metamorphism stretch back into the early Devonian (Pankhurst et al., 2006; Chernicoff et al., 2013). Interestingly, a case may be made for a magmatic break there between ~390 and 340 Ma, as will be discussed in Section 4. In contrast, northeast-dipping subduction beneath the southwest margin of the southern block may have started at ~390 Ma and continued into the Mesozoic (Table 1) (Kato et al., 2008; Chernicoff et al., 2013). Collision of the southern and northern blocks commenced in the late Carboniferous and Pankhurst et al. (2006) attributed the subsequent occurrence of widespread Permian magmatism to slab breakoff following terminal basin closure.

Along the proto-Andean margin to the west and north of Patagonia, the apparent absence of a typical Andean-type magmatic arc of early to middle Devonian age has led many to conclude that the margin was passive at that time, following widespread arc-magmatism and terrane collision during the Famatinian orogenic cycle (Bahlburg et al., 2009). However, the recognition of middle Devonian HP metamorphic rocks adjacent to a discontinuous belt of ultramafic bodies in the Frontal Cordillera and North Patagonian Andes of Argentina supports a ~390 Ma collision between Gondwana and a poorly-characterized allochthonous terrane ('Chilenia'; Fig. 2) (Ramos et al., 1986; Massonne and Calderón, 2008; Willner et al., 2011; Martínez et al., 2012). The polarity of subduction associated with pre-collisional convergence of Gondwana and Chilenia is equivocal, but indirect clues from detrital zircon ages (in detritus inferred to be derived from Chilenia) and the distribution of possibly arc-related to post-orogenic igneous rocks have been used to argue for east-dipping subduction (Álvarez et al., 2011; Martínez et al., 2012). For ~50–60 Myr following the accretion of Chilenia, arc-magmatism and deformation were notably absent along the entire proto-Andean margin north of Patagonia, leading again to the interpretation that the margin may have been passive then (Table 1) (Chew et al., 2007; Bahlburg et al., 2009). Late Devonian–early Carboniferous magmatic rocks are found to the east, in the Precordillera and foreland Sierras Pampeanas, but are predominantly A-type granitoids that were probably emplaced in a regime of prevailing tension (Grosse et al., 2009; Dahlquist et al., 2010; Martina et al., 2011). The earliest indications of subduction resumption appeared in the late-early Carboniferous (~340 Ma), with the onset of calc-alkaline magmatism in the Eastern Cordillera of Peru and the appearance of first-cycle detrital zircons in late Paleozoic accretionary complexes of Chile (Chew et al., 2007; Bahlburg et al., 2009; Miskovic et al., 2009; Hervé et al., 2013). However, unambiguous evidence of an active margin has not been documented before the late Carboniferous (~320 Ma), when HP metamorphism and a coeval calc-alkaline magmatic arc in the southern proto-Andes formed a classic paired metamorphic belt (Willner, 2005). High-grade metamorphism also occurred in the central proto-Andes at that time and arc-magmatic activity conspicuously increased, suggesting that the onset of late Paleozoic subduction may have been rapid across the entire proto-Andean margin (Miskovic et al., 2009). Subduction beneath the proto-Andean margin then continued unabated into the Permian (Table 1). During the mid-Permian to Triassic a phase of regional extension was accompanied by a dramatic change in the geochemical character of proto-Andean magmatism—from arc-related to intra-plate—and the locus of magmatism shifted inboard (Kleiman and Japas, 2009; Miskovic et al., 2009). The geodynamic origin of those occurrences remains unclear, but it could relate to changes in the rate of plate convergence, perhaps accompanied or caused by slab break-off.

### 3.3. Siberia and Amuria

#### 3.3.1. East Siberia (proto-Verkhoyansk margin)

The eastern margin of Siberia was passive from the Cambrian to the mid-Paleozoic, as evident by the typical passive margin sedimentary sequence in the southern sector of the Mesozoic Verkhoyansk fold and thrust belt (Fig. 3) (Khudoley and Guriev, 2003; Bradley, 2008). In the middle to late Devonian the passive margin was interrupted by a tensional episode, recognized by widespread mafic magmatism and rift-related deposits across the east Siberian margin and abundant extensional structures in the Sette-Daban zone of the southern Verkhoyansk fold and thrust belt (Table 1) (Khudoley and Guriev, 2003). Passive margin sedimentation was re-established in the early Carboniferous and continued into the Mesozoic; shortening associated with Verkhoyansk orogenesis began in the Jurassic (Bradley, 2008).

#### 3.3.2. Northwest Siberia (Uralian margin and West Siberian Basin)

Much about the Paleozoic history of the northwestern margin of Siberia is unknown due to the thick and expansive Jurassic to Recent sedimentary cover of the West Siberian Basin, which extends from the Altai-Sayan fold belt in the southeast, north to the Arctic Ocean, and along the Uralian orogen to the west (Fig. 3) (Vyssotski et al., 2006). Nevertheless, a window into that margin is found in central and southern Taimyr, where Paleozoic rocks are exposed on the Taimyr Peninsula to the north of the Mesozoic to Recent sediments of the Yenisey-Khatanga depocenter. There, the occurrence of lower Paleozoic to mid-Carboniferous continental shelf and slope deposits imply that the northwestern margin of

Siberia was passive then (Bradley, 2008). The passive margin was destroyed by the accretion of allochthonous northern Taimyr, which may have arrived in the late Carboniferous according to the occurrence of thrusting, metamorphism and granitoid magmatism of late Carboniferous–Permian age in central Taimyr (Table 1) (Pease and Scott, 2009; Pease, 2011). However, we reiterate that most of the contractional deformation in Taimyr was generated during the Mesozoic (Torsvik and Andersen, 2002; Buiter and Torsvik, 2007).

### 3.3.3. Southwest Siberia (Altai-Sayan margin)

The southwest margin of the Siberian craton is flanked by the notoriously complex Altai-Sayan area: a consolidation of micro-continental blocks, island arcs, backarc basins and accretionary complexes that largely amalgamated with the Siberian craton in the late Neoproterozoic to Ordovician (Fig. 3). By the mid-Paleozoic, the active southwest margin of greater Siberia had relocated to the western edge of that Altai-Sayan tectonic mosaic. In the northern (Siberian) and southern (Chinese) Altai, Devonian subduction-related granitoid magmatism occurred in the Rudny-Altai/Altai-Mongolian zones and the inboard Western-Altai zone (including the Charysh-Terekta and Gorny-Altai zones) (Xiao et al., 2004; Wang et al., 2009; Cai et al., 2011; Glorie et al., 2011a, 2012). That magmatic activity appears to have peaked at ~410–400 Ma (perhaps diachronously, younging to the northwest) and by ~370–360 Ma intrusions become sporadic and volumetrically limited (Cai et al., 2011; Glorie et al., 2011a). To the west of the Rudny-Altai zone, across the Ertix (or Irtysh or Erqis) shear zone, the Kalba-Narym and Chara zones have been recognized as a forearc basin and accretionary complex corresponding to the Devonian magmatic arc (Fig. 3) (Wilhem et al., 2012). The accretionary complex contains elements of late Devonian–early Carboniferous island arc rocks and oceanic crust and was sealed by late Carboniferous volcaniclastic rocks and intrusions (Buslov et al., 2004; Safonova et al., 2012). To the northwest those zones are obscured by deposits of the West Siberian Basin, but likely continue into the Ob-Saisan-Surgut area, where a late Devonian–early Carboniferous accretionary complex has been identified from boreholes and geophysical surveys (Fig. 3) (Cocks and Torsvik, 2007). Collectively, those observations imply that the southwest margin of greater Siberia was positioned above an east-dipping subduction zone during the Devonian–early Carboniferous, and this is reflected in most paleogeographic models of the region (Table 1). Some models significantly differ in arguing that the Altai-Mongolian microcontinent and/or an island arc to its south collided with greater Siberia in the early–middle Devonian or late Devonian–early Carboniferous (Buslov et al., 2004; Xiao et al., 2004; Glorie et al., 2011a, 2012). Although structural observations and the occurrence of ophiolitic bodies may support some such argument (the details remain vague), the restricted distribution of the *Tuvaella* brachiopod fauna to the north of the Ertix boundary implies that the affected zones were already proximal to Siberia in the Silurian (Cocks and Torsvik, 2007). The observations may thus be better explained by the strike-slip relocation of terranes and/or the opening and closing of a marginal back-arc basin in the Devonian (Wilhem et al., 2012).

Late Carboniferous–Permian magmatism (~320–250 Ma) of the Siberian and Chinese Altai was characterized by small, A-type intrusives that first invaded areas near the Ertix shear zone and later appeared across the entire Altai-Sayan region; they are commonly classified as post-orogenic to intraplate (Wang et al., 2009; Cai et al., 2011; Glorie et al., 2011a, 2012). Partly concurrent with that magmatic phase, major transcurrent motion occurred in the late Carboniferous–early Permian along the Ertix shear zone and other parallel strike-slips systems, notably within the Chara and Charysh-Terekta zones (Buslov et al., 2004; Buslov, 2011). That episode of regional transcurrent motion, coupled with attendant contractional deformation and magmatism, was associated with a protracted oblique collision between Siberia and Kazakhstan, which may have begun as early as the late Devonian and which continued into the early Permian (Briggs et al., 2007; Buslov, 2011; Wilhem et al., 2012).

### 3.3.4. Southeast Siberia and northern Amuria

From at least Silurian to mid-Mesozoic time, the southeastern margin of Siberia was flanked by the Mongol-Okhotsk Ocean (MOO), the vestiges of which are recognized in and along a WSW/ENE-trending suture that runs from central Mongolia to the Sea of Okhotsk (Fig. 3). Relics of that ocean basin include: late Silurian to early Carboniferous typical ocean plate stratigraphy (basaltic rocks overlain by Pridolian to Frasnian radiolarian chert passing upward into shale and turbidite) in the Khangay-Khentey basin, Devonian–early Carboniferous intraoceanic Onon arc rocks, the dismembered mid-Carboniferous (~325 Ma) Adaatsag ophiolite, and coarsening Permian–early Mesozoic marine sediments in the suture zone (Tomurtogoo et al., 2005; Kurihara et al., 2009; Bussien et al., 2011). That ocean separated Siberia from the so-called 'Amuria' terrane, which includes elements of the Tuva-Mongolian and Altai-Mongolian microcontinents that had purportedly accreted to Siberia in the early Paleozoic (Fig. 3) (Wilhem et al., 2012). That implies that the MOO opened in the late-early to mid-Paleozoic, dividing the collage of terranes previously assembled against the southeast margin of the Siberian craton. Additionally, the abrupt western termination of the suture zone in central Mongolia suggests that the ocean basin did not continue into the Altai-Sayan realm; rather the early Paleozoic-accreted terranes there remained coherent with the Siberian craton. Therefore, the MOO was probably wedge-shaped and narrowed to the west.

On the northern (Siberian) margin of the MOO, mid-Carboniferous to Triassic subduction-related igneous rocks are recognized in the Angara-Vitim, Khangay and Khentey batholiths and the Selenga (Western Transbaikalian) volcano-plutonic belt and have been ascribed to north-dipping subduction beneath Siberia (Table 1) (Tomurtogoo et al., 2005; Donskaya et al., 2013). Because of the prevalence of Devonian–early Carboniferous detrital zircons in late Paleozoic–early Mesozoic sediments of the Khangay-Khentey accretionary wedge to the south of the arc, Bussien et al. (2011) argued that subduction and arc magmatism may have started in the Devonian. Mid-Carboniferous to Triassic subduction-related igneous rocks are also recognized in the Middle Gobi volcano-plutonic belt along the southern (Amurian) margin of the MOO, signifying that subduction of the MOO was also south-directed and thus bivergent (Tomurtogoo et al., 2005; Bussien et al., 2011). However, unlike the northern margin of the MOO, there are no strong indications that subduction beneath the southern margin began prior to the Carboniferous.

### 3.3.5. Southern Amuria

South of the Mongol-Okhotsk suture, the constituents of Amuria—which include microcontinents, island- and continental magmatic arcs, back-arc basins, and ophiolitic- and accretionary complexes—exhibit a general trend of southward-younging, reflecting significant southward growth of that terrane during the Paleozoic. In particular, a major E–W trending structural divide that bisects Amuria, the 'main Mongolian lineament', separates a principally early Paleozoic domain to the north from a predominantly late Paleozoic domain to the south (Fig. 3) (Windley et al., 2007). To the south of that lineament, Silurian to Carboniferous island arc magmatic rocks in the Tseel, Edren, Zoolen, Gurvansayhan and Enshoo zones of Badarch et al. (2002) (Trans-Altai zone of Kroner

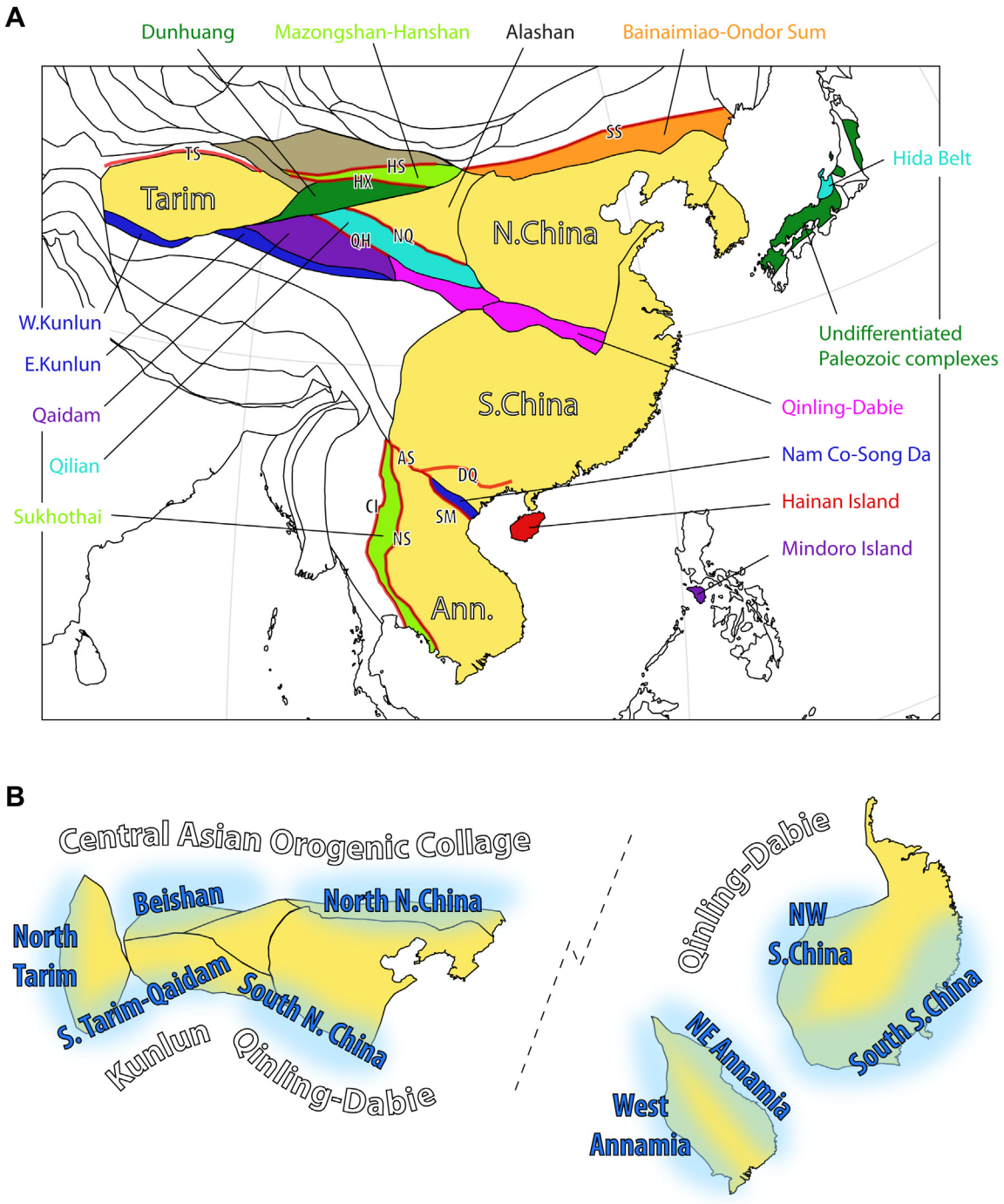


**Figure 4.** (A) Modern map showing the present-day location of the Tarim, North China, South China and Annamia cratons (yellow), the various terranes that were accreted to, rifted from, or remobilized along their margins in late Paleozoic time (various bright colors), and other features discussed in Sections 3.5–3.7. Brown areas are late Paleozoic terranes not explicitly discussed. *Abbreviations*: AS, Ailaoshan suture; CI, Changning-Menglian-Inthanon suture; DQ, Dian-Qiong suture; HS, Hongshishan belt; HX, Hongliuhe-Xichangjing belt; QH, North Qaidam belt; NQ, North Qilian belt; NS, Nan-Sra Kaeo suture; SM, Song Ma suture; SS, Solonker suture; TS, Tian Shan suture. (B) Schematic early Devonian reconstruction of North China-Tarim, South China and Annamia, showing their margins as we define and discuss them in Sections 3.5–3.7.

et al., 2010) are flanked by contemporaneous continental arc-back-arc successions to the north (Gobi Altai, Mandalovoo and Nuhetdavaa zones) and forearc/accretionary complexes to the south (Fig. 3) (Helo et al., 2006; Yarmolyuk et al., 2008; Demoux et al., 2009; Blight et al., 2010; Wainwright et al., 2011; Wilhem et al., 2012; Rippington et al., 2013). Mafic-ultramafic bodies inferred to be fragments of a Devonian–Carboniferous ophiolite occur in the Zoolen and Gurvansayhan zones (Rippington et al., 2008, 2013), and could represent a basin of such age that separated the island- and continental arcs. Wainwright et al. (2011) have argued that xenocrystic zircons found in juvenile Devonian–Carboniferous island arc rocks from the south Gurvansayhan zone indicate that the arc could not have been far from the continental margin. Collectively, those observations are consistent with a north-dipping Devonian–Carboniferous subduction zone that alternately retreated and advanced to open and close a backarc basin behind a marginal island arc (Table 1) (Kroner et al., 2010). During the late Carboniferous to Permian the character of magmatism in southern

Mongolia changed from calc-alkaline to A-type to bimodal, presumably due to the cessation of subduction and the onset of transtensive tectonics (Hanzl et al., 2008; Blight et al., 2010; Yarmolyuk et al., 2008). However, Economos et al. (2012) argued that subduction-related magmatism continued into the early Permian in the South Gobi zone of southernmost Mongolia, which has been contentiously identified as either an allochthonous Precambrian microcontinent (Badarch et al., 2002; Kroner et al., 2010) or a Paleozoic accretionary complex (Taylor et al., 2013).

To the east, in northeast China (Inner Mongolia), the Devonian–Carboniferous Uliastai continental magmatic arc represents a continuation of the Nuhetdavaa zone of Mongolia (Fig. 3) (Xiao et al., 2003, 2009b). As in Mongolia, the late Paleozoic Baolidao island arc is located to the south of the continental arc, and the two are separated by the late Paleozoic Hegenshan backarc ophiolite-accretion complex of disputed age (Miao et al., 2008; Chen et al., 2009; Liu et al., 2013). To the south of the Baolidao arc is the Xilinhot metamorphic complex, which exhibits middle–late Devonian blueschists and has been interpreted to constitute a mid-to-late Paleozoic forearc accretionary complex (Chen et al., 2009; Xiao et al., 2009b; Liu et al., 2013). Interestingly, the high-grade metamorphic rocks of the Xilinhot complex, like those of the South Gobi zone, have led to controversial suggestions that it may represent a Precambrian microcontinent (Xiao et al., 2003).

The late Paleozoic tectonic history of southern Mongolia and northeast China are thus highly-similar, but many critical details of their evolution remain vague and contested. For example, the inception and duration of the marginal backarc(s) (Miao et al., 2008; Liu et al., 2013), or even its existence (Jian et al., 2012), are matters of continuing debate. Nonetheless, it is clear that the southern margin of Amuria was active in the Devonian and Carboniferous and that the locus of arc magmatism periodically migrated, either due to the opening and closing of one or more marginal backarc basins or to a change in the angle of subduction. Similarly critical, but also controversial, is the timing of collision between Amuria and North China along the Solonker (Sulinheer) suture zone (Fig. 3). Late Carboniferous–early Permian relics of subduction and accretion offer a lower age constraint on the timing of final basin closure, but an unambiguous upper age constraint is not provided until ~234 Ma, when the suture zone was stitched by the Halatu granites (Xiao et al., 2003; Chen et al., 2009). More equivocal ages on bimodal magmatism and metamorphism from the northern periphery of the suture zone have likewise been used to propose that collision broadly occurred in the late Carboniferous to Triassic (Blight et al., 2010; Zhang et al., 2011a; Li et al., 2013), but there is no strong consensus on finer constraints.

### 3.4. Kazakhstania

Kazakhstania is a complicated and highly-deformed terrane collage of microcontinents, island arcs and accretionary complexes which largely amalgamated prior to the Devonian (Windley et al., 2007). In the Devonian and Carboniferous that entire composite terrane was deformed in a crustal-scale process that transformed the previously-rectilinear feature into an orocline (Fig. 3) (Abrajevitch et al., 2008; Levashova et al., 2012). The geometry of the pre-Permian margins of Kazakhstania were profoundly modified during that event, thus complicating our margin-by-margin style of discussion; here we group the present-day central and east areas (the 'internal' margin of the deforming orocline) and the west and south areas (the 'external' margin of the orocline).

#### 3.4.1. 'Internal' (central and east) Kazakhstania

In East Kazakhstan, the strongly NW-concave structural trend of the orocline is delineated by an early–middle Devonian continental magmatic arc that exhibits a ~180° change in strike between the southwest and northeast arms of the belt. Paleomagnetic data indicate that belt was nearly linear in the early Devonian and that the northeast arm was subsequently rotated clockwise to its present position (with respect to the southwest arm) during the middle Devonian to late Carboniferous (Abrajevitch et al., 2008; Levashova et al., 2012). The presence of forearc accretionary complexes in the core of the present orocline (or outboard of the restored early–middle Devonian magmatic arc) indicates that subduction was dipping beneath Kazakhstania (Table 1) (Windley et al., 2007; Levashova et al., 2012; Wilhem et al., 2012). In the late Devonian the continental magmatic arc migrated eastward—partly overlapping the former (early–middle Devonian) forearc—where it remained active throughout the Carboniferous as the Balkhash-Yili arc (Fig. 3) (Windley et al., 2007; Levashova et al., 2012). Levashova et al. (2012) speculated that relocation of the magmatic arc could reflect a sudden jump of the subduction zone, which may have been forced to adopt a more ocean-ward position by the tightening of the orocline.

The Balkhash-Yili arc of east Kazakhstania may continue into West Junggar, where late Devonian to late Carboniferous magmatic arc rocks have been found to the northwest of the attendant Karamay arc-accretionary complex (Geng et al., 2011; Choulet et al., 2012b; Yang et al., 2012). Although a minor mid-to-late Paleozoic back-arc basin may have opened and closed behind the Karamay complex (as suggested by the Darbut ophiolitic mélange), it is generally agreed that the prevailing subduction zone was located outboard of that unit and that subduction was northwest-directed, beneath central West Junggar. Subduction beneath that margin probably ceased in the late Carboniferous, according to the appearance of regionally widespread latest Carboniferous to late Permian alkaline magmatism and the early Permian deposition of coarse terrestrial molasse and nonmarine volcanics (Choulet et al., 2012b; Xu et al., 2013). Along the opposing internal margin of the orocline, latest Carboniferous to Permian magmatism in the Yili arc was similarly characterized by post-collisional granitoids and nonmarine volcanics, and the youngest oceanic material incorporated into the neighboring accretionary complex to the north was mid-Carboniferous in age (~325 Ma) (Han et al., 2010). Additionally, a ~316 Ma stitching pluton crosscut the North Tian Shan suture zone between the Devonian–Carboniferous accretionary complex and the adjacent Junggar terrane to the north, thereby providing an upper age constraint on the closure of the intervening ocean basin then (Han et al., 2010).

A second late Devonian to Carboniferous magmatic belt in West Junggar has been identified in the Saur arc to the north and correlated with the coeval Zharma arc of east Kazakhstan (Fig. 3). Together, those magmatic belts are thought to be the products of a south-dipping subduction zone that helped to close the ocean basin between Kazakhstania and Siberia (Table 1) (Chen et al., 2010; Choulet et al., 2012a; Xu et al., 2013). Thus, the Zharma-Saur arc constituted part of the 'external' margin of Kazakhstania. As in the south, latest Carboniferous to Permian magmatism in the Zharma-Saur region was dominated by post-collisional A-type granitoids and bimodal volcanics, suggesting that subduction there had also ceased in the late Carboniferous (Chen et al., 2010). Accordingly, the Chara suture zone between Kazakhstania and the Siberian/Chinese Altai was stitched by a ~307 Ma pluton and locally sealed by early Permian molasse (Chen et al., 2010; Han et al., 2010). In the Permian, many of the regional suture zones acted as major strike-slip faults during an interval of protracted transcurrent tectonism (Choulet et al., 2012b; Levashova et al., 2012).

#### 3.4.2. 'External' (west and south) Kazakhstania

In the west, the Devonian margin of Kazakhstania runs parallel to the Urals, along the East Uralian suture zone in Russia and Kazakhstan (Fig. 3). To the south, the strike of that margin follows the arcuate shape of the orocline, curving through Uzbekistan and northern Tajikistan into an E–W orientation that continues into Kyrgyzstan and China; there the Devonian margin is demarcated by the boundary between the Kyrgyzstan Middle Tian Shan/Chinese Central Tian Shan and the Kyrgyzstan/Chinese South Tian Shan. At the dawn of the Devonian that entire margin is thought to have been active, from relics of a Silurian to early–middle Devonian continental magmatic arc identified in the Turgai belt of Kazakhstan (Bykadorov et al., 2003; Windley et al., 2007), the Kyrgyzstan North and Middle Tian Shan (Biske and Seltmann, 2010; Glorie et al., 2011b; Seltmann et al., 2011), and the Chinese Central Tian Shan (Fig. 3) (Gao et al., 2009; Dong et al., 2011b; Long et al., 2011; Ren et al., 2011; Ma et al., in press-b). In the middle to late Devonian, arc magmatism appears to have waned or ceased altogether across much of the western and southwestern margin. In Kazakhstan and Kyrgyzstan that magmatic hiatus has been associated with the establishment of a passive margin (Table 1) (Windley et al., 2007; Biske and Seltmann, 2010; Wilhem et al., 2012). In the early Carboniferous arc magmatism continued in the Chinese Central Tian Shan (having been largely uninterrupted in the late Devonian) and re-appeared in the Valerianovsky arc of Kazakhstan (Bea et al., 2002; Windley et al., 2007), but apparently did not resume in the Kyrgyzstan Tian Shan until the late Carboniferous (Biske and Seltmann, 2010; Seltmann et al., 2011). The late Carboniferous (~320 Ma) recommencement of subduction-related magmatism in Kyrgyzstan was short-lived, and broadly synchronous with the termination of arc magmatism in Kazakhstan and the Chinese Central Tian Shan.

The Kyrgyzstan/Chinese South Tian Shan is an accretionary zone that delineates the suture between Kazakhstania to the north and Tarim to the south (Fig. 3). Within it, remnants of the formerly intervening Turkestan Ocean have been recognized in ophiolitic mélanges that yield material of late Ordovician to early Carboniferous age, indicating that final basin closure post-dated the early Carboniferous (Han et al., 2011). Tighter constraints on the age of collision are provided by the timing of peak UHP metamorphism (~319 Ma) and the earliest occurrence of stitching plutons (~300 Ma) in the South Tian Shan, which together limit that event to the late Carboniferous (~319 to 300 Ma) (Table 1) (Han et al., 2011). Correspondingly, regional subduction-related magmatism in the Kyrgyzstan Middle Tian Shan and Chinese Central Tian Shan ceased in the mid- to late Carboniferous (as discussed above), and was succeeded by a latest Carboniferous to mid-Permian episode of widespread post-collisional magmatism which affected the entire Tian Shan as well as the northern margin of Tarim (Konopelko et al., 2007; Gao et al., 2009; Ren et al., 2011; Seltmann et al., 2011; Ma et al., in press-a). Following continental collision, the Tian Shan region was dominated by large-scale E–W transcurrent motion in the Permian, resulting in trans-crustal shear zones that may have controlled the emplacement of post-collisional plutons and accelerated regional post-orogenic exhumation (Laurent-Charvet et al., 2003; Konopelko et al., 2007; Glorie et al., 2011b; Seltmann et al., 2011).

### 3.5. North China and Tarim

#### 3.5.1. Northern North China

Our understanding of the late Paleozoic history of the northern margin of North China has been advancing rapidly, following the recognition that a belt of plutonic rocks exposed along the margin of the North China craton is Carboniferous to Permian in age, rather than Precambrian, as had been previously supposed (Zhang et al., 2007b, 2009a,b; Bai et al., 2013). Those subduction-related intrusive rocks, which have yielded ages of ~330 to 270 Ma, have been interpreted to represent a continental magmatic arc that developed above a southward-dipping subduction zone. Late Paleozoic arc-related volcanic rocks and volcanic detritus have also been documented across the northern margin of the North China craton (Cope et al., 2005; Zhang et al., 2007a). Cope et al. (2005) concluded from detrital zircon age distributions in Carboniferous–Permian strata that magmatic arc was active from ~400 to 275 Ma, although perhaps with an early Carboniferous hiatus (Table 1). Continental arc magmatism appears to have ceased in the mid-Permian, and was succeeded in the late Permian to mid-Triassic by a more spatially distributed phase of plutonism with a post-orogenic geochemical character (Zhang et al., 2009b). To the north of the late Paleozoic continental magmatic arc, the mid-Paleozoic margin of North China is delineated by the Ondor Sum subduction-accretion complex, which formed outboard of the early Paleozoic Bainaimiao arc (Fig. 4) (Xiao et al., 2003). Although the Ondor Sum complex had already been developing in the early Paleozoic, the occurrence of mid-to-late Permian metamorphic rocks and ophiolitic fragments reflect its continued development in the late Paleozoic (Miao et al., 2007; Xiao et al., 2009b). To the north of the Ondor Sum complex lies the diffuse collisional boundary between North China and Amuria, the Solonker (Sulinheer) suture (Xiao et al., 2003, 2009b). The timing of their collision is contentious, but may be late Permian–Triassic (Cope et al., 2005; Miao et al., 2007; Xiao et al., 2009b; Zhang et al., 2009b; Wilhem et al., 2012). However, following clear relics of Early Permian subduction, unequivocal evidence of basin closure has not been documented before ~234 Ma, when granites crosscut the suture (Chen et al., 2009).

#### 3.5.2. Beishan

Beishan, located between the Precambrian Dunhuang Block to the south and the peri-Siberian terranes of southern Mongolia to the north, is a collage of volcanic arcs, accretionary complexes, ophiolitic belts and, controversially, microcontinent blocks (Fig. 4). We begin our discussion by cautioning that the origins of the mafic-ultramafic belts in Beishan are contentious and their ophiolitic nature is not unequivocally demonstrated. Correlations between the various belts are likewise debated and here we simply adopt one prevailing interpretation. Of the numerous Paleozoic ocean basins inferred from the region, at least one, corresponding to the Hongliuhe-Xichangjing belt (Fig. 4), closed by the early Devonian according to the occurrence of cross-cutting and undeformed granitoids of that age (Zhang et al., 2011b). The closure of that basin may correspond to the poorly characterized late Silurian–early Devonian 'Beishan orogeny', which has been attributed to either an intraoceanic amalgamation of island arcs (Xiao et al., 2010) or to collision along the margin of the Dunhuang block (Wilhem et al., 2012). The Xingxingxia-Xiaohuangshan belt further to the north has previously been thought to represent another ocean basin that closed in the early to middle Paleozoic, but Zheng et al. (2013a) have reported early Carboniferous ages (~345–336) from basalts and gabbros of that unit. Carboniferous to Permian-age mafic-ultramafic rocks occur in the northernmost Hongshishan belt (Xiao et al., 2010; Song et al., 2013a) and the southernmost Liuyuan-Yin'aoxia belt (Mao et al., 2011; Zhang et al., 2011b). Ill-defined episodes of Devonian and Carboniferous arc-related magmatism reported from the variously-defined Mazongshan and Hanshan units (between the Hongliuhe-Xichangjing and Hongshishan belts; Fig. 4) have been related to subduction of one or more of those inferred ocean basins, but corresponding reconstructions vary considerably (e.g. Xiao et al., 2010; Wilhem et al., 2012; Zhang et al., 2012a; Zheng et al., 2013a). Complex, multi-phase deformation chronicled the progressive consolidation of the Beishan orogenic

collage, but final collision between the Dunhuang block and southern Amuria is constrained in central Beishan to have occurred between ~273 and 227 Ma (Tian et al., 2013). Post-orogenic plutonism appeared in Beishan in the middle and late Triassic (Li et al., 2012a).

We proceed here with a simplistic interpretation that draws reference from the neighboring regions. Following the interpretation of an early Paleozoic closure of the Hongliuhe-Xichangjing basin, we assume that the Beishan orogeny was the result of a collision between the Dunhuang block and the Mazongshan-Hanshan unit by the earliest Devonian. The constituents of the Mazonghsan-Hanshan unit have traditionally been considered microcontinents of Tarim or Kazakhstania affinity, but that association is challenged by geochronological and geochemical data (Song et al., 2013a,b), and they may rather be an agglomeration of island arcs. To the north of the Mazongshan-Hanshan unit, the Hongshishan basin was existent prior to the Devonian and remained open until at least the late Permian. Consumption of the Honshishan basin was achieved by south-dipping subduction beneath the Mazongshan-Hanshan unit, giving rise to the widespread late Paleozoic magmatic arc rocks there. Carboniferous mafic-ultramafic rocks in the Xingxingxia-Xiaohuangshan belt may signify the opening and closing of a minor backarc basin within the Mazonshan-Hanshan unit then. Similarly, Permian mafic-ultramafic rocks in the Liuyuan-Yin'aoxia belt and Permian rift-related sedimentation in the northern Dunhuang block (Li et al., 2012a) and Mazongshan unit (Tian et al., 2013) may reflect the evolution of a successor backarc basin. To the east, the Xingxingxia-Xiaohuangshan and Liuyuan-Yin'aoxia belts may continue as the Devonian to Carboniferous Engger Us and late Carboniferous to Permian Quaganchulu ophiolitic belts respectively (Feng et al., 2013; Zheng et al., 2013b).

Even assuming that the various mafic-ultramafic belts of Beishan are ophiolites, it is important to note that the true location of the 'principal' Paleoasian Ocean basin between the Dunhuang block and Amuria is not well-established, despite being critical for an accurate reconstruction of that region. We have adopted the Hongshishan belt as the marker of the former Paleoasian Ocean, but if, for example, the Liuyuan-Yin'aoxia belt represents the true boundary, the Mazongshan-Hanshan unit would have been on the far side of the main ocean from the Dunhuang block. In such a case the Mazongshan-Hanshan unit could be correlative with the Baolidao arc of southern Amuria. As another alternative, Xiao et al. (2010) considered the Mazongshan-Hanshan unit to be an amalgamation of intraoceanic island arcs that bisected the Paleoasian Ocean and thus remained independent of both the Dunhuang block and Amuria until the Permian. Still others would place the main ocean between the Mazongshan-Hanshan arcs (Zheng et al., 2013a,b). Obviously, additional work is urgently needed there to improve our understanding of that complicated region, and our present interpretation must be considered provisional.

### 3.5.3. Northern Tarim

In the northwest Tarim basin, thick Neoproterozoic to Permian sedimentary sequences of marine platform carbonates and terrestrial siliciclastic rocks have conventionally been interpreted to reflect a long-lasting passive margin along the north Tarim craton then (Table 1) (Carroll et al., 2001; Bradley, 2008). A major angular unconformity divides the late Paleozoic sedimentary sequence, separating gently folded Silurian and Devonian strata from a deepening-upward Carboniferous sequence, which is in turn sharply overlain by early Permian coarsening-upward nonmarine rocks and intercalated basaltic lavas (Carroll et al., 2001; Xiao et al., 2013). Notable changes in sedimentary provenance and transport accompanied the transition in depositional environment during the early Permian, reflecting an influx of volcanic-derived material from the northwest, probably from a then newly-emergent Tian Shan region (Carroll et al., 2001; Xiao et al., 2013). In the context of a passive margin approaching a subduction zone, those features have been attributed to the development of a flexural forebulge followed by foreland basin sedimentation (Carroll et al., 2001; Han et al., 2011). Thus, the conventional late Paleozoic model supposes that the northern passive margin of Tarim was destroyed by its collision with Kazakhstania, driven by north-dipping subduction beneath the South Tian Shan (Table 1). That is supported by the presence of a Devonian to late Carboniferous magmatic arc in the Central Tian Shan to the north, which ceased at ~320 Ma (Section 3.4.2). Correspondingly, eclogite-facies metamorphism occurred in the South Tian Shan suture zone from ~345 to 320 Ma, and the younger dates have been interpreted to represent the age of peak HP metamorphism (Gao et al., 2011; Han et al., 2011) Exhumation and retrograde metamorphism of those HP metamorphic rocks followed in the latest Carboniferous–early Permian, and locally they were intruded by early Permian dikes and unconformably overlain by Permian molasse (Gao et al., 2011; Glorie et al., 2011b; Han et al., 2011). Early Permian plutons—which are generally undeformed and intrusive to late Paleozoic thrusts and ophiolitic mélanges of the suture zone—invaded a wide region in both the greater Tian Shan and the northern margin of Tarim (Han et al., 2011). Together with an early- to mid-Carboniferous age for the youngest ophiolitic rocks in the South Tian Shan suture zone, that suggests that the passive margin of Tarim collided with the South Tian Shan in the late Carboniferous–earliest Permian (Gao et al., 2011; Han et al., 2011).

Alternative interpretations of the late Paleozoic history of northern Tarim remain controversial. Arguments for south-dipping subduction beneath northern Tarim have been made according to observations of structural vergence in the South Tian Shan (Charvet et al., 2011; Wang et al., 2011) and inferred arc-related Devonian plutonism in northern Tarim (Ge et al., 2012). However, the evidence for a late Paleozoic arc in northern Tarim is spatiotemporally restricted, and the significance of the structural observations and their relationship to the regional subduction polarity are debated (Xiao et al., 2009b, 2013). The timing of collision between Tarim and Kazakhstania is also contested; for example, a late Permian to Triassic event has been asserted, in part, on the basis of disputed late Permian radiolaria and Permian–Triassic HP metamorphic rocks in the South Tian Shan suture zone (Xiao et al., 2009a,b, 2013; Gao et al., 2011; Han et al., 2011).

### 3.5.4. Southern Tarim and Qaidam (Kunlun orogen)

The Kunlun belt, which fringes the southern margins of Tarim and Qaidam (but is offset by the Altyn Tagh fault into the West and East Kunlun; Fig. 4), is a composite orogen that was built along an active margin in the early and late Paleozoic. Most tectonic models agree that there was an Ordovician to early Devonian collision between Tarim and some Precambrian constituent of the Kunlun belt ('South Kunlun'), leaving them juxtaposed along the Oytag-Kudi ophiolitie-bearing suture zone (Mattern and Schneider, 2000; Xiao et al., 2005; Jia et al., 2013). That is broadly consistent with the occurrence of Silurian to mid-Devonian deformation and metamorphism and subsequent post-orogenic magmatism in the Kunlun belt, and with the deposition of late Devonian molasse above a regional mid-Paleozoic unconformity (Mattern and Schneider, 2000; Cowgill et al., 2003; Xiao et al., 2005; Ye et al., 2008). In the Carboniferous to early Mesozoic, a southward-growing accretionary complex developed along the southern margin of the Kunlun belt, reflecting the operation of a north-dipping subduction system (Xiao et al., 2005, 2002). The timing of corresponding late Paleozoic arc magmatism in the Kunlun belt is very poorly resolved, but may have spanned the late Paleozoic to early Mesozoic (Schwab et al., 2004; Xiao et al., 2005). Detrital zircon age-distributions suggest there

was a magmatic lull in the late Devonian to early Permian (~380–280 Ma) (Cowgill et al., 2003; Ding et al., 2013), although sparse plutonic and volcanic rocks of that age have been reported along the margin from the northern Pamir to the eastern Kunlun (Schwab et al., 2004; Xiao et al., 2005; Jiang et al., 2013). In the mid-Permian to early Mesozoic, arc magmatism was more clearly established along the Kunlun belt: in the Sailiyak arc of the West Kunlun and the north Kunlun batholith of the East Kunlun (Xiao et al., 2002, 2005; Schwab et al., 2004). Thus, following the mid-Paleozoic collision of the 'South Kunlun', the southern margin of Tarim may have remained active above a north-dipping subduction zone throughout the late Paleozoic (Table 1).

#### 3.5.5. Southern North China (Qilian and Qinling-Dabie orogen)

Between the Alashan block (here considered coherent with the North China craton from the mid-Paleozoic) and the northern Qaidam block lies the Qilian orogen, which has been treated in various ways, but is usually subdivided into a North Qilian arc-accretionary belt, a Central/South Qilian block and a North Qaidam UHP metamorphic belt (Fig. 4) (Song et al., 2013c). Early Paleozoic subduction resulting in a Silurian collision along the North Qilian belt is evident by the occurrence of Cambrian to late Ordovician ophiolites, ~500–440 Ma arc volcanic rocks, ~454–446 Ma HP metamorphic rocks, and Silurian flysch and post-orogenic Devonian molasse (Wang et al., 2005; Song et al., 2013c). To the south, collision along the North Qaidam belt may have been slightly younger, as UHP metamorphism associated with northward-directed continental subduction of the Qaidam block is dated to ~430–420 Ma (Xiao et al., 2009a; Song et al., 2013c). Thus, the Qilian orogen may have been fully assembled by the latest Silurian. Alternatively, due to continued granitoid magmatism through the Devonian in the Qilian block and North Qilian belt, Xiao et al. (2009a) proposed that southward subduction beneath the Qilian block had endured until the late Devonian, and ended with the collision of the Qilian and Alashan blocks. We note, however, that the tectonic environment of those granitoids remains to be established; Song et al. (2013c) have speculatively treated them as syn- to post-orogenic.

To the southeast, along the southern margin of the North China craton, the composite Qinling-Dabie orogen may be broadly correlative with both the Qilian and Kunlun orogens (Fig. 4). As in the Kunlun, the Qinling orogen experienced subduction-accretion and collisional events throughout the Paleozoic and into the early Mesozoic. In the early Paleozoic, the Kuanping, Erlangping and North Qinling units of the Qinling orogen are thought to have amalgamated together with the North China craton, resulting in several episodes of high-grade metamorphism and magmatism then (Ratschbacher et al., 2003; Dong et al., 2011a; Wu and Zheng, 2013). Consolidation of those units may have continued into the late Silurian–early Devonian, according to the persistence of high-grade metamorphism and magmatism until ~420–400 Ma. However, the regional mid-Paleozoic subduction-related magmatic rocks may be composite in origin, since they have also been attributed to north-dipping subduction of a southern ocean basin beneath the North Qinling unit (Ratschbacher et al., 2003; Dong et al., 2011a). Ophiolitic remnants of that ocean basin in the Shangdan fault delineate a first-order boundary in the Qinling orogen, separating the North and South Qinling units. Notably, early Paleozoic to early Devonian magmatic arc rocks appear near-exclusively north of that suture, thus supporting a north-dipping polarity of subduction (Ratschbacher et al., 2003; Wang et al., 2013b).

The closure timing of that 'Shangdan' Ocean remains a subject of debate, largely hinging on differing interpretations of the middle Devonian–early Carboniferous Liuling Group clastic rocks which lie along the boundary between the North and South Qinling units. Provenance studies have indicated that the sediments of that sequence were sourced from both the North and South Qinling (Wu and Zheng, 2013), which, together with the cessation of regional metamorphism and magmatism at ~400 Ma and contemporaneous transpressive wrenching of the units north of the suture (Ratschbacher et al., 2003; Liu et al., 2012b), could signify that the intervening ocean closed in the early Devonian (Dong et al., 2011a). In contrast, the Liuling Group has also been interpreted as a composite unit, in which a northern forearc-accretionary complex that was deposited along the active margin of the North Qinling was juxtaposed with sediments derived from the South Qinling during closure of the basin that separated them (Ratschbacher et al., 2003; Yan et al., 2012). That interpretation, in conjunction with possibly late Devonian plutonic rocks in the North Qinling (Yan et al., 2012; Wang et al., 2013b) and late Carboniferous HP metamorphism in the Huwan shear zone (Peters et al., 2013; Wu and Zheng, 2013), alternatively implies a post-Devonian collision.

An understanding of the tectonic evolution of that margin is further complicated by the identification of a second ophiolitic belt in the Mianlue area, which has been proposed to represent a suture between the South Qinling and the South China craton (Dong et al., 2011a). Because those two blocks exhibit strong early Paleozoic lithostratigraphic similarities, it is probable that any late Paleozoic ocean that appeared between them had originally opened by their separation. A mid-Paleozoic rifting event could explain an episode of rapid sedimentation and coincident mafic to ultramafic magmatism that occurred in the South Qinling in the Silurian to early Devonian, and would accord with the oldest rocks identified in the Mianlue ophiolite, which are upper Devonian to Carboniferous radiolarian cherts (Dong et al., 2011a; Wu and Zheng, 2013).

The basin(s) between North and South China must have closed by the time those two continental blocks collided in the Triassic. A wealth of research on the HP/UHP metamorphic rocks of the Dabie orogen (Fig. 4) has established that South China occupied the lower plate during that collision, indicating that the preceding destruction of the intervening basin (at least shortly before collision) was accomplished by north-dipping subduction (Hacker et al., 2006). However, the time at which that subduction initiated is unclear. If the Shangdan Ocean basin had remained open until the Triassic collision, subduction beneath the North Qinling unit may have been continuous from the early Devonian, punctuated by Carboniferous HP metamorphism (Ratschbacher et al., 2003; Liu et al., 2011). In that case the basin represented by the Mianlue belt could have been minor. Alternatively, if the Shangdan Ocean closed in the early Devonian, subduction would have ceased beneath the North Qinling unit and later initiated south of the South Qinling unit at some time prior to the Triassic collision, perhaps coincident with late Carboniferous HP metamorphism in the Huwan shear zone (Dong et al., 2011a). Yet another possibility—and the one that we tentatively adopt—is that north-dipping subduction of the Shangdan Ocean ended with a mid-to-late Carboniferous collision between North China and the South Qinling unit, whereupon subduction jumped to the southern (previously passive) margin of the latter (Table 1) (Wu and Zheng, 2013). Magmatism in the southern Qinling orogen was virtually absent in the late Paleozoic, but Ratschbacher et al. (2003) have suggested that a manifestation of mid-Carboniferous to early Permian subduction-related magmatism may be located further inboard, in a NE-trending belt of andesitic volcanics in the eastern North China craton.

### 3.6. South China and Japan

#### 3.6.1. Northwestern South China (Longmen Shan and Qinling-Dabie orogens)

In the late Neoproterozoic to Ordovician the basement of the western Sichuan Basin was host to the deposition of shallow-

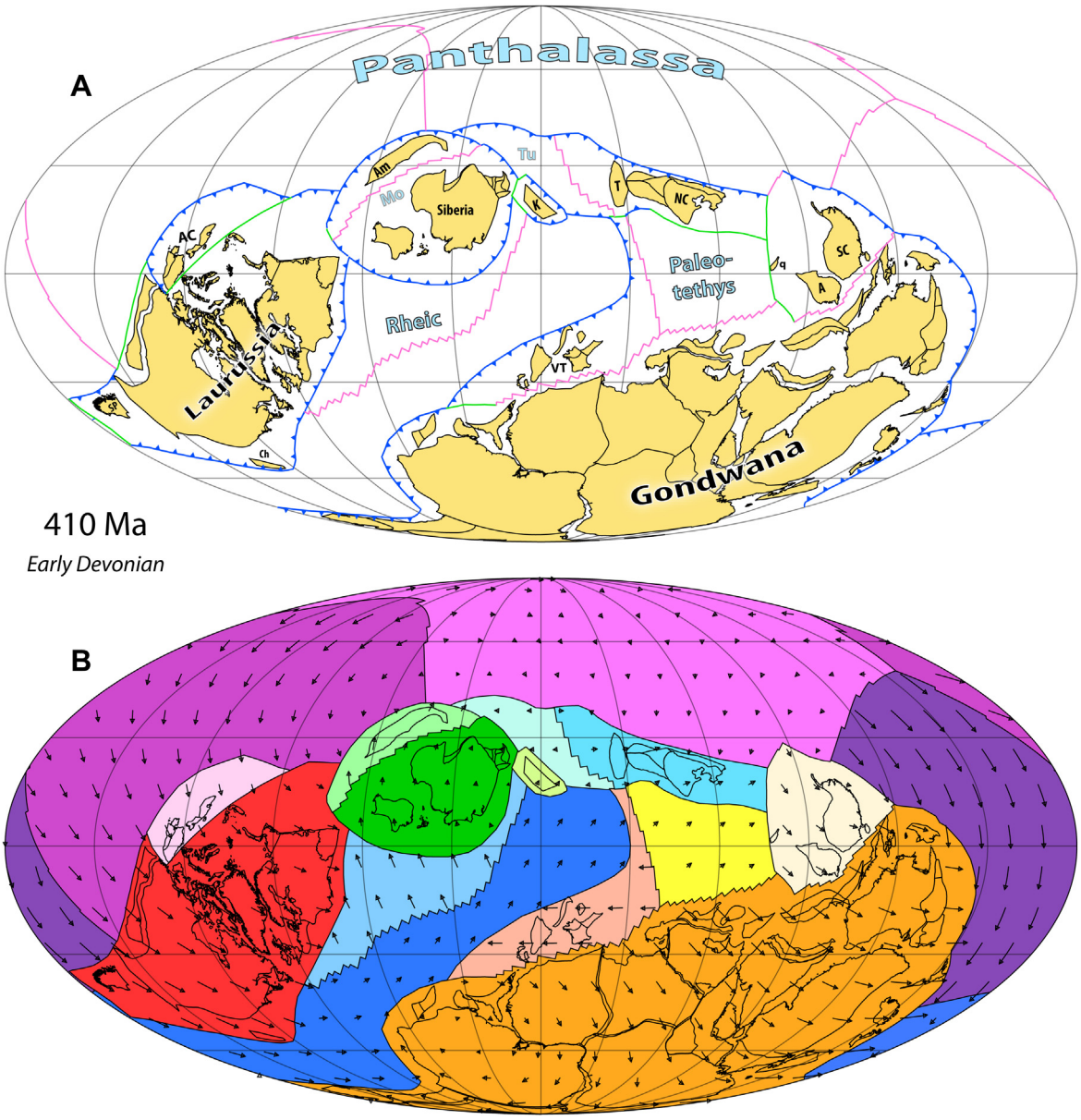


**Figure 5.** (A) 410 Ma (early Devonian) paleogeographic reconstruction showing simplified plate boundaries and labels of some major features. *Abbreviated continental units*: A, Annamia; AC, Arctic Alaska-Chukotka; Am, Amuria; Ch, Chilenia; K, Kazakhstania; NC, North China; q, South Qinling; SC, South China; SP, South Patagonia; T, Tarim; VT, Variscan terranes; *oceanic domains*: Mo, Mongol-Okhotsk Ocean; Tu, Turkestan Ocean. (B) Plate velocity field.

marine carbonate and siliciclastic rocks, reflecting the passivity of the northwest margin of South China during that interval (Bradley, 2008). In contrast, Silurian and Devonian rocks are missing from most of the western Sichuan Basin, but are preserved as a thick clastic sequence along its northwestern Longmen Shan margin (Burchfiel et al., 1995; Jia et al., 2006). That westward-thickening deposition, together with seismically-imaged mid-to-late Paleozoic extensional grabens in the western Sichuan Basin, argues for a Silurian–Devonian episode of rifting along the Longmen Shan margin (Jia et al., 2006). That timing is broadly coincident with the onset of rapid sedimentation and concurrent mafic to ultramafic magmatism in the South Qinling (Wu and Zheng, 2013), and may reflect a continuous rifting event along the entire northwestern margin of South China then. A passive margin was reestablished in the Carboniferous to Permian and remained until South China collided with North China in the Triassic.

### 3.6.2. Southern South China

In southeastern South China the Devonian opened to the waning stages of the late Ordovician–Silurian Kwangsian (or Wuyi-Yunkai) orogeny, which was associated with intra-continental closure of the failed Precambrian Nanhua rift between the Yangtze and Cathyasia blocks (Li et al., 2010; Wang et al., 2013a,c). That event caused regional deformation and widespread magmatism between ~460 and 420 Ma and left a broad Silurian–Devonian unconformity. In the Devonian, southeastern South China was affected by an episode of regional transtension, which first manifested in the early Devonian with the appearance of major NE–SW trending strike-slip faults and intervening NW–SE oriented extensional basins that locally hosted submarine volcanism (Xun et al., 1996; Chen et al., 2001). That episode probably denoted the rifting of South China from northeast Gondwana—frequently conjectured to have been conjugate margins in the mid-Paleozoic—where an analogous Devonian episode of

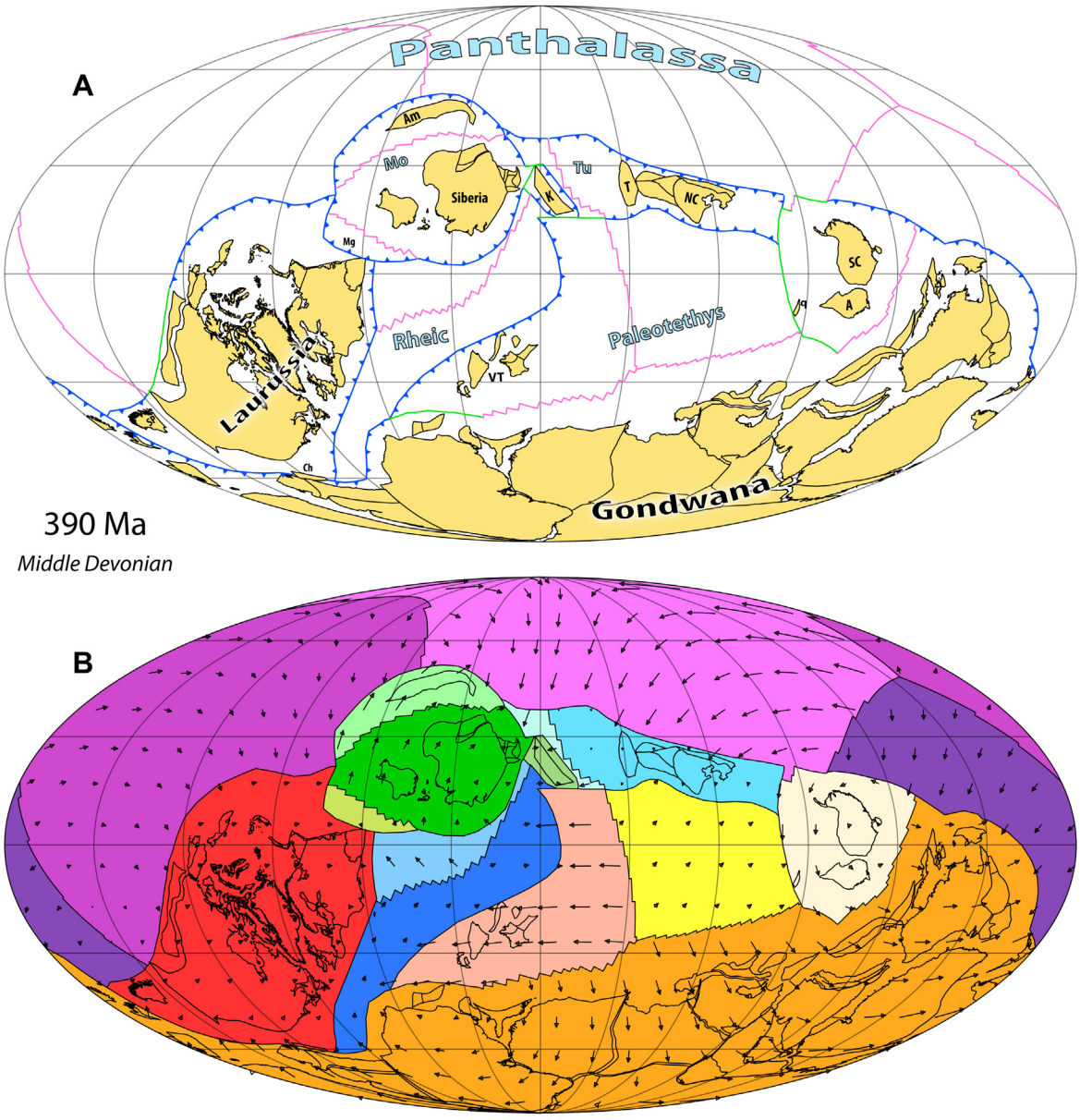


**Figure 6.** (A) 390 Ma (middle Devonian) paleogeographic reconstruction showing simplified plate boundaries and labels of some major features. *Abbreviated continental units*: A, Annamia; Am, Amuria; Ch, Chilenia; K, Kazakhstania; Mg, Magnitogorsk arc; NC, North China; q, South Qinling; SC, South China; SP, South Patagonia; T, Tarim; VT, Variscan terranes; *oceanic domains*: Mo, Mongol-Okhotsk Ocean; Tu, Turkestan Ocean. (B) Plate velocity field.

transtension-extension has been recognized (Shen et al., 2008). Subsequent to Devonian extension, shallow to deep marine sedimentation persisted in southeastern South China until the Permian (Table 1) (Wang et al., 2013c). Middle to late Permian arc-related magmatism in Hainan Island (Li et al., 2006) and Mindoro Island (Knittel et al., 2010) (Fig. 4), and the discovery of late Paleozoic detrital zircons in Permian sedimentary rocks from Cathyasia (Hu et al., 2012; Li et al., 2012b), may indicate that the margin of southeastern South China was active in the Permian. However, Cai and Zhang (2009) have interpreted the Hainan Island igneous rocks as products of subduction directed beneath Annamia (see Section 3.7.1), and Wang et al. (2013c) cautioned that the detrital zircons alone do not provide unambiguous evidence of a magmatic arc.

In southwestern South China a late Devonian to Permian passive margin sequence with intercalated mafic volcanics occurs above a middle Devonian basal conglomerate lying unconformably on lower Paleozoic flysch-type sediments (Cai and Zhang, 2009; Jian et al., 2009a). That sequence has been interpreted to reflect a Devonian rifted margin, but its conjugate margin was inferred to lie along Simao, where a similar middle Devonian basal conglomerate overlies early Paleozoic sediments (Table 1).

### 3.6.3. Japan

The Japanese islands are now recognized as a complex of subhorizontal nappes stacked with a general downward/oceanward-younging polarity that reflects a long history of convergence and growth along an active margin. In southwest Japan, specific intervals of active convergence/orogenesis in the mid-to-late Paleozoic have been recognized in the accretionary complexes and HP metamorphic belts of the Silurian–Devonian Oeyama and Kurosegawa belts, the Carboniferous–Permian Nedamo and Renge belts and the Permian–Triassic Akiyoshi, Maizuru, Suo, and Ultra-

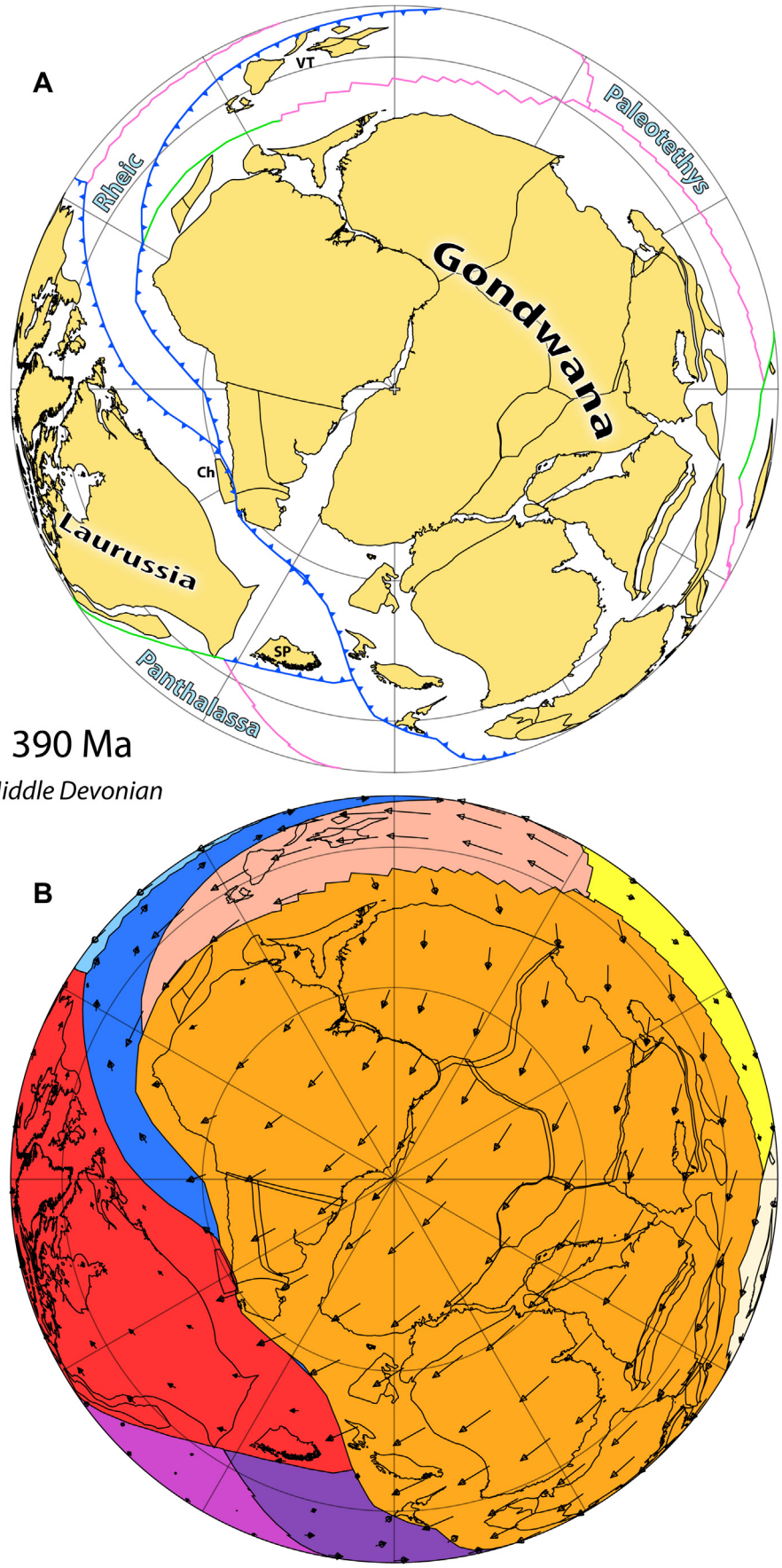
A
VT
Paleotethys
Rheic
Gondwana
Ch
Laurussia
SP
Panthalassa
390 Ma
Middle Devonian
B

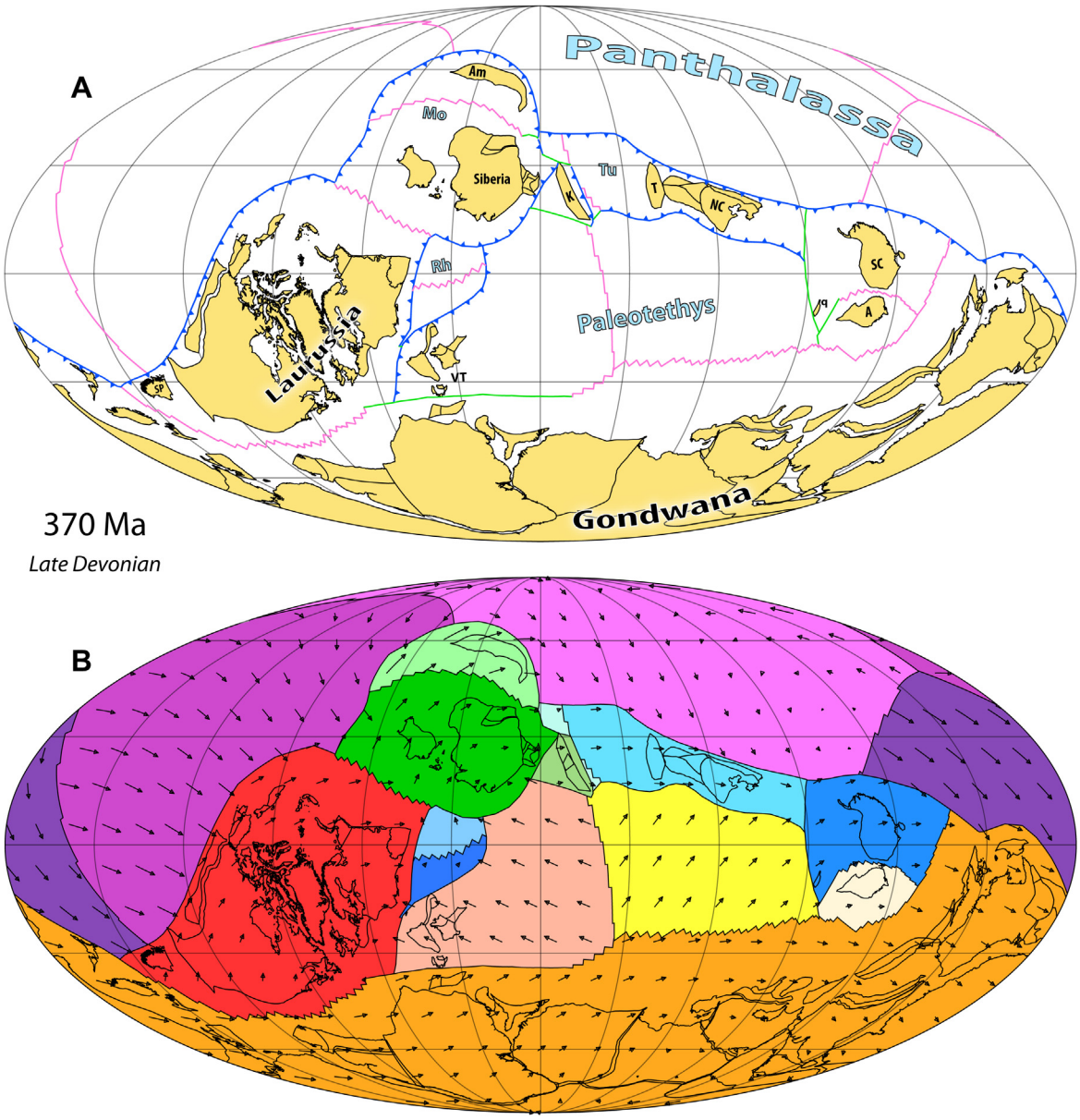


**Figure 8.** (A) 370 Ma (late Devonian) paleogeographic reconstruction showing simplified plate boundaries and labels of some major features. *Abbreviated continental units*: A, Annamia; Am, Amuria; K, Kazakhstania; NC, North China; q, South Qinling; SC, South China; SP, South Patagonia; T, Tarim; VT, Variscan terranes; *oceanic domains*: Mo, Mongol-Okhotsk Ocean; Rh, Rheic Ocean; Tu, Turkestan Ocean. (B) Plate velocity field.

Tamba belts (Oh, 2006; Isozaki et al., 2010; Wakita, 2013). Attendant magmatic activity was recorded in the Hida belt to the northwest, where Silurian–Devonian, mid-to-late Carboniferous, and mid-to-late Permian igneous rocks have been inferred to represent products of a continental margin arc (Fig. 4) (Oh, 2006; Wakita, 2013). Tectonic erosion along the long-active margin of Japan was likely substantial and the true extent of Paleozoic accretionary/collisional orogenesis and arc-related magmatism may be greatly underrepresented by the documented remnants (Isozaki et al., 2010; Charvet, 2013). Thus, the margin may have been continuously active from the early Paleozoic, with the aforementioned units representing peak episodes of orogenesis and/or exceptional preservation (Table 1). The Paleozoic affinity of Japan is uncertain and has been assigned both to eastern North China and eastern South China; however, we believe the physiographical, paleontological and geochemical arguments make a stronger case for its proximity to South China (Isozaki et al., 2010; Jahn, 2010).

### 3.7. *Annamia (Indochina + Simao)*

#### 3.7.1. *Northeast margin*

Although debated, the Song Ma and Ailaoshan sutures have usually been accepted as the principal tectonic boundary separating Annamia from South China to the north (Fig. 4). Within the Song Ma suture zone, greenschist- to lower amphibolite-facies residual mantle peridotites and mafic rocks with MORB-type

**Figure 7.** (A) 390 Ma (middle Devonian) paleogeographic reconstruction as in Fig. 6, but shown in an orthogonal projection centered on the South Pole. Abbreviations as in Fig. 6. (B) Plate velocity field.

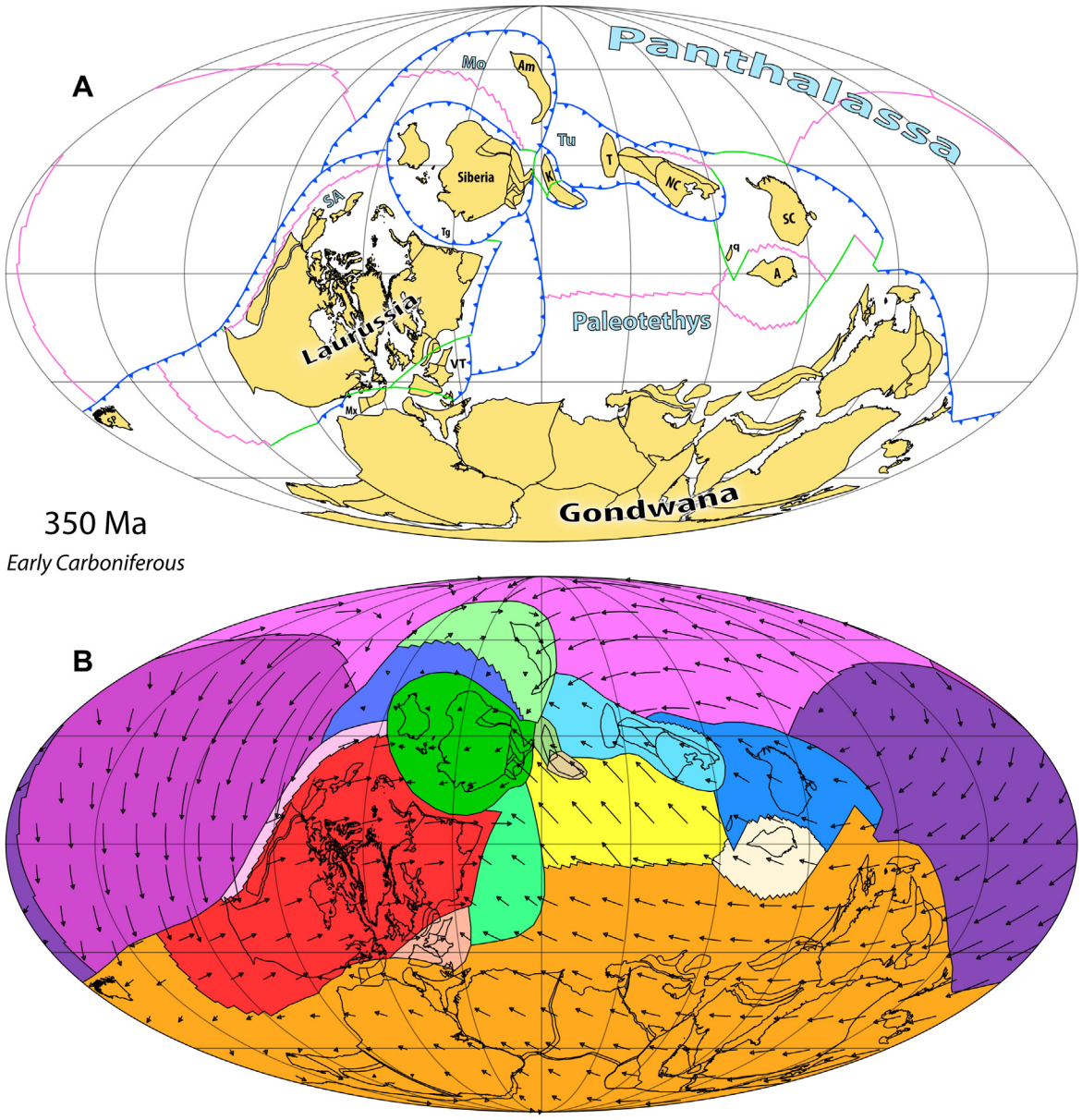


**Figure 9.** (A) 350 Ma (early Carboniferous) paleogeographic reconstruction showing simplified plate boundaries and labels of some major features. *Abbreviated continental units*: A, Annamia; Am, Amuria; K, Kazakhstania; Mx, Mixteca-Oaxacan; NC, North China; q, South Qinling; SC, South China; SP, South Patagonia; T, Tarim; Tg, Tagil arc; VT, Variscan terranes; *oceanic domains*: Mo, Mongol-Okhotsk Ocean; SA, Slide Mountain-Angayucham Ocean; Tu, Turkestan Ocean. (B) Plate velocity field.

geochemical affinities have been recognized as an ophiolitic suite (Zhang et al., 2013a). The mafic rocks from that suite have yielded middle Devonian to late Carboniferous ages (387–313 Ma)—inferred to date the timing of crystallization—and late Permian to early/middle Triassic metamorphic ages (265–240 Ma) (Van Vuong et al., 2012). Jian et al. (2009a, b) reported middle–late Devonian ages (~387–374 Ma) from the Ailaoshan ophiolite. Northeast of the Song Ma ophiolite suite, in the Nam Co antiform (Fig. 4), HP metamorphic rocks yielded middle Triassic ages which are thought to reflect the timing of peak metamorphism (Nakano et al., 2010; Zhang et al., 2013a). Together, those observations suggest that Annamia and South China collided along the Song Ma-Ailaoshan suture in the late Permian–early Triassic. From the structure and kinematic indicators of metamorphic rocks along that suture and in shear zones in the Truong Son metamorphic belt to the south, it has been inferred that collision was oblique, with a strong component of right-lateral translation (Lepvrier et al., 2008; Van Vuong et al., 2012). However, the polarity of preceding subduction along that boundary is more equivocal and both northeast-dipping (beneath South China) and southwest-dipping (beneath Annamia) models have been proposed. To the southwest of the Song Ma suture, the NW–SE trending, Truong Son granitoids and Song Ca volcanics have been recognized as a Permian to Triassic magmatic arc lying along the northern margin of the Truong Son metamorphic belt (Liu et al., 2012a). The early Permian to middle Triassic magmatic rocks (~280–245 Ma) have a subduction-related geochemical affinity, whereas the geochemistry of the middle to late Triassic rocks has been inferred to reflect post-collisional extension (Liu et al., 2012a). Equivalently, middle Permian subduction-related volcanism has been recognized to the southwest of the Ailaoshan ophiolite in the Yaxianqiao arc (Jian et al., 2009a, b). Permian to Triassic volcanism has also been recognized in the Song Da belt to the northeast of the

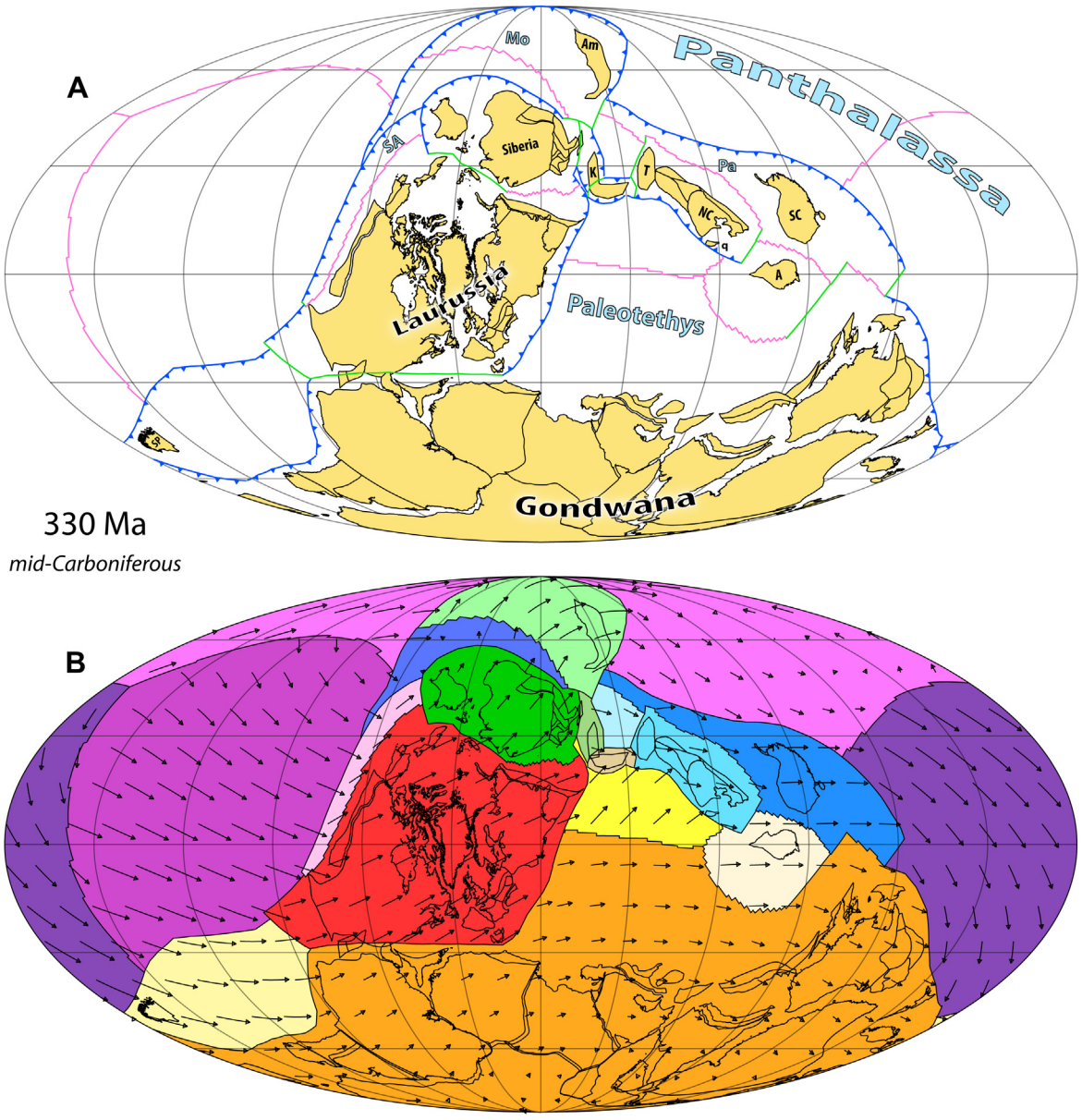


**Figure 10.** (A) 330 Ma (mid-Carboniferous) paleogeographic reconstruction showing simplified plate boundaries and labels of some major features. *Abbreviated continental units*: A, Annamia; Am, Amuria; K, Kazakhstania; NC, North China; q, South Qinling; SC, South China; SP, South Patagonia; T, Tarim; *oceanic domains*: Mo, Mongol-Okhotsk Ocean; SA, Slide Mountain-Angayucham Ocean; Pa, Paleoasian Ocean. (B) Plate velocity field.

Song Ma suture, where a Permian–Triassic volcano-sedimentary sequence exhibits mafic to ultramafic early Permian to early Triassic volcanics and middle to late Triassic felsic volcanics (Liu et al., 2012a). There, early Permian to early Triassic volcanism was associated with rifting rather than subduction, but that rifting has been ascribed to back-arc extension due to north-directed subduction (Lepvrier et al., 2008). Cai and Zhang (2009) proposed that the Dian-Qiong suture to the north of the Song Da belt is a structural duplication of the Song Ma-Ailaoshan suture that developed by sinistral strike-slip in Cenozoic time (Fig. 4), which would allow southwest-dipping subduction to account for both the Truong Son arc magmatism and marginal rifting along the Song Da belt. Along the Dian-Qiong suture Cai and Zhang (2009) reported Carboniferous (and presumed Devonian to early Permian) ophiolitic material with MORB-type and OIB-type geochemical affinities, late Permian (~261 Ma) mafic and minor felsic island arc volcanics, and late Devonian to early Permian deep-water siliceous rocks with radiolarians of Paleotethyan affinity. Late Permian continental arc granitoids are also documented in Hainan Island south of the Dian-Qiong suture (Li et al., 2006). In the Nanpanjiang basin to the north of the Dian-Qiong suture, middle Devonian to Permian carbonate platform to deep marine sedimentary rocks have been attributed to the establishment of a passive margin on the southern margin of South China, which was interrupted by the deposition of late Permian terrestrial molasse and S-type granites (Cai and Zhang, 2009).

### 3.7.2. West margin

The western boundary of Annamia is juxtaposed with Sibumasu along the Changning-Menglian (and correlative Inthanon) suture zone (Fig. 4). The suture zone contains ophiolitic mélange, Devonian to late Permian mafic volcanics and associated shallow

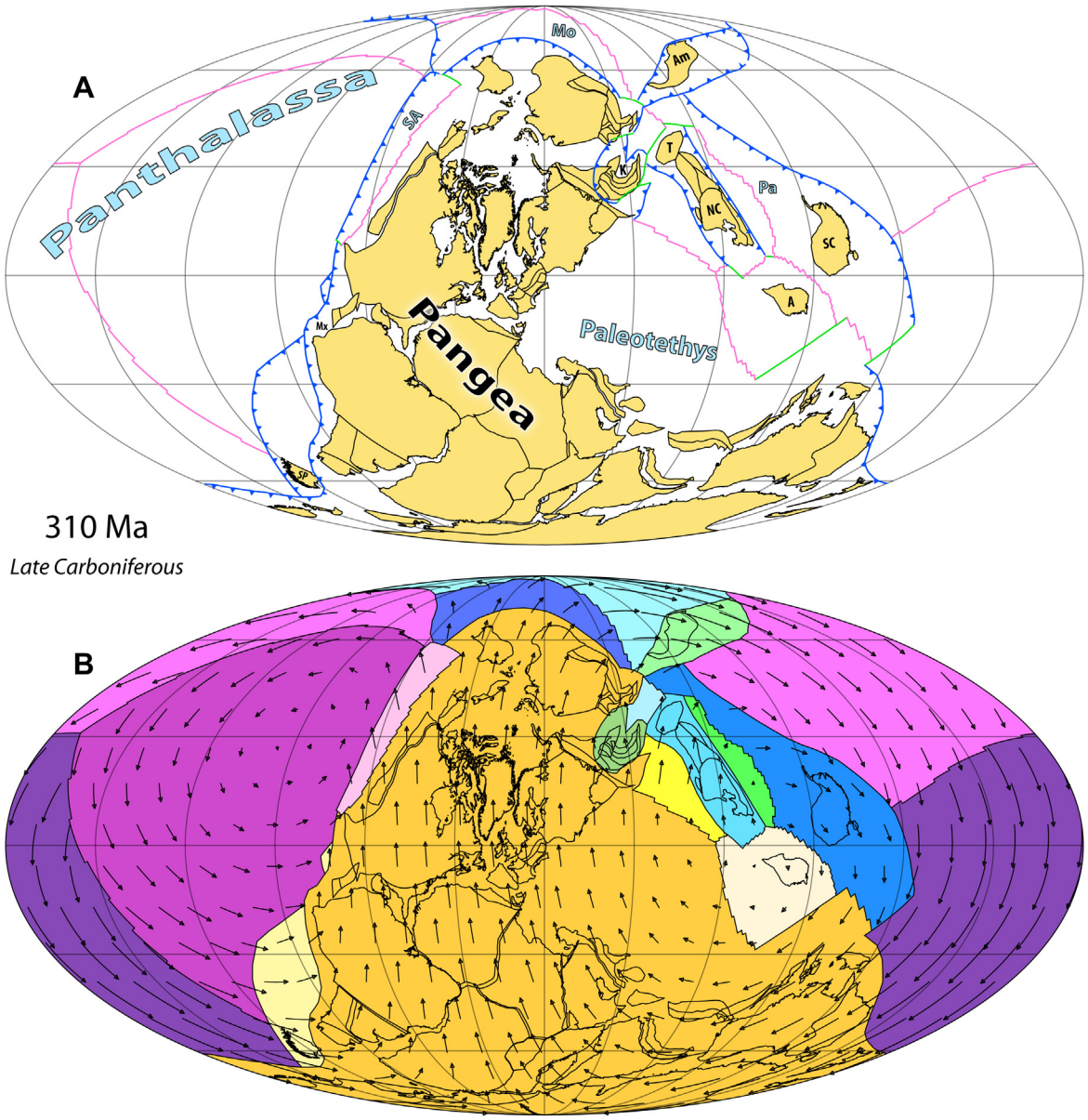


**Figure 11.** (A) 310 Ma (late Carboniferous) paleogeographic reconstruction showing simplified plate boundaries and labels of some major features. *Abbreviated continental units*: A, Annamia; Am, Amuria; K, Kazakhstania; Mx, Mixteca-Oaxacan; NC, North China; SC, South China; SP, South Patagonia; T, Tarim; *oceanic domains*: Mo, Mongol-Okhotsk Ocean; SA, Slide Mountain-Angayucham Ocean; Pa, Paleoasian Ocean. (B) Plate velocity field.

marine carbonates, and radiolarian-bearing deep marine sedimentary rocks of middle Devonian to middle Triassic age. Ophiolitic rocks are also found in the parallel Nan-Sra Kaeo suture zone to the east, but are thought to represent a marginal back-arc basin restricted to the latest Carboniferous–late Permian (Sone and Metcalfe, 2008; Ridd et al., 2011). Between those parallel suture zones, in the Sukhothai terrane, Permian–Triassic paired metamorphic belts and magmatic arc rocks have been interpreted to reflect the operation of an east-dipping subduction system beneath it (Table 1). The oldest dated magmatic arc rocks are late early Permian (~280 Ma), but if east-dipping subduction gave rise to the Nan-Sra Kaeo back-arc basin, subduction possibly started earlier, in the latest Carboniferous (Sone and Metcalfe, 2008; Ridd et al., 2011). North of the 25th parallel, the 311–277 Ma Gicha complex may be correlative with the Nan-Sra Kaeo back-arc basin, whereas the Permian Tuoba-Nanzuo arc may be a continuation of the Sukhothai arc (Jian et al., 2009a, b).

## 4. Plate model

In the following we present and discuss our plate model, drawing both from our compiled geological observations and from the paleogeographic data used to construct the continental rotation model. Because it is helpful to use both reference systems in our presentation, we use *italics* for model-based directions to distinguish them from present-day directions (in normal font). The plate reconstructions (Figs. 5–14) are here shown in 20-Myr intervals and in a paleomagnetic reference frame (not corrected for true polar wander). The complete digital plate model accompanying this paper is described in Appendix 1.

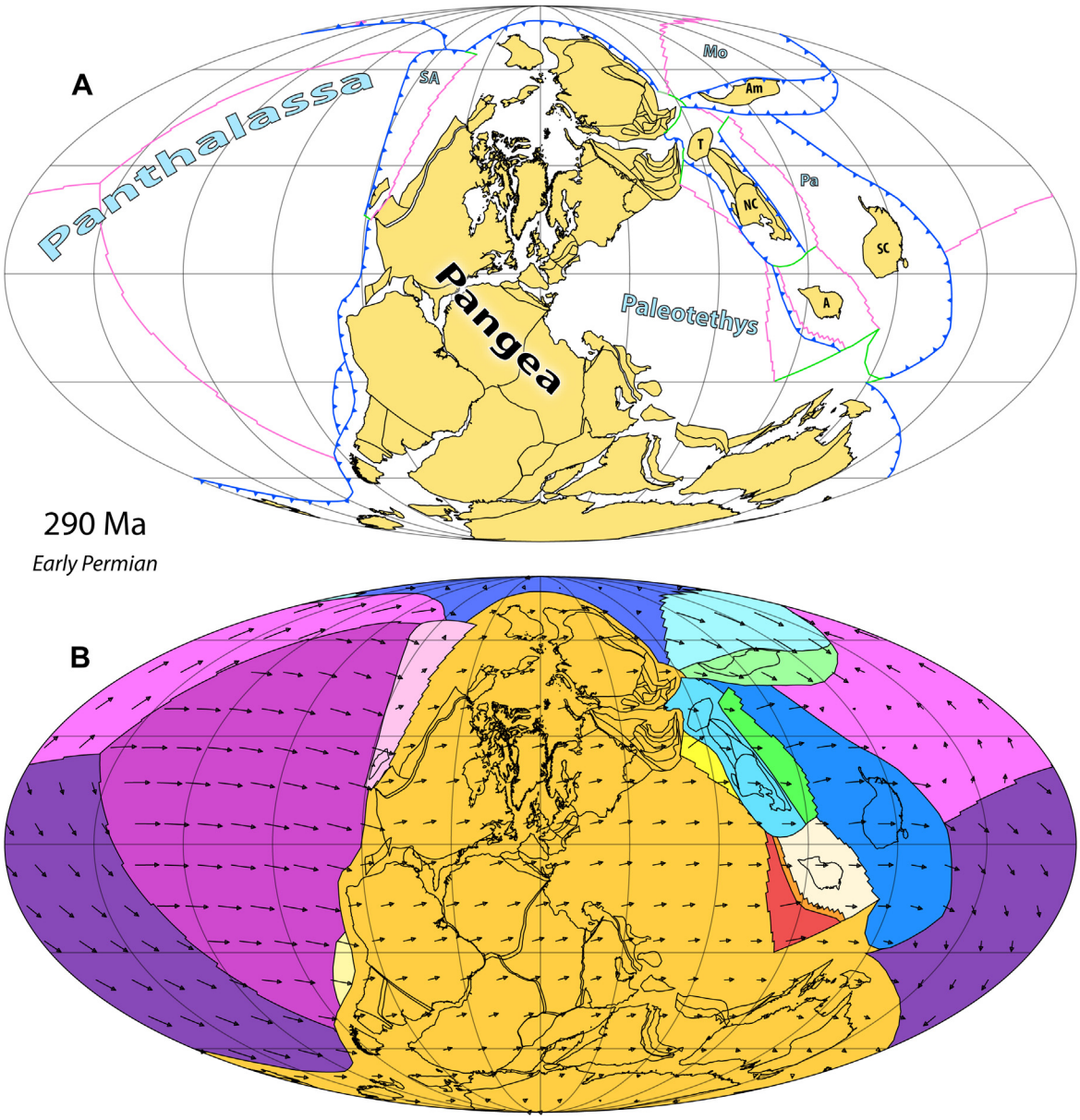


**Figure 12.** (A) 290 Ma (early Permian) paleogeographic reconstruction showing simplified plate boundaries and labels of some major features. *Abbreviated continental units*: A, Annamia; Am, Amuria; NC, North China; SC, South China; T, Tarim; *oceanic domains*: Mo, Mongol-Okhotsk Ocean; SA, Slide Mountain-Angayucham Ocean; Pa, Paleoasian Ocean. (B) Plate velocity field.

### 4.1. Devonian

#### 4.1.1. Closing of Rheic Ocean

At the dawn of the Devonian, continental crust was largely collected into four landmasses: Gondwana, Laurussia, Siberia and North China-Tarim (Fig. 5). Laurussia had formed through the amalgamation of Baltica, Avalonia and Laurentia via terminal closure of the intervening Tornquist and Iapetus Oceans in the late Ordovician and Silurian. Paleomagnetic data reveal that Laurussia was located in low southerly latitudes in the earliest Devonian and kimberlite occurrences in western Laurentia and northern Baltica allow its reconstruction over the eastern arm of the Pacific LLSVP. To the *southeast*, across the Rheic Ocean, which had opened between Avalonia and Gondwana in the latest Cambrian–earliest Ordovician, western Gondwana laid at high southerly latitudes with the South Pole in south-central South America (Fig. 5) (but paleomagnetic data from Gondwana are particularly sparse for the Silurian to middle Devonian). During the early Devonian, Laurussia drifted slowly *south* and rotated slightly counter-clockwise, closing the Rheic Ocean as it approached west Gondwana, which was pivoting about the South Pole. The polarity of Rheic Ocean subduction is an open question, especially since magmatic arc rocks are largely missing. HP metamorphic rocks in the Frontal Cordillera of Argentina argue for *south-dipping* subduction of the *southwestern* Rheic (Álvarez et al., 2011), but in the *northeast*, deformation and magmatism in the northern Appalachians and structural observations in southern Avalonia have been interpreted to reflect *north-dipping* subduction of the Rheic (Woodcock et al., 2007). Pe-Piper et al. (2010) reconciled those observations by invoking a large intra-Rheic transform (approximately at the Gulf of Maine) across which subduction polarity inverted. Such a transform could have been a primary feature installed by the drift of Avalonia (in which

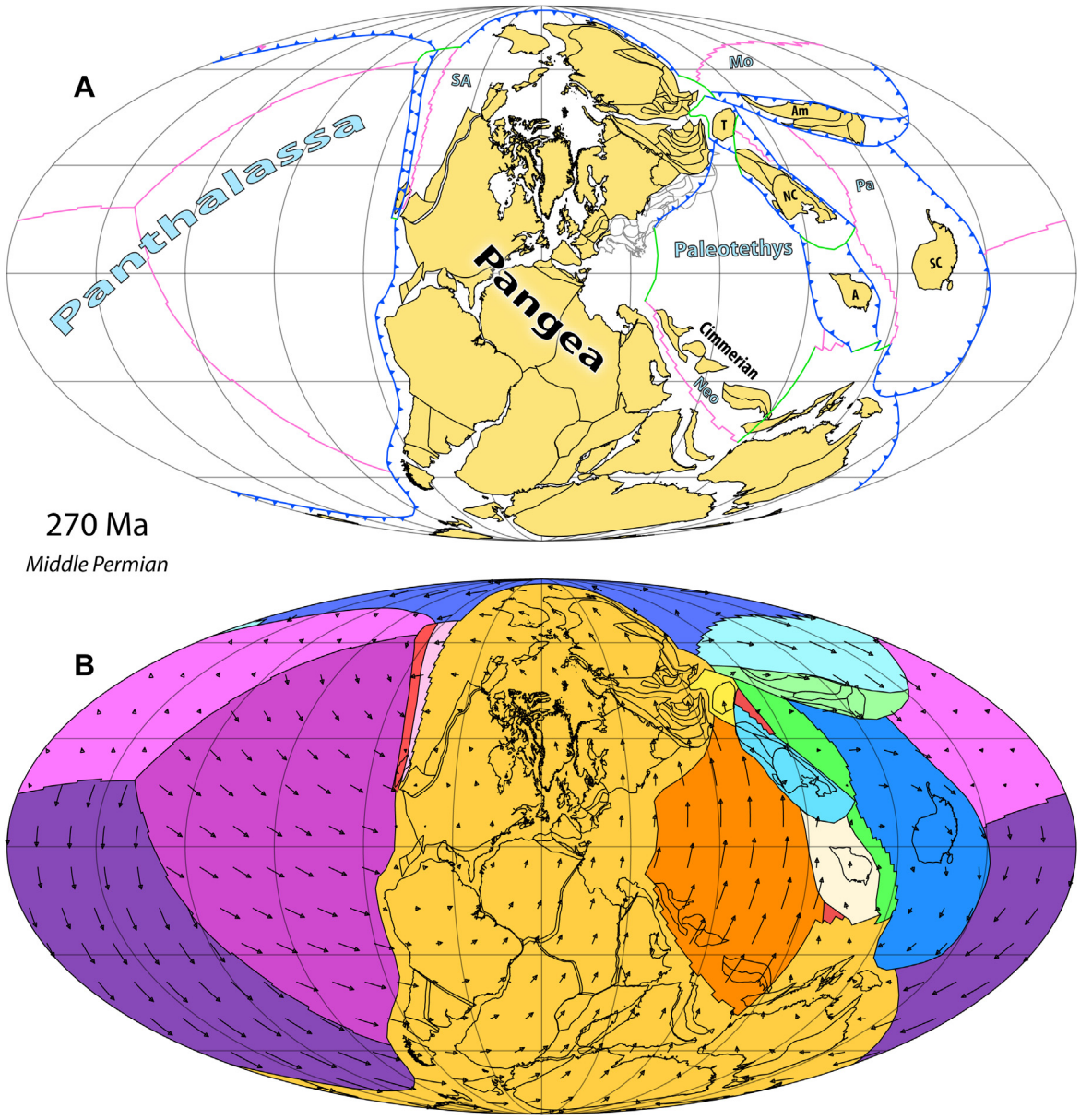


**Figure 13.** (A) 270 Ma (middle Permian) paleogeographic reconstruction showing simplified plate boundaries and labels of some major features. *Abbreviated continental units*: A, Annamia; Am, Amuria; NC, North China; SC, South China; T, Tarim; *oceanic domains*: Neo, Neotethys Ocean; Mo, Mongol-Okhotsk Ocean; SA, Slide Mountain-Angayucham Ocean; Pa, Paleoasian Ocean. (B) Plate velocity field.

case the *southwestern* "Rheic" would rather be remnant Iapetus) and merits further study. But here we have adopted a simpler kinematic scenario in which subduction was bivergent and active along the entirety of both margins (Fig. 5). According to our kinematic scenario, the *southwestern* Rheic closed at ~390 Ma, coincident with the accretion of the Chilenia terrane to west Gondwana (Figs. 6 and 7) (Willner et al., 2011; Martínez et al., 2012). Suggestions that Chilenia has a Laurentian affinity are thus in strong accordance with our model (Keppie and Ramos, 1999; Álvarez et al., 2011). The accretion of the (Gondwana-derived) Meguma terrane to Laurentia was likewise concomitant with *southwestern* Rheic closure in that scenario (van Staal et al., 2009), and thus "Neo-Acadian" deformation could be ascribed to an initial, soft collision with peri-Gondwana. Further afield, the 400–390 Ma "Acadian" deformation of the southern British Isles and HP metamorphism of the upper allochthons of NW Iberia could also be related to that soft collision, if not the preceding subduction that gave rise to it (Woodcock et al., 2007; Arenas et al., in press). Importantly, the relative orientation of Laurussia and Gondwana at that time was very different than that of their final configuration in Pangea, precluding the possibility that accretion of the Suwannee terrane was responsible for Neo-Acadian deformation in the southern Appalachians (Figs. 6 and 7), as suggested by Hibbard et al. (2010).

Sparse middle–late Devonian paleomagnetic data (one paleomagnetic pole at 370 Ma) and kimberlite occurrences from Laurussia suggest that it drifted *northeast* during that interval, returning to 0–30°S by ~360 Ma (Fig. 8). Comparatively more numerous paleomagnetic data from Gondwana reveal that it remained relatively stationary about the South Pole during that time (the pole remained near Angola from 390 to 360 Ma; Fig. 7), while late Devonian kimberlites in Australia enable its reconstruction in longitude above the western margin of the Pacific LLSVP. In our

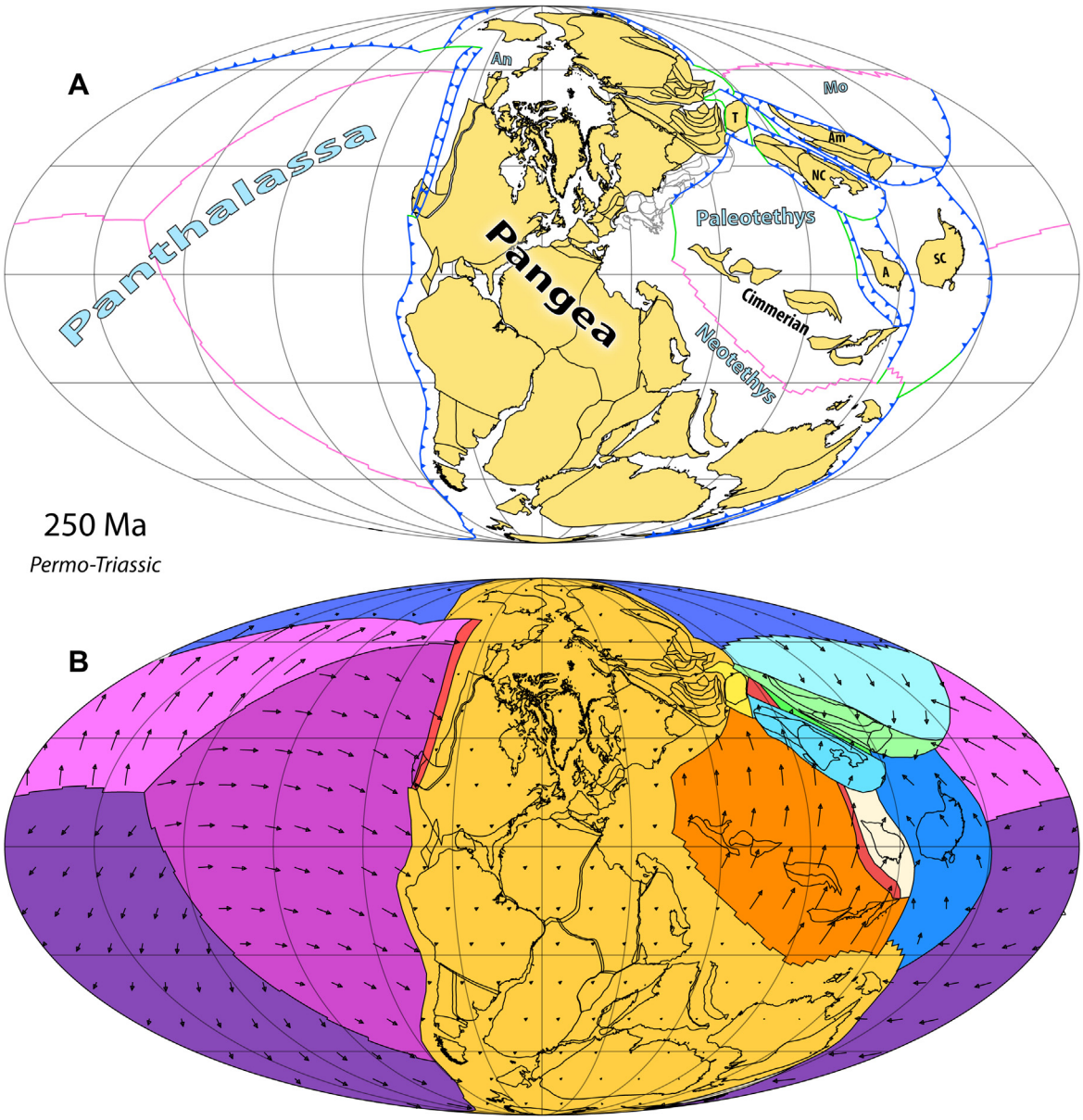


**Figure 14.** (A) 250 Ma (Permo-Triassic) paleogeographic reconstruction showing simplified plate boundaries and labels of some major features. *Abbreviated continental units*: A, Annamia; Am, Amuria; NC, North China; SC, South China; T, Tarim; *oceanic domains*: An, Angayucham Ocean; Mo, Mongol-Okhotsk Ocean. (B) Plate velocity field.

model, relative motion between Laurussia and Gondwana in the middle–late Devonian was slightly divergent to transcurrent, requiring an ephemeral spreading center along the former Rheic suture that rapidly evolved into a transform boundary (Fig. 8). That time frame corresponds with an interval of intra-plate extension and possibly the installation of a passive margin along the proto-Andean margin (Bahlburg et al., 2009; Grosse et al., 2009; Martina et al., 2011). Similarly, the southern margin of the northern block of Patagonia may have experienced a ~50 Myr magmatic hiatus beginning then, reflecting an interruption of subduction. Contemporaneously, along the Appalachian margin, Neo-Acadian deformation was supplanted by a protracted regime of dextral strike-slip motion that continued through the early Carboniferous.

*4.1.2. Opening of Paleotethys Ocean*

Rifting of the Variscan terranes and the corollary opening of the Paleotethys Ocean along the northern margin of Gondwana began in the early Devonian, with initial spreading of the ocean occurring at 410 Ma in our model (Fig. 5). Stampfli et al. (2013) alternatively delayed the opening of the Paleotethys until the middle–late Devonian, although other models placed the event in the Ordovician to Silurian (Stampfli and Borel, 2002). According to the relative longitudinal positioning of Laurussia and Gondwana in our model, a middle–late Devonian opening of the Paleotethys would necessitate that the Variscan terranes moved at an unreasonably high plate speed in order to have reached southern Baltica by the early Carboniferous. As an aside, such a condition highlights a potential opportunity by which to evaluate our reconstructed paleolongitudes, but requires further detailed work on the evolution of the Paleotethys.

Contemporaneous with the Paleotethys opening, *southeast-dipping* intraoceanic subduction of the Rheic may have initiated to the *northwest* of the Variscan terranes (Fig. 5), as evident by the rocks preserved in the MGCH and, speculatively, offshore in the

Léon domain of North Armorica (Franke, 2006; Faure et al., 2010). Further relics of that intraoceanic subduction zone may be preserved in Devonian supra-subduction ophiolites of the Galicia-Trás-os-Montes zone of NW Iberia (Arenas et al., 2007) and/or in Devonian arc-related detritus in SW Iberia (Pereira et al., 2012). Notably, the structure of the allochthonous thrust stack of the Galicia-Trás-os-Montes zone is antithetic to that expected from a *southeast-dipping* subduction zone, and may instead reinforce the notion of bivergent subduction of the Rheic. To the *southwest* of the Variscan terranes, along the *northwest* margin of Gondwana, early Devonian granitoids in the Maya block may reflect the continuation of that *southeast-dipping* subduction zone, if not early Devonian extension (Fig. 5) (Weber et al., 2012).

Devonian paleomagnetic data from Armorica, Bohemia, Iberia and Saxothuringia are few, but indicate that the Variscan terranes remained at relatively constant latitude throughout the period (Tait et al., 1996, 2000; Tait, 1999; Zwing and Bachtadse, 2000). Thus, in order to realize Devonian convergence and early Carboniferous collision with southern Baltica, the Variscan terranes must have drifted almost due *westward*. To accomplish that we have modeled the Paleotethys opening via a triple-junction of spreading ridges, with a *NNW–SSE-oriented* ridge-axis meeting the margin of *northern* Gondwana just to the *east* of the Variscan terranes (Fig. 5) (technically here "Paleotethys" then refers to a composite ocean). Spreading along the *NNW–SSE* ridge continued until the mid-late Devonian (~370 Ma) when nascent interactions began between the Variscan terranes and southern Baltica (Fig. 8); at that time the ridge inverted to become a *west-dipping* intraoceanic subduction zone (Fig. 9). Importantly, our modeling of the Variscan terranes is distinct from the 'Hun superterrane' concept of Stampfli (2000) and Stampfli and Borel (2002) in that we do not include continental elements from the so-called Asiatic Hunic terranes (including Tarim, Qiangtang and North China). In our model those 'Asiatic' units are either already in the northern hemisphere (i.e. Tarim-North China) or are separated from the departing Variscan terranes by the *NNW–SSE-oriented* Paleotethys ridge and instead rift from Gondwana later during opening of the Neotethys. Another Paleotethys opening scheme by Stampfli et al. (2013) is more similar to our own, but the starting distribution of the Variscan terranes (termed 'Galatian superterrane' by them) is considerably different.

The notorious complexities of the late Devonian–early Carboniferous Variscan orogeny are beyond the scope of our global model and we have thus adopted a representation which is simplistic. Preceding the first direct interaction between the Variscan terranes and southern Baltica in the late Devonian, *northwest-dipping* subduction beneath Baltica and *southeast-dipping* subduction beneath the intraoceanic MGCH arc ceased with the closure of the main Rheic Ocean. Contemporaneously, subduction initiated along the northwest margin of Bohemia, where *southeast-dipping* subduction of the remnant Rheic (or some minor basin internal to the Variscan terranes) continued into the early Carboniferous (Fig. 8). Following the closure of the main Rheic, relative motion between Baltica and the Variscan terranes was increasingly accommodated by a major transpressive zone between them (Fig. 9). The occurrence and importance of such early transform motion has been established by Martínez Catalán et al. (2007), Woodcock et al. (2007) and Braid et al. (2011), among others. In conjunction with the effective closure of the Rheic Ocean between the Variscan terranes and Baltica and the inversion of the Paleotethys *NNW–SSE-oriented* ridge, the Paleotethys also began to subduct *westward* beneath the margin of the Variscan terranes in the mid-late Devonian (Fig. 9) (Stampfli et al., 2002; von Raumer et al., 2013). That Devonian–Carboniferous *westward-dipping* subduction zone continued to the *north* along the Scythian and Turan platforms, which may have eventually grown through accretion of the outboard Paleotethys intraoceanic arc.

Paleomagnetic, paleobiologic and sedimentologic data suggest that South China was adjacent to northeast Gondwana in the mid-Paleozoic (Shen et al., 2008; Cocks and Torsvik, 2013). However, early Devonian regional strike-slip faults and extensional basins in South China are understood to denote the initiation of its rifting from Gondwana. Along the southwestern margin of South China and the northeastern margin of Annamia—which were likely then conjugate—an early Devonian unconformity and middle Devonian to Permian ophiolitic and passive margin rocks have been interpreted to signify a near-contemporaneous separation of Annamia and South China (Jian et al., 2009a, b). In western Annamia, similar late Paleozoic rocks reflect the respective early Devonian separation of that continent from Gondwana. Thus, we implemented a rift system that separated South China + Annamia and northeast Gondwana in the early Devonian (Fig. 5); by the middle Devonian the system progressed to include the separation of South China and Annamia (Fig. 8). Given the broad spatio-temporal concurrence of those events with the development of the Paleotethys, it is tempting to directly link those rift systems. However, the paleomagnetic (though sparse) and geologic data from South China are enough to demonstrate that it cannot have moved passively with the (*northeastern*) Paleotethys as modeled, and we have instead decoupled them with an intraoceanic transform boundary. During the Devonian we also included the South Qinling terrane as a passive element of the greater South China plate, the former having been previously rifted from the northwest margin of South China in the Silurian.

#### 4.1.3. The northern hemisphere

Throughout the Devonian, Siberia and North China-Tarim remained isolated at low latitudes in the northern hemisphere. The paleolatitude of Siberia is almost entirely interpolated for the Devonian as there are no reliable data from the mid-Silurian (~430 Ma) to the latest Devonian (360 Ma) (Cocks and Torsvik, 2007). Nonetheless, those data indicate that Siberia was 'upside down' (azimuthally inverted) at the beginning of the Devonian and centered at about 15°N (Fig. 5). As the Devonian progressed, Siberia rotated clockwise and drifted *north* to become centered at ~30°N by 360 Ma (Figs. 6 and 8). Early Devonian kimberlites in east Siberia and the ~400 Ma Altai-Sayan LIP in its southwest support the reconstruction of that continent above the northwest arm of the African LLSVP. Abundant late Devonian kimberlites and the ~360 Ma Yakutsk LIP in east Siberia indicate that the continent remained over the LLSVP throughout the Devonian, perhaps drifting only slightly *east*.

Given that positioning, the Uralian margin of Baltica progressively approached the northern margin of Siberia (*south-facing* in the early Devonian) through the Devonian. That is interesting because the Uralian margin of Baltica records the accretion of the Magnitogorsk island arc in the middle–late Devonian (and later the Tagil island arc in the early Carboniferous) (Brown et al., 2011), whereas the northern margin of Siberia was passive during the Devonian, according to observations from central and southern Taimyr (Bradley, 2008). To satisfy those different observations we hypothesize that the Devonian Magnitogorsk island arc was situated above a *north-dipping* intraoceanic subduction zone to the *south* of northern Siberia (Fig. 5). The island arc would have initiated on oceanic crust on the outboard passive margin of northern Siberia, but, as Siberia rotated clockwise in the early Devonian, a back-arc basin opened behind the island arc and it became an independent plate (Fig. 6). By the late middle Devonian, *north-dipping* subduction had destroyed the basin separating Baltica and the Magnitogorsk arc and the latter was accreted in the early late

Devonian (Fig. 8). We further posit that the Tagil island arc—which was also active in the Devonian—was the *eastward* continuation of the Magnitogorsk arc, and so also sat above a *north-dipping* intra-oceanic subduction zone outboard (to the *south*) of northern Siberia. To the *northeast*, that intraoceanic subduction zone would have continued into the Altai-Sayan active margin of southwest peri-Siberia (Fig. 5). The Altai-Sayan margin remained active through the Devonian, first subducting oceanic crust of the Rheic Ocean and then, during the late Devonian, crust of the Paleotethys Ocean. Further to the *north* the Turkestan Ocean was also subducting beneath the southwest margin of Siberia until the end of the Devonian.

The southeastern margin of Siberia (*northwest-facing* in the early Devonian) was passive through nearly the entire Devonian, facing the slowly-spreading MOO which had opened in the Silurian (Figs. 5–7) (Bussien et al., 2011). In the latest Devonian (360 Ma) the passive margin collapsed and *south-dipping* subduction commenced beneath Siberia (Fig. 9). The margin of east Siberia was likewise passive throughout the Devonian, save for a middle–late Devonian episode of extension that was probably due to the impingement of a plume (Cocks and Torsvik, 2007).

Paleomagnetic data from Kazakhstania reveal that the present-day orocline was rectilinear in the early–middle Devonian, oriented *NW–SE* and located at mid-low northern latitudes above a *southwest-dipping* subduction zone (Figs. 5 and 6) (Abrajevitch et al., 2007; Bazhenov et al., 2012). Given its early interaction with the Altai-Sayan region of Siberia and their similar paleolatitude, it is likely that Kazakhstania was already proximal to southwestern Siberia in the early Devonian and we speculate that their active margins were contiguous. Incessant Devonian arc magmatism in Kazakhstania indicates that *southwest-dipping* subduction endured throughout that period, as it did in the neighboring Altai-Sayan region (Windley et al., 2007; Glorie et al., 2011a; Wilhem et al., 2012). Along the 'external' margin of Kazakhstania (opposite the one just discussed), oblique subduction of the Rheic Ocean had occurred in the early Devonian but ceased in the middle Devonian with the passage of an intraoceanic subduction zone that heralded the expansion of the Paleotethys (Figs. 5–7). In the middle to late Devonian the margin remained passive behind an outboard transform boundary. That scenario is compatible with the observation that late Silurian–early Devonian arc-related magmatism along that margin waned by the middle to late Devonian (Windley et al., 2007; Biske and Seltmann, 2010).

Devonian paleomagnetic data from North China (Cocks and Torsvik, 2013) and Tarim (Li et al., 1990) are sparse, but indicate that those blocks occupied the same mid-low latitudes in the northern hemisphere. In considering also the geological data that suggest that the Qilian orogen was assembled by the latest Silurian and that the composite Qinling-Dabie orogen is correlative with the Qilian and Kunlun orogens, we contend that Tarim and North China were drifting as one tectonic unit by the early Devonian (although not in their present-day relative positioning) (Fig. 4). Throughout the Devonian the passive northern margin of Tarim faced the Turkestan Ocean, which was subducting *westward* beneath Kazakhstania and Siberia (Figs. 5–7). Along the shared Kunlun-Qinling-Dabie margin of North China-Tarim, *north-dipping* subduction of the Paleotethys was continuous through the Devonian, following a brief interval of minor transform motion in the earliest Devonian. Simultaneous *southward-directed* subduction of the Panthalassa occurred to the *north* beneath northern North China and Beishan until 370 Ma, when the neighboring intraoceanic subduction zone of the South China plate passed by northern North China, converting its active margin into a transform boundary.

#### 4.1.4. Marginal seas and the Panthalassa

The Panthalassa, like the present-day Pacific, was a vast ocean. But despite covering a hemisphere throughout the late Paleozoic, little is known about that composite basin due to the complete destruction of its constituent plates. Moreover, a near-continuous subduction zone encircled the Panthalassa along its boundary with the continents, thereby limiting the inferences that can be drawn about its late Paleozoic kinematics. We have adopted the simplest scenario that allows us to meet that condition of near-constant convergence all along the boundary of the domain: a stable triple-junction of spreading ridges, but it is important to note that this model of the Panthalassa is grossly naïve. As it is first necessary to correctly reconstruct the continental domain—from which we have a wealth of observational data—we have not yet attempted a realistic construction of the Panthalassa, but we discuss potential avenues for such future work in Section 5.2.

The western margin of Laurentia exhibits no indicators of an active margin prior to the middle–late Devonian. Accordingly, our Panthalassa model begins with one ridge of the three-plate system aligned near-orthogonally to the western margin of Laurentia, with strike-slip motion occurring along the Laurentia-Panthalassa boundary (Figs. 5 and 6). Strike-slip motion predominated along that margin until the middle Devonian, when we initiated relative convergence to coincide with the first appearance of arc-related magmatism there (Fig. 8) (Colpron and Nelson, 2009). In the late Devonian we adjusted the relative motion to become more obliquely convergent, in anticipation of the latest Devonian–Carboniferous opening of the Slide Mountain and Angayucham Oceans (Fig. 9).

The Innuitian margin of Laurentia is more challenging to understand. Bearing in mind the Baltic affinities of the Pearya and Arctic Alaska-Chukotka terranes and their late Silurian–early Devonian arrival by sinistral transpression, we consider their accretion to have been a continuation of Caledonide orogenesis. The persistence of their motion after peak-Caledonide orogenesis could be attributed to the lack of an immediate 'backstop'; or in other words, their accretion could have been delayed because of the irregular shape of the converging margins. Accordingly, we treated those terranes as a small, unified plate that detached from Baltica when the latter collided with Laurentia, only to continue slowly drifting for ~20 Myr until colliding with Laurentia itself (Figs. 5 and 6). The late Devonian–early Carboniferous Ellesmerian orogeny is yet more mystifying, and here we can only speculate that it was an expression of convergence between northern Laurussia and its conjugate plates (Siberia and Panthalassa).

To the *north* of southern Siberia, the MOO slowly widened throughout the Devonian as Amuria drifted away from Siberia. Kravchinsky et al. (2002) and Zhao et al. (2013) have published the only paleomagnetic studies of Devonian rocks from Amuria, but their results are unfortunately ambiguous. Although Kravchinsky et al. (2002) interpreted their four paleomagnetic poles (from Devonian rocks) as primary, we note that the associated foldtests for three of them were statistically inconclusive and the fourth peaked at 78% unfolding. The Devonian formations studied by Zhao et al. (2013) likewise yielded negative to inconclusive foldtests. Since the age of folding is very poorly constrained (Permian to Cenozoic), and the paleomagnetic poles are very similar to Permian results from the same areas, we regard those Devonian data as untrustworthy. Thus, the location of Amuria in the Devonian is not directly constrained, but following the assumption that western-most Amuria was loosely contiguous with the Altai-Sayan region of Siberia, its position can be partly fixed. We thus treated Amuria as semi-coupled to Siberia, but allowed the widening MOO to slowly separate their eastern margins (Figs. 5–7). The MOO must have been expanding in the Devonian as its north and south margins

were both passive until the latest Devonian, when subduction began along the southern margin of Siberia (Fig. 9). On the southern margin of Amuria (*north-facing* in the Devonian) subduction of the Panthalassa continued unabated through the Devonian.

In the Silurian to early Devonian, subduction of the Panthalassa along the southeast margin of Gondwana was occurring beneath the outboard Gamilaroi-Calliope arc (Figs. 5 and 6). During the middle–late Devonian Tabberabberan orogeny, the backarc of the Gamilaroi-Calliope arc collapsed and the arc was accreted to the continental margin by 380 Ma. Subsequently, *west-dipping* subduction of the Panthalassa began directly beneath the continental margin of eastern Australia, where it persisted through the Carboniferous (Fig. 8). Elsewhere along the perimeter of the Panthalassa, relative motion remained predominantly convergent throughout the Devonian; a continuous subduction zone operated from south to east Gondwana, along the northern margin of North China-Tarim and further on across the southern margin of Amuria and the northern extension of Laurussia.

### 4.2. Carboniferous

#### 4.2.1. Formation of Pangea

In the Carboniferous, paleomagnetic data from Laurussia and Gondwana remain few in number for the first 20 Myr, but become more abundant after 340 Ma. At the start of the Carboniferous, Laurussia was positioned at low latitude in the southern hemisphere (Fig. 9). It drifted *northward* throughout the period, crossing the Equator in the mid-to-late Carboniferous and accelerated *northward* after 320 Ma (Figs. 10 and 11). By the end of the Carboniferous Laurussia occupied the latitudes ~0–30°N. With respect to the drift of Gondwana during the Carboniferous, the South Pole moved across southern Africa during the early Carboniferous and to the central Transantarctic Mountains region of East Antarctica by the end of the Carboniferous. No LIPs were erupted into either Laurussia or Gondwana during the Carboniferous, but late Carboniferous kimberlites were emplaced in northern Baltica and western Australia. The constraints imposed by those kimberlites can be satisfied by placing Baltica on the northeastern margin of the African LLSVP and Australia on the southeastern tip. That positioning requires Laurussia to move strongly *eastward* in the early Carboniferous (Figs. 9 and 10), whereas a comparatively minor *westward-drift* of Gondwana is only broadly constrained to the Carboniferous.

Associated with that strong *eastward-drift* of Laurussia, and continuing from the late Devonian, relative motion between Laurussia and Gondwana was dominated by dextral strike-slip through the early Carboniferous (Figs. 9 and 10). However, transpression to highly oblique subduction was locally important along the transform system, as evident in the Mauritanide belt of Morocco and Mixteca-Oaxacan terrane of Mexico where there was Devonian–early Carboniferous HP metamorphism (and, in the latter, perhaps coeval arc magmatism) (Fig. 9) (Keppie et al., 2008, 2012; Michard et al., 2010). Arc magmatism recurred in the Mixteca-Oaxacan terrane in the late Carboniferous, when it reached the *east-dipping* subduction zone fringing the Panthalassa along the *western* margin of Pangea (Fig. 11).

We stress that our implementation of considerable dextral transform motion between Laurussia and Gondwana during the early Carboniferous is not tantamount to the adoption of Pangea "B" (Muttoni et al., 2009a; Domeier et al., 2012), since Pangea did not form until ~320 Ma. At 320 Ma relative motion between Laurussia and Gondwana ceases in our model, and the Pangea "A-type" reconstruction that is reached persists through the Permian (Fig. 11). Such timing for Pangea's ultimate amalgamation is corroborated by evidence of regional shortening along the Appalachians in the late Mississippian–early Pennsylvanian, including basin inversion in the Canadian Maritimes and the development of a clastic wedge in the southern Appalachians (Hatcher, 2010; Hibbard et al., 2010). Analogously, pronounced regional shortening and dextral wrenching of that same age has been recognized in the Moroccan Meseta (Michard et al., 2010). In passing, we note that the absence of late Devonian–Carboniferous arc magmatism and other clear indications of subduction along the former Rheic margins may have been due to the dominance of transcurrent vs. convergent tectonics (see also: Mueller et al., in press), which enhances the difficulty in establishing which was the upper plate.

Variscan orogenesis culminated in the early Carboniferous (350–340 Ma) with a series of terrane collisions marked by HP/UHP metamorphism and pronounced crustal thickening. The detailed kinematic evolution of the Variscan orogen is beyond our present scope, but we note that strike-slip tectonics continued to play a key role through the Carboniferous (Martínez Catalán et al., 2007; Azor et al., 2008). In our simplified model, the Variscan terranes continued to move relative to Baltica by means of a major zone of dextral transpression until 340 Ma, when the terranes coalesced with Laurussia (Figs. 9 and 10). To the *south*, the boundary between the Variscan terranes and northwest Gondwana remained a pure transform fault for most of the early Carboniferous, but became slightly transpressive in the mid-Carboniferous during the final convergence between Laurussia and Gondwana. In the *east*, *west-dipping* subduction of the Paleotethys beneath the Variscan terranes and the Scythian-Turan domains continued (from the late Devonian) until at least the late Carboniferous (Figs. 9 and 10).

Siberia has no reliable paleomagnetic data between 360 Ma and 275 Ma, and we are faced with a span of precarious interpolation for most of the Carboniferous and early Permian. However, an abundance of early Carboniferous kimberlites in east Siberia (continuing from the numerous Devonian occurrences) suggests that the continent lingered above the northwest arm of the African LLSVP then. Proceeding with such a reconstruction, the relative motion between Siberia and Laurussia was obliquely convergent in the early Carboniferous, following an interval of transcurrent relative motion in the late Devonian. Destruction of the basin between Siberia and Laurussia was achieved initially by *northeast-dipping* subduction beneath the Tagil island arc and the then-inverted ridge that once lay behind the Magnitogorsk island arc (Fig. 9). By 345 Ma the Tagil island arc had accreted to the Uralian margin of Baltica (Puchkov, 2009a; Brown et al., 2011) and the polarity of subduction had flipped to allow closure of the remnant (backarc) basin by subduction beneath Baltica. However, that latter phase of convergence was short-lived, and by 340 Ma motion along the boundary became transcurrent to weakly divergent, producing a minor but long-lived basin between Baltica and west Siberia that later filled to form the West Siberian Basin (Fig. 10). To the *northwest* along that boundary, from 340 to 320 Ma, transcurrent to transpressive motion between the 'Kara terrane' (kept coherent with Baltica in our model, following Lorenz et al., 2008) and north Siberia would have been responsible for the late Paleozoic deformation in Severnaya Zemlya and Taimyr, which would therefore have been kinematically distinct from Uralian orogenesis to the south. At 320 Ma relative motion along the Siberia-Laurussia plate boundary ceases in our model. In reality, sluggish convergence and transform motion between Siberia and Laurussia continued into the early Mesozoic (Buiter and Torsvik, 2007; Cocks and Torsvik, 2007), but, for simplicity, we considered that as intra-plate deformation and treated Siberia, Laurussia and Gondwana together as one plate (Pangea) after 320 Ma (Fig. 11).

#### 4.2.2. Solitary continents

Having rifted both from Gondwana and from each other in the Devonian, South China and Annamia continued to drift in isolation during the Carboniferous, being situated between the Paleotethys (to the *southwest*) and the Panthalassa (to the *northeast*) and otherwise surrounded by marginal seas (Figs. 9–11). Unfortunately, there are no quantitative Carboniferous constraints on paleolatitude or paleolongitude for either of those continents, so their exact positions are unknown for that period and their reconstruction is based on interpolation. In accordance with the geological observations, we maintained passive margins all around both continents for the whole of the Carboniferous, with the exception of the east margin of South China, where the proto-Japanese islands were positioned above a subduction zone consuming the Panthalassa (Figs. 9–11). At the beginning of the Carboniferous, active divergence in the region was largely restricted to a branch of the Paleotethys to the *southwest* of Annamia and along a slowly-spreading ridge between South China and Annamia. In the early Carboniferous, *northwest-dipping* subduction beneath southeast North China brought that continent very close to South China and Annamia, but at 340 Ma the *west-dipping* segment of the subduction zone converted to a sinistral transform boundary, perhaps due to its impingement on the South China-Annamia ridge (Figs. 9 and 10). Continued subduction beneath the southern margin of North China resulted in the accretion (and translation) of the South Qinling unit to the North China margin in the mid- to late Carboniferous (Figs. 10 and 11). On the north side of North China, a backarc basin started to develop behind the intraoceanic South China (proto-Japan) subduction zone in the earliest Carboniferous (Fig. 9). By the mid-Carboniferous that basin had substantially grown to become the Paleoasian Ocean, which separated North China-Tarim and Kazakhstania from Amuria and the Panthalassa (Fig. 10).

Sparse paleomagnetic data from North China suggest that it rotated clockwise during the Carboniferous (although vertical axis rotations in the Hexi corridor are a concern) but remained at low latitude in the northern hemisphere (Zhao et al., 1996; Huang et al., 2001). Though no Carboniferous LIPs or kimberlites were emplaced into North China, its possible paleolongitude is restricted by its snug positioning between Kazakhstania and Siberia to the *west* and South China and east Gondwana to the *east* (Figs. 9–11). Following subduction of the Turkestan ridge in the late Devonian, continued subduction of the Turkestan Ocean beneath Kazakhstania and southern Amuria drew North China-Tarim progressively *westward* in the early Carboniferous (Fig. 9). By the mid-early Carboniferous the Turkestan Ocean had been consumed between Tarim and *east* Kazakhstania and direct interaction between those terranes began at ~340 Ma (Fig. 10). That timing is consistent with the occurrence of early to mid-Carboniferous (~345–320 Ma) eclogite-facies metamorphism in the South Tian Shan suture zone and the waning of arc magmatism in Kazakhstan and the Chinese Central Tianshan by the mid-Carboniferous (Gao et al., 2009, 2011; Han et al., 2011; Ren et al., 2011). Additionally, Abrajevitch et al. (2008) suggested that the impingement of Tarim on Kazakhstania could have driven (or assisted in driving) oroclinal bending of the latter, which was underway by the early Carboniferous. Alternatively, the occurrence of early Carboniferous ophiolitic material in the South Tian Shan suture may indicate that our preferred timing for both ridge subduction and final collision is slightly too early (Han et al., 2011); nevertheless, post-340 Ma convergence between North China-Tarim and Kazakhstania must have been minor according to the paleolongitude constraints imposed by the plates to the *east* (South China, Annamia and east Gondwana). It is also possible that some of the ophiolitic material in the South Tian Shan suture was extracted from the Paleotethys Ocean after initial contact between Tarim and Kazakhstania, but prior to their final consolidation (for example, note the active margin of *south* Kazakhstania in Fig. 10).

Like many previous models, we contend that consumption of the Paleotethys in the Carboniferous was partly achieved by subduction beneath the southern (Kunlun-Qinling-Dabie) margin of North China-Tarim (Figs. 9–11), although the geological evidence remains vague. On the opposite side of the terrane, along Beishan and northern North China, the Devonian active margin was progressively supplanted in the early Carboniferous by a passive margin via the passage of the intraoceanic arc (proto-Japan) of the eastern South China plate and the growth of the Paleoasian Ocean behind it (Figs. 9 and 10). However, by the beginning of the late Carboniferous, subduction had recommenced along the Beishan/northern North China margin and the young Paleoasian Ocean began subducting beneath it (Fig. 11). That short-lived early Carboniferous subduction hiatus in northern North China is consistent with the ~360–330 Ma gap in detrital zircon ages from Carboniferous–Permian strata across that margin (Cope et al., 2005).

Paleomagnetic data place Kazakhstania in mid-low latitudes in the northern hemisphere during the Carboniferous, permitting its reconstruction to a position adjacent to southwest Siberia (Abrajevitch et al., 2008; Levashova et al., 2012). The oroclinal bending of Kazakhstania may have begun already in the middle–late Devonian, but was certainly underway by the earliest Carboniferous. We simplistically modeled the evolution of that orocline by dividing Kazakhstania into two discrete units and rotating them semi-independently (Figs. 8–11). Subduction of the Turkestan Ocean beneath the 'Internal' margin of Kazakhstania continued during the early Carboniferous as the orocline tightened (Fig. 9). Following the initial collision of Tarim at 340 Ma, oroclinal bending proceeded more rapidly through the mid-Carboniferous until its conclusion at 310 Ma, at which time subduction along the 'internal' margin also ceased (Figs. 10 and 11). Along the 'external' margin of Kazakhstania, subduction of the Paleotethys beneath the Chinese Tian Shan continued throughout the late Devonian and mid-Carboniferous, whereas in the Kyrgyzstan Tian Shan subduction did not recommence (following its middle–late Devonian interruption) until the mid-Carboniferous (Figs. 9 and 10). That resumption of subduction in the Kyrgyzstan Tian Shan approximately coincided with the time at which Kazakhstania began to override the young ocean basin developing between Siberia and Baltica. The subduction of that basin was short-lived, as Kazakhstania docked with Baltica along the Uralian margin at 310 Ma; the remnant basin to the *northwest* formed the West Siberian Basin (Fig. 11). Following complex transpressive motion between Kazakhstania and the Altai-Sayan margin of Siberia throughout the early to mid-Carboniferous, we treat Kazakhstania and Siberia as consolidated after 310 Ma; Kazakhstania thus constitutes part of Pangea from then on.

#### 4.2.3. Marginal seas and the Panthalassa

Prior to the mid-early Carboniferous, the proto-Andean and north Patagonian margins remained passive following the closure of the Rheic Ocean and the collision of Chilenia (Chew et al., 2007; Bahlburg et al., 2009). We suppose that was due to an extension of the Laurussian plate that separated those margins from the Panthalassa, which could have been subducting beneath an outboard (partly intraoceanic) boundary during the late Devonian–early Carboniferous (Figs. 8 and 9). At 340 Ma the proto-Andean and north Patagonian passive margins collapsed to form a subduction zone that linked with the one fringing southeast Gondwana (Fig. 10). That subduction zone first began to consume the young oceanic plate which was created by the divergence of Laurussia and south Gondwana in the late Devonian–early Carboniferous (Figs. 9

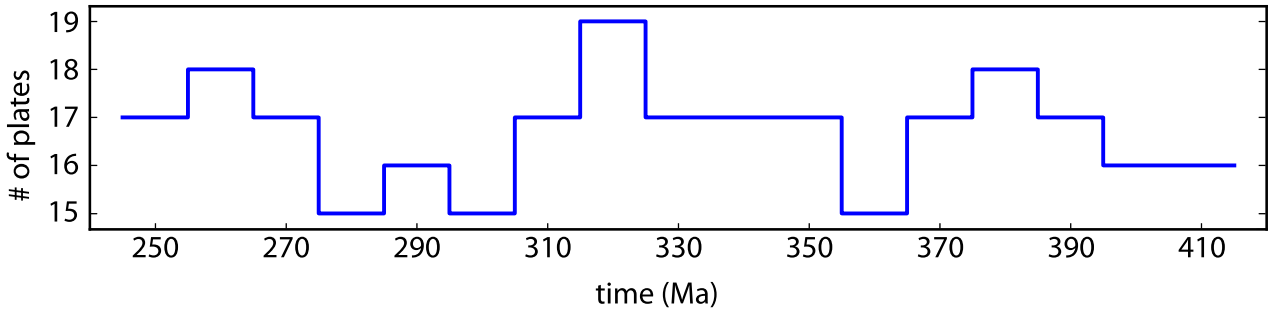


**Figure 15.** Average number of plates per 10-Myr interval in our model.

and 10). Considering the timing, it is possible that the allochthonous (southern) block of Patagonia was resident on that young oceanic plate and that its late Carboniferous accretion was due to the operation of the *east-dipping* proto-Andean subduction zone (Figs. 10 and 11). Working backwards, that interpretation would place south Patagonia proximal to southern Laurentia in the late Devonian, and we speculate that they may have been united prior to the late Devonian–early Carboniferous spreading (i.e. the ridge cleaved south Patagonia from peri-Laurentia) (Figs. 8 and 9). We note that there are some indications that south Patagonia had a Laurentian affinity (Chernicoff et al., 2013). Furthermore, the possible inception of subduction along the southwest margin of south Patagonia at 390 Ma would have been coincident with the onset of subduction along western Laurentia. Hence, we modeled the south block of Patagonia as a detached fragment of Laurentia which later collided with north Patagonia at 310 Ma (Figs. 8–11). With the closure of the intervening basin between north and south Patagonia, western Gondwana began to directly override oceanic lithosphere of the Panthalassa.

Along the western margin of Laurentia the start of the Carboniferous roughly coincided with the opening of the Slide Mountain Ocean between the Laurentian parautochthon and the outboard Yukon-Tanana arc terrane and its correlatives. With the Panthalassa persistently, if obliquely, subducting beneath the Yukon-Tanana terrane along its western margin, the back-arc spreading of the Slide Mountain Ocean continued unabated throughout the Carboniferous and into the Permian (Figs. 9–12). Further to the *northeast*, along the Arctic-Alaska-Chukotka terrane, the Angayucham Ocean also opened in the late Devonian–early Carboniferous. The contiguity of and similarities between those basins have previously led to the interpretation that they were unified, and we embraced this simplifying concept in our model (Figs. 9–12).

Between Siberia and Amuria the wedge-shaped MOO continued to spread during the Carboniferous. In the early Carboniferous, subduction of that ocean only occurred along the southeast margin of Siberia, but in the mid-Carboniferous it also began along the northern margin of Amuria (Figs. 9–11). On the opposite side of Amuria, along its southern margin, subduction of the Panthalassa continued uninterrupted throughout the Carboniferous. Unfortunately, we had to dismiss the Carboniferous paleomagnetic data from Amuria (Xu et al., 1997; Kravchinsky et al., 2002; Zhao et al., 2013), for the same reasons outlined above, so the reconstructed position of Amuria was again constrained only by its western continuation into the Altai-Sayan region.

Elsewhere along the perimeter of the Panthalassa, subduction was sustained and consistently outward-dipping (i.e. beneath the continents) during the Carboniferous, with specific relative motion that ranged from orthogonal to highly oblique. Along eastern Australia the relative motion of the Panthalassa changed several times during the course of the Carboniferous, giving rise to the Kanimblan orogeny and the regimes of regional tension that pre- and post-dated it. As in the late Devonian, the subduction zone along the perimeter of the Panthalassa was near-continuous during the Carboniferous, and so there was little direct communication between the Panthalassa and the continental domain.

### 4.3. Permian

#### 4.3.1. Drift of Pangea and opening of Neotethys Ocean

Paleolatitude and paleolongitude constraints for Pangea are excellent for the Permian. A wealth of paleomagnetic data reveal that the supercontinent drifted *north* and rotated counterclockwise during that period (Figs. 12–14), such that its center of mass moved from ~30°S at 300 Ma to ~10°S at 250 Ma (Torsvik et al., 2012). Early Permian paleolongitude constraints are provided by kimberlites in northwest Laurentia and by the Skagerrak LIP (~297 Ma) and the Panjal Traps (~285 Ma). Late Permian kimberlites were emplaced in northwest Laurentia, southern Africa and eastern Australia, and the Siberian Traps erupted at ~251 Ma. Those occurrences allow Pangea to be reconstructed such that its overall longitudinal drift from 300 to 250 Ma was *eastward*, resulting in a progressive centering of the supercontinent above the African LLSVP (Figs. 12–14).

In the early to mid-Permian a large area of the Pangean plate consisted of the south Paleotethys Ocean (*southwest* of the Paleotethys ridge) (Fig. 12). By the beginning of the middle Permian that oceanic lithosphere had become independent through the rifting of the Cimmerian terranes from northeast Gondwana and the corollary opening of the Neotethys Ocean (Fig. 13). The prevailing explanation for that event postulates that rifting was instigated by slab-pull forces transmitted from the northward subduction of the south Paleotethys (beneath Baltica and proto-Asia), following subduction of the Paleotethys ridge (Stampfli and Borel, 2002; Gutiérrez-Alonso et al., 2008). We have adopted that scenario, but note the great uncertainties in the timing and style of ridge subduction. Many interpretations of that event have been drawn from the late Carboniferous and early Permian stratigraphy and magmatism of southern Baltica, but the kinematic and geometric constraints imposed by our model necessitate that the Paleotethys ridge was at high-angle to the southern margin of Baltica then (Figs. 10–12). Furthermore, following final consolidation of Pangea at 320 Ma, the motion between the south Paleotethys and Baltica must have ceased, and the relative motion between Baltica and the north Paleotethys would have been highly oblique to transcurrent. The widespread late Carboniferous–early Permian rifting and magmatism across southern Baltica has been attributed to subduction of the Paleotethys ridge (Dostal et al., 2003; Gutiérrez-Alonso et al., 2008), but we speculate that it could rather have been a consequence of margin-wide break-off of the Paleotethys slab following the abrupt cessation of convergence at 320 Ma. In our model the Paleotethys ridge was subducted beneath the *northeast-dipping* subduction zone flanking southern North China

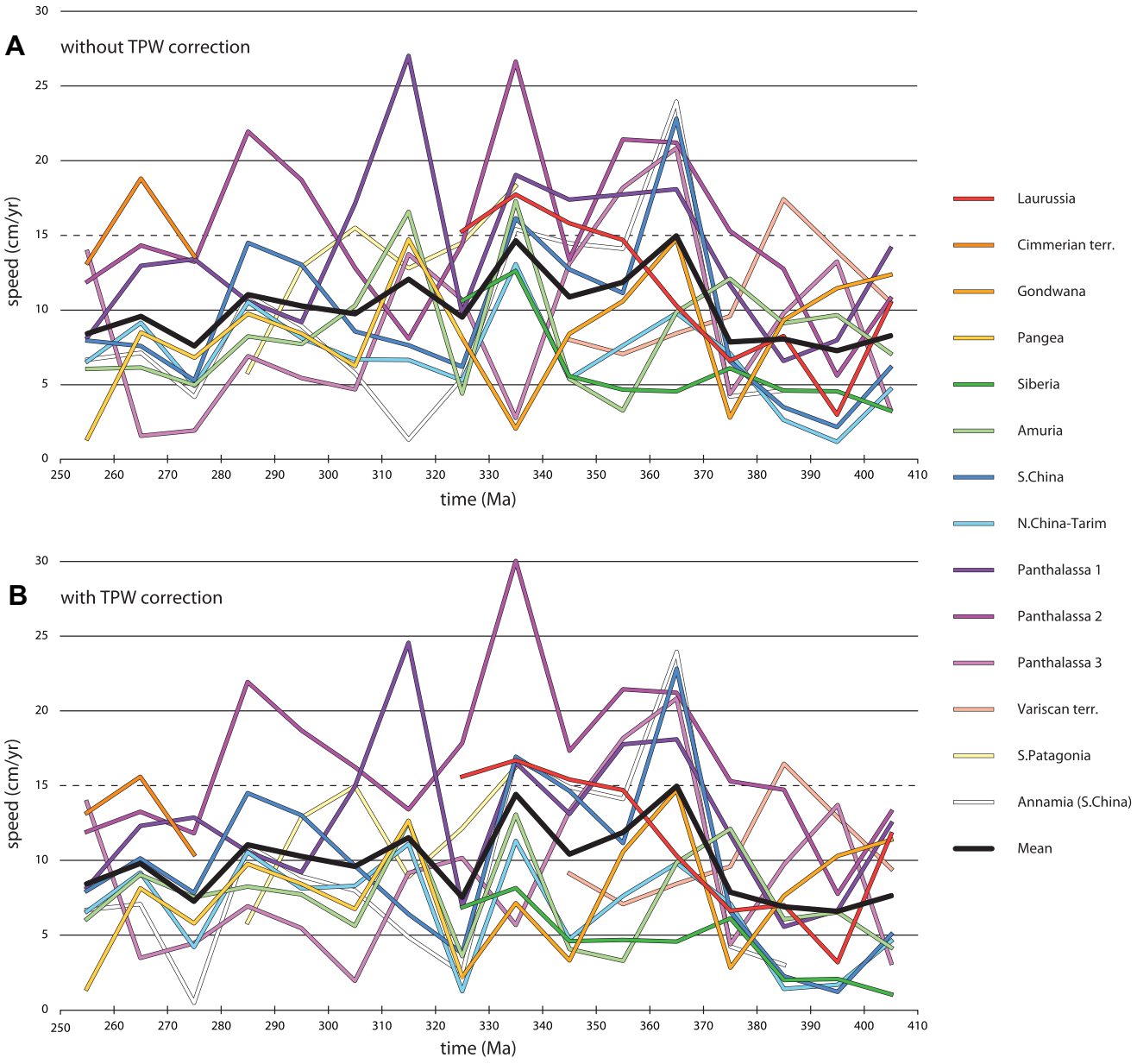


**Figure 16.** 10-Myr averaged speeds (cm/yr) for the continental and Panthalassa plates, calculated from their approximate centroids. (A) Before correction for true polar wander (TPW). (B) After correction for TPW.

and western Annamia in the Early to mid-Permian (Figs. 12 and 13). Subduction beneath those margins could have continued uninterrupted during initial rifting and subsequent spreading of the Neotethys, whereas subduction beneath the southern margin of Baltica must have recommenced following the opening of the Neotethys. Subduction of the Paleotethys and the corollary expansion of the Neotethys continued throughout the Permian and into the Triassic (Fig. 14).

Paleomagnetic studies of late Paleozoic and Triassic rocks from Iran provide strong support for its Permian-Triassic northward drift (Besse et al., 1998; Muttoni et al., 2009b), whereas hints of corresponding motion have been gleaned from meager paleomagnetic results from other Cimmerian terranes (Huang et al., 1992; Muttoni et al., 2009a; Ran et al., 2012). Although future work may corroborate variable rates of spreading along the Neotethys ridge (Muttoni et al., 2009a), the available data are not yet sufficient to resolve such detail, particularly given the rapid rate of drift of the terranes. We have simply modeled the drift of the Cimmerian terranes by a single, time-varying rotation defined by the paleomagnetic data from Iran. However, to avoid a premature (Permian) collision between Annamia and Sibumasu we have delayed the drifting of the latter from northeast Gondwana (by 7 Myr), and therefore invoked a short-lived transform between Qiangtang and Sibumasu (Fig. 13).

#### 4.3.2. *Proto-Asia*

The early Permian position of South China is unconstrained, but the 258 Ma Emishan LIP has provided both paleomagnetic data and a paleolongitude constraint (Torsvik et al., 2008b; Cocks and Torsvik, 2013). Together those data indicate that South China was positioned on the Equator and most likely above the westernmost margin of the Pacific LLSVP (Figs. 13 and 14). No paleogeographic

constraints are available from Annamia for the Permian, but its possible locations are limited by the positions of neighboring continents. As in the Carboniferous, the northwest and southwest margins of South China remained passive through the Permian, while *west-dipping* subduction of the Panthalassa continued beneath the proto-Japan arc outboard of the east margin (Figs. 12–14). In contrast, both the western and eastern passive margins of Annamia failed during the Permian: the former collapsed already at the start of the period and the latter developed into an active margin by 280 Ma (Figs. 12 and 13). Along the western margin, the occurrence of Permian subduction is indicated by the paired metamorphic belts and magmatic arc rocks of the Sukhothai terrane, which we have modeled as an independent unit beginning in the earliest Permian. To accord with the latest Carboniferous–Late Permian basinal deposits to the east of the Sukhothai terrane, we opened an ephemeral back-arc basin behind the Sukhothai arc that collapsed by the latest Permian (Figs. 12–14). In eastern Annamia, early Permian to Triassic arc-magmatic rocks in the Truong Son-Yaxianqiao arc reflect the operation of a *west-dipping* subduction zone that closed the basin separating Annamia and South China (Figs. 13 and 14). The age of HP metamorphic rocks as well as the youngest ophiolitic and magmatic arc rocks along the now-juxtaposed margins of those continents indicates that their collision occurred in the late Permian–early Triassic.

Early to late Permian paleomagnetic data from Tarim (Bai et al., 1987; Li et al., 1988; McFadden et al., 1988; Sharps et al., 1989; Gilder et al., 1996) and North China (Cocks and Torsvik, 2013) reveal that those continents remained stable at mid-low latitudes during the early Permian, but began to drift *north* after ~280 Ma (Figs. 12–14). North China also underwent a counterclockwise rotation in the middle–late Permian that is not reflected in the paleomagnetic data from Tarim, so we have allowed the two blocks to move relative to one another by transform motion roughly along the Altyn Tagh fault (Fig. 13). Relative motion also occurred between Tarim and Pangea during the Permian, so the *northwest* extension of the Tarim plate is also bounded by transform faults. Due to the dextral motion between Pangea and Tarim and the encroachment of Amuria on the latter, the oceanic lithosphere to

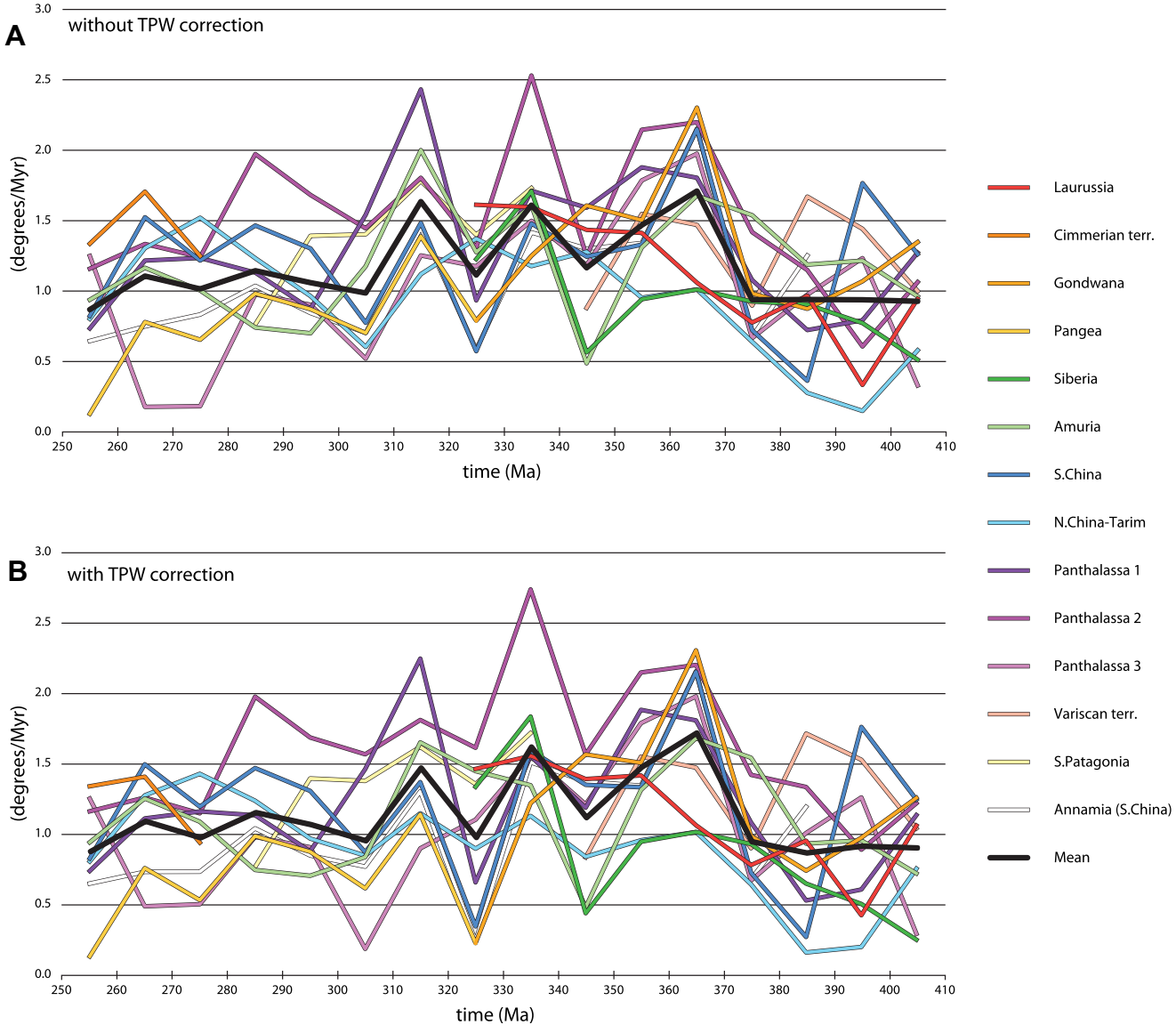


**Figure 17.** 10-Myr average rotations (degrees/Myr) for the continental and Panthalassa plates. (A) Before correction for true polar wander (TPW). (B) After correction for TPW.

the *northwest* of northern Tarim was progressively destroyed during the Permian, so that only the remnant Junggar Basin survived at 250 Ma (Figs. 12–14). Along the Kunlun-Qinling-Dabie margin, subduction of the Paleotethys continued throughout the Permian; terminal subduction of the Paleotethys ridge occurred in the mid-early Permian, just prior to the opening of the Neotethys. In Beishan and northern North China, subduction of the Paleoasian Ocean continued from the Carboniferous until the end-Permian, when the basin closed and North China collided with Amuria (Figs. 12–14). To accommodate the counterclockwise rotation of North China in the late early Permian we have allowed the opening of a minor backarc basin along the margin of Beishan; intriguingly, the Liuyuan-Yin'aoxia belt could represent the preserved relics of that ephemeral basin (Fig. 13). By the late Permian, subduction had also begun along the east margin of North China due to the convergence of South China and Annamia, and ultimately led to the amalgamation of the three blocks in the early Mesozoic.

#### 4.3.3. Marginal seas and the Panthalassa

Following on from the Carboniferous, the Slide Mountain Ocean continued to widen between western Laurentia and the Yukon-Tanana arc terrane during the early Permian (Fig. 12). However, the mid-Permian appearance of a magmatic arc and HP metamorphic rocks on the east side of the Yukon-Tanana terrane indicates that formerly-passive margin had collapsed by then, and that the Slide Mountain Ocean had begun subducting to the *west* (Fig. 13). By the end of the Permian the Slide Mountain Ocean had been consumed and the arc terranes of the upper plate were thrust *eastward* onto western Laurentia during the Sonoma orogeny (Fig. 14) (Dickinson, 2009). In contrast, passive margin sediments deposited in the Angayucham Ocean to the *north* reveal that it remained open until the Jurassic, suggesting either that the two systems had become decoupled in the mid-Permian (i.e. *west-dipping* subduction of the Angayucham Ocean did not commence in the mid-Permian) or that subduction was interrupted in the *north* before the basin was entirely destroyed. We have adopted the latter scenario and speculate that *west-dipping* subduction of the Angayucham Ocean ceased together with subduction to the *south* in the latest Permian to Triassic, leaving a remnant basin to the *east* that survived until the mid-Mesozoic (Fig. 14). Furthermore, we have adjusted the mid-to-late Permian relative motion between the Yukon-Tanana arc and the Panthalassa so as to be nearly-orthogonal in the *south* and highly oblique in the *north*; in that scenario, the accretion of the southern segment of the arc terrane could have disrupted the continuation of subduction to the north (Figs. 13 and 14).

Bivergent subduction of the MOO continued during the Permian, but as in the Carboniferous, spreading outpaced subduction and the ocean basin widened then (Figs. 12–14). Along its northeastern edge, the wedge-shaped MOO rode over the Panthalassa upon an intraoceanic subduction zone which had progressively lengthened throughout the late Paleozoic. The southern margin of Amuria also remained active throughout the Permian, first consuming the Panthalassa and later the Paleoasian Ocean, until terminal closure of the latter—which thus instigated collision between Amuria and North China—at the end of the Permian (Figs. 12–14).

In the latest Carboniferous, *southwest-dipping* subduction of the Panthalassa jumped outboard from the margin of southeast Gondwana to the intraoceanic Gympie-Brook Street island arc. However, at 270 Ma the remnant basin behind the Gympie-Brook Street terrane began to collapse by *west-dipping* subduction beneath the continental margin of Antarctica and Australia and by the end of the Permian the basin had been entirely consumed. The arc terrane accreted to the margin of Gondwana in the earliest Mesozoic during the Gondwanide/Hunter-Bowen orogeny. Along the west margin of Gondwana, subduction of the Panthalassa continued throughout the Permian (Figs. 12–14). Although we have not attempted to model it, an important episode of dextral transpression affected the entire margin of south Gondwana (from Chile to east Australia) during the Permian, producing a wide variety of tectonomagmatic features which are collectively associated with the nebulous "Gondwanides" orogeny. Future work in detailed modeling of the Panthalassa is necessary to decipher that tectonic puzzle.

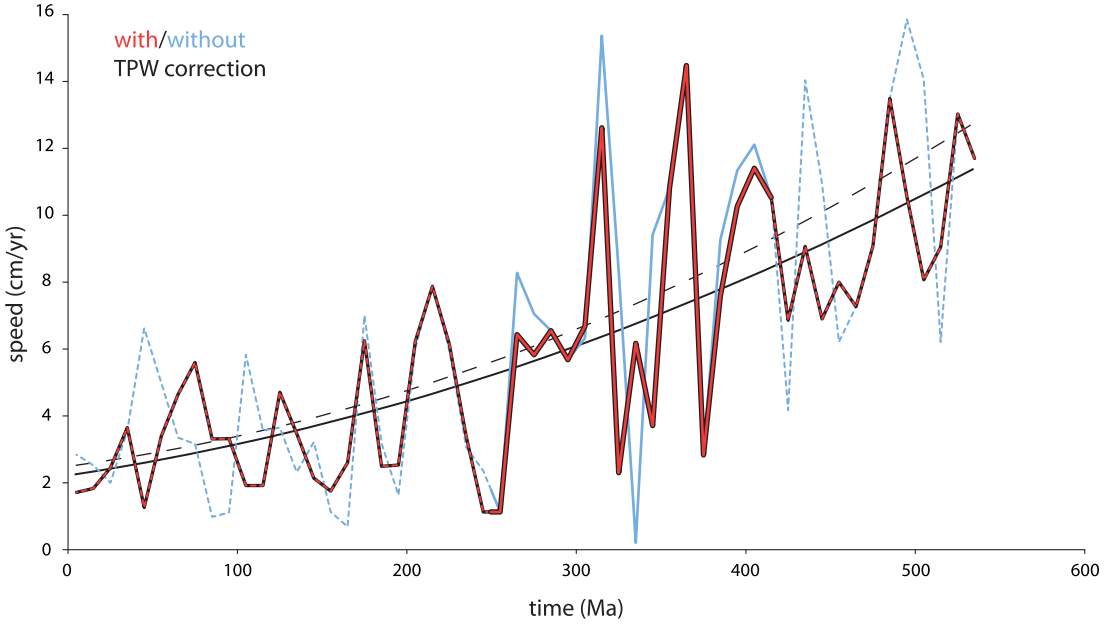


**Figure 18.** Plate speed of Africa (=Pangea before 200 Ma; =Gondwana before 320 Ma) through time, both before and after correction for true polar wander (TPW). Solid line segments highlight the late Paleozoic interval studied in this paper (410–250 Ma). Background polynomial curves highlight a trend of increasing plate speed with increasing age (solid/dashed = with/without TPW correction).

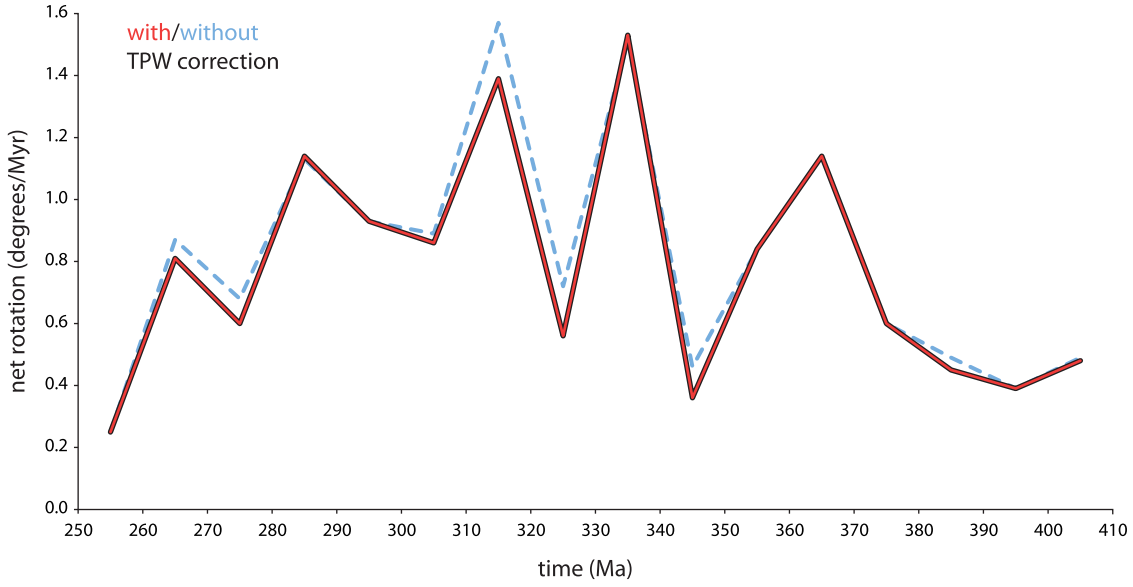


**Figure 19.** Net rotation of the lithosphere with and without correction for true polar wander (TPW).

## 5. Discussion

### 5.1. Model aspects and comparisons

The plates in our model number between 15 and 19 through time (Fig. 15), which is similar to the ~14–25 moderate-to-large sized plates today (Bird, 2003; DeMets et al., 2010) and to the 12–26 plates specified by Seton et al. (2012) for the Mesozoic. An important aspect of any plate model—but one rarely considered in Paleozoic paleogeography—is the speed of the specified plates. Observational data and geodynamic considerations suggest that large continental plates should not generally exceed speeds of ~15–20 cm/yr, whereas smaller oceanic plates may be capable of moving faster (Meert et al., 1993; Gurnis and Torsvik, 1994). In Fig. 16 we show the 10-Myr average speeds of the major plates in our model (those with continents and the Panthalassa plates), as determined at their approximate centroids (re-calculated every 10-Myr). Presented in cm/yr, those results communicate an intuitive metric of speed, but they do not fully describe plate motion as rotations do, and so we also show 10-Myr average rotation rates (Fig. 17).

In Figs. 16 and 17 plate motions are shown with and without correction for true polar wander (TPW)—which, if non-zero, should diminish the resultant motion of the global plate system. Prior to TPW correction most of the plates in our model already moved less than 15 cm/yr (Figs. 5–14). Five plates exhibited transient bursts of speed greater than 20 cm/yr, but three of those were Panthalassa plates, which are highly simplistic. Thus, those speeds could very likely be reduced through future work on the Panthalassa. The two other plates (South China and Annamia) were not constrained by any quantitative data during the interval of their shared high-speed (370–360 Ma), and so were semi-coupled to Gondwana through a transform boundary at that time. During that 10-Myr interval, Gondwana rotated very strongly about an Euler pole located in eastern Amazonia (Fig. 17), which was nearly 90° from South China and Annamia and nearly along strike of their mutual transform boundary with Gondwana. Thus, South China and Annamia were required to move at a relatively high-speed in order to maintain the transform boundary; otherwise it would have been necessary to invoke an ephemeral subduction zone. Because the positions of those blocks are poorly known before and after that interval, it is likely that better constraints on their paleogeography would also see their speeds fall.

The most notable plate that moved in excess of 15 cm/yr is Laurussia, which, before TPW correction, moved an average of 15.9 cm/yr between 360 and 320 Ma. Because the movement of Laurussia in the early Carboniferous was dominantly east-west (Figs. 9 and 10), its relatively high speed has not hitherto been recognized. That east-west movement of Laurussia must have been accommodated by dextral strike-slip along the northwest margin of Gondwana—and is substantiated by the widespread early Carboniferous dextral structures found in southeast Laurentia. We reiterate that the apparent difficulty of determining the 'upper-plate' during Rheic Ocean closure could be a reflection of great obliquity in the convergence of the continents, which would imply significant east-west motion of Laurussia (and/or Gondwana). With TPW correction, the speed of Laurussia dropped slightly over that interval to an average of 15.6 cm/yr. Likewise, the speeds of 15–20 cm/yr exhibited by the Variscan terranes, Amuria, South Patagonia and the Cimmerian terranes were reduced with TPW correction, although as small continents occupying larger oceanic plates, their pre-corrected speeds were not unreasonable.

To put the plate speeds observed in our model into a broader temporal context, in Fig. 18 we compare the mean plate speed for Pangea/Gondwana with that of the equivalent plate (Africa before 200 Ma, Gondwana after 320 Ma) from Torsvik et al. (submitted for publication) for the whole of the Phanerozoic. Ideally, we would compare the global mean plate speed over time, but that is not yet possible without a plate model for the early Paleozoic; we have thus opted to use the largest continental plate. It would be premature to draw any firm inferences about global tectonics from the time-dependent behavior of that single plate, but we cautiously note two prominent features of Fig. 18: the amplitude of plate speed increased dramatically for times prior ~300 Ma and the background trend shows increasing plate speed with increasing age. We think these features are probably manifestations of the uncertainty in the Paleozoic plate reconstructions (increasing uncertainty with age) and/or unaccounted TPW corrections, and that plate speeds in the Paleozoic could prove comparable to those of today. This highlights the need to routinely consider plate speeds in Paleozoic

reconstructions, and suggests that the apparently fast-moving plates in our model require further scrutiny. Speculatively, higher pre-Pangean plate speeds could alternatively be related to a more dynamic Earth.

Because our polygon coverage is global, another geodynamic consideration that we have used to evaluate the model is the net rotation of the lithosphere. In a spherical convective system with a viscosity structure that is uniform or only radially heterogeneous (stratified), the surface flow field will be purely poloidal (divergent-convergent). On Earth, however, lateral variations in viscosity occur in the upper mantle—particularly between suboceanic and subcontinental lithosphere—and are responsible for the toroidal (transform) component of plate motion (O'Connell et al., 1991; Ricard et al., 1991). Net rotation corresponds to the degree one harmonic of that toroidal field, and it, if calculated from an absolute mantle reference frame, describes the rigid rotation of the entire lithosphere with respect to the underlying mantle. Models of recent ($\leq$30 Ma) plate motion reveal that net rotation is currently directed westward and estimates of its rate of drift mostly fall below 0.2°/Myr (Conrad and Behn, 2010; Torsvik et al., 2010a,b). Broadly comparable estimates of net rotation have been deduced from numerical models and observations of seismic anisotropy (Becker, 2008; Conrad and Behn, 2010). Using a global polygon model, Torsvik et al. (2010a,b) computed net rotation back to 150 Ma and recognized a linear trend (increasing with age) superimposed on an otherwise fluctuating amplitude with an average of ~0.12°/Myr. By further considering the net rotation of different sub-sets of plates, they demonstrated that the linear trend was likely an artefact of increasing uncertainty with increasing model age (60% of the lithosphere is missing by 150 Ma), which implies that net rotation for the past 150 Ma has been similar in magnitude to that in the recent past.

In our model, net rotation ranged from 0.25°/Myr (at 255 Ma) to 1.53°/Myr (at 335 Ma), with an average of 0.77°/Myr (Fig. 19). Comparably, in the similarly-constructed 0–200 Ma global plate polygon model of Seton et al. (2012), rates of net rotation reached up to 1.0°/Myr in the Cretaceous. Under the assumption that net rotation in the Paleozoic and Mesozoic was broadly similar in magnitude to today, the rates predicted by these models are excessive. However, considering the degree of uncertainty in the reconstruction of now-subducted oceanic basins and that neither model was explicitly designed to minimize net rotation, the relatively high values are unsurprising. In our model, the Panthalassa constitutes an entire hemisphere and so strongly influenced net rotation; however, as the model of that basin is presently naïve, the high rates of net rotation are not especially concerning. This does, however, suggest that future work seeking to improve upon the reconstruction of the Panthalassa could exploit net rotation, by striving to reduce the rates to something more comparable to modern estimates.

### 5.2. Future directions

Opportunities for further testing and future improvement of our model are abundant. The most glaring over-simplification is our reconstruction of the Panthalassa, but improvements to our rudimentary kinematics could be achieved through consideration of ophiolite formation/emplacement ages or from inferences of relative motion drawn from the upper (continental) plates along the Panthalassa margin (for example, Kleiman and Japas, 2009; Fergusson, 2010). During the Mesozoic, several substantial terranes were accreted to west Laurentia and east Siberia—they were omitted from our model but must have been in the Panthalassa in the late Paleozoic; their reconstruction would thus provide more kinematic constraints for the Panthalassa. Broader approaches could aim to meet specified theoretical criteria, such as a particular global rate of subduction or oceanic crust production, or minimized net lithosphere rotation (as described above), but are themselves ad hoc.

Direct checks on the veracity of the underlying continental reconstruction model are also important. One of the exciting aspects of our plate model is the ease with which it can offer testable predictions. For example, even in the absence of paleomagnetic data, the model can generate a synthetic apparent polar wander path (APWP) for any plate. In lieu of paleomagnetic data, such a synthetic APWP would be predicated entirely on the other data-types built into the model (geology, paleobiology, derivative kinematics), but would be directly testable by newly-acquired paleomagnetic data.

Applications of our plate model will be important for numerical simulations of mantle convection (as a surface kinematic input), specifically in expanding their temporal reach (Bower et al., 2013; Bull et al., submitted for publication). Work is on-going to develop oceanic age-grids for the model, which should further expand its utility as an input, in serving geodynamic considerations in mantle models but also in providing possible paleo-bathymetry for paleo-ocean/climate simulations. Future efforts will be focused on the temporal expansion of the plate model back to the early Paleozoic and on merging it with plate models for younger times (Seton et al., 2012).

## 6. Conclusions

Paleogeography is fundamental to our understanding of the history of plate tectonics and thus vital in efforts to link plate kinematics and mantle dynamics. Unfortunately, the relentless operation of subduction has obliterated Paleozoic and early Mesozoic oceanic lithosphere, making pre-Cretaceous 'full-plate' paleogeographic reconstructions exceptionally challenging. However, with the development of new geodynamic concepts and analytical tools, it is now feasible to construct, test and share such models, even though they can only be considered provisional. Here we present a global plate model for the late Paleozoic (410–250 Ma), together with a review of the underlying data and interpretations. We trust that this model will be useful in extending the temporal reach of mantle models, but also hope that it may serve more broadly as a late Paleozoic tectonic framework for future testing and further improvement.

## Acknowledgements

We thank Editor M. Santosh for extending an invitation for this review, and reviewer Joseph Meert for providing constructive feedback. Robin Cocks is thanked for discussions and for reading the manuscript. The European Research Council under the European Union's Seventh Framework Programme (FP7/2007-2013)/ERC Advanced Grant Agreement Number 267631 (Beyond Plate Tectonics) and the Research Council of Norway through its Centres of Excellence funding scheme, project number 223272 (CEED) are acknowledged for financial support.

## Appendix A

Our plate model is shown in 20-Myr increments in Figs. 5–14 but a plate model can be generated at any age between 410 and 250 Ma using the supplementary data. Visualization of the data requires the latest version of Gplates (version 1.3.0 or newer; www.gplates.org). Download the supplementary data: http://www.earthdynamics.org/data/Domeier2014_data.zip and unzip all files

to a common subdirectory. Six files contain the supplementary data:

1. *LP TPW.rot* is a standard format Gplates rotation file for 410–250 Ma. The header (top 14 lines) includes our true polar wander (TPW) corrections.
2. *LP land.shp* (and other extensions) is an ARC-GIS shapefile that contains select, present-day continent outlines (coastlines).
3. *LP ridge.gmpl*, *LP subduction.gpml*, and *LP transform.gpml* are Gplates feature datafiles (in Gplates markup language format) containing our interpreted spreading ridge, subduction zone and transform plate boundaries, respectively.
4. *LP. topos.gpml* is a Gplates feature datafile (in Gplates markup language format) containing the topological plate polygons built from the ridge, subduction and transform plate boundary polyline files.

At Gplates start-up, select all the unzipped files ('File' > 'Open Feature Collection'). Gplates defaults to a mantle reference frame (plate ID = 0) and reconstructions will be displayed as TPW-corrected because of our header in the rotation file. To show reconstructions with respect to the spin-axis (i.e. a paleomagnetic reference frame), as in Figs. 5–14, change the Anchored Plate ID to 1. ('Reconstruction' > 'Specify Anchored Plate ID'). For further information on gplates and instructions on its use, visit www.gplates.org

## References


Abrajevitch, A., Van der Voo, R., Bazhenov, M.L., Levashova, N.M., McCausland, P.J.A., 2008. The role of the Kazakhstan orocline in the late Paleozoic amalgamation of Eurasia. Tectonophysics 455 (1–4), 61–76.

Abrajevitch, A., Van der Voo, R., Levashova, N.M., Bazhenov, M.L., 2007. Paleomagnetic constraints on the paleogeography and oroclinal bending of the Devonian volcanic arc in Kazakhstan. Tectonophysics 441 (1–4), 67–84.

Adams, C.J., 2008. Geochronology of Paleozoic terranes at the Pacific Ocean margin of Zealandia. Gondwana Research 13 (2), 250–258.

Al-Belushi, J., Glennie, K., Williams, B., 1996. Permo-Carboniferous Glaciogenic Al Khlata Formation, Oman: a new hypothesis for origin of its glaciation. GeoArabia 1 (3), 389–404.

Alexandre, P., Chalot-Prat, F., Saintot, A., Wijbrans, J., Stephenson, R., Wilson, M., Kitchka, A., Stovba, S., 2004. The $^{40}Ar/^{39}Ar$ dating of magmatic activity in the Donbas Fold Belt and the Scythian Platform (Eastern European Craton). Tectonics 23, TC5002.

Alirezaei, S., Hassanzadeh, J., 2012. Geochemistry and zircon geochronology of the Permian A-type Hasanrobat granite, Sanandaj–Sirjan belt: a new record of the Gondwana break-up in Iran. Lithos 151, 122–134.

Álvarez, J., Mpodozis, C., Arriagada, C., Astini, R., Morata, D., Salazar, E., Valencia, V.A., Vervoort, J.D., 2011. Detrital zircons from late Paleozoic accretionary complexes in north-central Chile (28°–32°S): possible fingerprints of the Chilenia terrane. Journal of South American Earth Sciences 32 (4), 460–476.

Amato, J.M., Toro, J., Miller, E.L., Gehrels, G.E., Farmer, G.L., Gottlieb, E.S., Till, A.B., 2009. Late Proterozoic-Paleozoic evolution of the Arctic Alaska-Chukotka terrane based on U-Pb igneous and detrital zircon ages: implications for Neoproterozoic paleogeographic reconstructions. Geological Society of America Bulletin 121 (9–10), 1219–1235.

Anfinson, O.A., Leier, A.L., Gaschnig, R., Embry, A.F., Dewing, K., Colpron, M., 2012. U–Pb and Hf isotopic data from Franklinian Basin strata: insights into the nature of Crockerland and the timing of accretion, Canadian Arctic Islands. Canadian Journal of Earth Sciences 49 (11), 1316–1328.

Angiolini, L., Balini, M., Garzanti, E., Nicora, A., Tintori, A., 2003. Gondwanan deglaciation and opening of Neotethys: the Al Khlata and Saiwan Formations of Interior Oman. Palaeogeography, Palaeoclimatology, Palaeoecology 196 (1–2), 99–123.

Arenas, R., Catalán, J.R.M., Martínez, S.S., García, F.D., Abati, J., Fernández-Suárez, J., Andonaegui, P., Gómez-Barreiro, J., 2007. Paleozoic ophiolites in the Variscan suture of Galicia (northwest Spain): distribution, characteristics, and meaning. Geological Society of America Memoirs 200, 425–444.

Arenas, R., Díez Fernández, R., Sánchez Martínez, S., Gerdes, A., Fernández-Suárez, J., Albert, R., 2014. Two-stage collision: exploring the birth of Pangea in the Variscan terranes. Gondwana Research 25 (2), 756–763.

Azor, A., Rubatto, D., Simancas, J.F., González Lodeiro, F., Martínez Poyatos, D., Martín Parra, L.M., Matas, J., 2008. Rheic Ocean ophiolitic remnants in southern Iberia questioned by SHRIMP U-Pb zircon ages on the Beja-Acebuches amphibolites. Tectonics 27, TC5006.

Badarch, G., Dickson Cunningham, W., Windley, B.F., 2002. A new terrane subdivision for Mongolia: implications for the Phanerozoic crustal growth of Central Asia. Journal of Asian Earth Sciences 21 (1), 87–110.

Bahlburg, H., Vervoort, J.D., Du Frane, S.A., Bock, B., Augustsson, C., Reimann, C., 2009. Timing of crust formation and recycling in accretionary orogens: insights learned from the western margin of South America. Earth-Science Reviews 97 (1–4), 215–241.

Bai, X., Liu, S., Wang, W., Yang, P., Li, Q., 2013. U–Pb geochronology and Lu–Hf isotopes of zircons from newly identified Permian–Early Triassic plutons in western Liaoning province along the northern margin of the North China Craton: constraints on petrogenesis and tectonic setting. International Journal of Earth Sciences, 1–15.

Bai, Y., Chen, G., Sun, Q., Sun, Y., Li, Y., Dong, Y., Sun, D., 1987. Late Paleozoic polar wander path for the Tarim platform and its tectonic significance. Tectonophysics 139 (1), 145–153.

Ballèvre, M., Bosse, V., Ducassou, C., Pitra, P., 2009. Palaeozoic history of the Armorican Massif: models for the tectonic evolution of the suture zones. Comptes Rendus Geoscience 341 (2–3), 174–201.

Baud, A., Richoz, S., Beauchamp, B., Cordey, F., Grasby, S., Henderson, C.M., Krystyn, L., Nicora, A., 2012. The Buday'ah Formation, Sultanate of Oman: a Middle Permian to Early Triassic oceanic record of the Neotethys and the late Induan microsphere bloom. Journal of Asian Earth Sciences 43 (1), 130–144.

Bazhenov, M.L., Levashova, N.M., Degtyarev, K.E., Van der Voo, R., Abrajevitch, A.V., McCausland, P.J., 2012. Unraveling the early–middle Paleozoic paleogeography of Kazakhstan on the basis of Ordovician and Devonian paleomagnetic results. Gondwana Research 22 (3), 974–991.

Bea, F., Fershtater, G.B., Montero, P., 2002. Granitoids of the Uralides: Implications for the Evolution of the Orogen, vol. 132, pp. 211–232.

Becker, T.W., 2008. Azimuthal seismic anisotropy constrains net rotation of the lithosphere. Geophysical Research Letters 35, L05303.

Beranek, L.P., Mortensen, J.K., 2011. The timing and provenance record of the Late Permian Klondike orogeny in northwestern Canada and arc-continent collision along western North America. Tectonics 30, TC5017.

Beranek, L.P., Mortensen, J.K., Lane, L.S., Allen, T.L., Fraser, T.A., Hadlari, T., Zantvoort, W.G., 2010. Detrital zircon geochronology of the western Ellesmerian clastic wedge, northwestern Canada: Insights on Arctic tectonics and the evolution of the northern Cordilleran miogeocline. Geological Society of America Bulletins 122 (11–12), 1899–1911.

Berberian, M., King, G., 1981. Towards a paleogeography and tectonic evolution of Iran. Canadian Journal of Earth Sciences 18 (2), 210–265.

Besse, J., Torcq, F., Gallet, Y., Ricou, L., Krystyn, L., Saidi, A., 1998. Late Permian to Late Triassic palaeomagnetic data from Iran: constraints on the migration of the Iranian block through the Tethyan Ocean and initial destruction of Pangaea. Geophysical Journal International 135 (1), 77–92.

Bird, P., 2003. An updated digital model of plate boundaries. Geochemistry, Geophysics, Geosystems 4 (3), 1027.

Biske, Y.S., Seltmann, R., 2010. Paleozoic Tian-Shan as a transitional region between the Rheic and Urals-Turkestan oceans. Gondwana Research 17 (2–3), 602–613.

Blendinger, W., van Vliet, A., Hughes Clarke, M.W., 1990. Updoming, rifting and continental margin development during the Late Palaeozoic in northern Oman. Geological Society, London, Special Publications 49 (1), 27–37.

Blight, J.H.S., Petterson, M.G., Crowley, Q.G., Cunningham, D., 2010. The Oyut Ulaan Volcanic Group: stratigraphy, magmatic evolution and timing of Carboniferous arc development in SE Mongolia. Journal of the Geological Society 167 (3), 491–509.

Boger, S.D., 2011. Antarctica — Before and after Gondwana. Gondwana Research 19 (2), 335–371.

Bower, D.J., Gurnis, M., Seton, M., 2013. Lower mantle structure from paleogeographically constrained dynamic Earth models. Geochemistry, Geophysics, Geosystems 14 (1), 44–63.

Bradley, D.C., 2008. Passive margins through Earth history. Earth-Science Reviews 91 (1–4), 1–26.

Braid, J.A., Murphy, J.B., Quesada, C., Mortensen, J., 2011. Tectonic escape of a crustal fragment during the closure of the Rheic Ocean: U-Pb detrital zircon data from the Late Palaeozoic Pulo do Lobo and South Portuguese zones, southern Iberia. Journal of the Geological Society 168 (2), 383–392.

Briggs, S.M., Yin, A., Manning, C.E., Chen, Z.L., Wang, X.F., Grove, M., 2007. Late Paleozoic tectonic history of the Ertix Fault in the Chinese Altai and its implications for the development of the Central Asian Orogenic System. Geological Society of America Bulletin 119 (7–8), 944–960.

Broska, I., Petrík, I., Majka, J., Bezák, V., 2013. Devonian/Mississippian I-type granitoids in the Western Carpathians: a subduction-related hybrid magmatism. Lithos 162, 27–36.

Brown, D., Herrington, R., Alvarez-Marron, J., 2011. Processes of Arc–Continent Collision in the Uralides, Arc-Continent Collision. Springer, pp. 311–340.

Brown, D., Juhlin, C., Ayala, C., Tryggvason, A., Bea, F., Alvarez-Marron, J., Carbonell, R., Seward, D., Glasmacher, U., Puchkov, V., Perez-Estaun, A., 2008. Mountain building processes during continent–continent collision in the Uralides. Earth-Science Reviews 89 (3–4), 177–195.

Brown, D., Juhlin, C., Tryggvason, A., Friberg, M., Rybalka, A., Puchkov, V., Petrov, G., 2006. Structural architecture of the southern and middle Urals foreland from reflection seismic profiles. Tectonics 25, TC1002.

Buiter, S.J.H., Torsvik, T.H., 2007. Horizontal movements in the Eastern Barents Sea constrained by numerical models and plate reconstructions. Geophysical Journal International 171, 1376–1389.

Bull, A.B., Domeier, M., Torsvik, T.H., 2014. The effect of Plate Motions on the Longevity of Deep Mantle Heterogeneties. Physics of the Earth and Planetary Interiors (under review).
Burchfiel, B.C., Zhiliang, C., Yupinc, L., Royden, L.H., 1995. Tectonics of the Longmen Shan and adjacent regions, Central China. International Geology Review 37 (8), 661–735.
Buslov, M.M., 2011. Tectonics and geodynamics of the Central Asian Foldbelt: the role of Late Paleozoic large-amplitude strike-slip faults. Russian Geology and Geophysics 52 (1), 52–71.
Buslov, M.M., Fujiwara, Y., Iwata, K., Semakov, N.N., 2004. Late Paleozoic-Early Mesozoic geodynamics of Central Asia. Gondwana Research 7 (3), 791–808.
Bussien, D., Gombojav, N., Winkler, W., von Quadt, A., 2011. The Mongol–Okhotsk Belt in Mongolia — An appraisal of the geodynamic development by the study of sandstone provenance and detrital zircons. Tectonophysics 510 (1–2), 132–150.
Bykadorov, V., Bush, V., Fedorenko, O., Filippova, I., Miletenko, N., Puchkov, V., Smirnov, A., Uzhkenov, B., Volozh, Y.A., 2003. Ordovician—Permian palaeogeography of Central Eurasia: development of Palaeozoic petroleum-bearing basins. Journal of Petroleum Geology 26 (3), 325–350.
Cai, J.-X., Zhang, K.-J., 2009. A new model for the Indochina and South China collision during the Late Permian to the Middle Triassic. Tectonophysics 467 (1–4), 35–43.
Cai, K., Sun, M., Yuan, C., Long, X., Xiao, W., 2011. Geological framework and Paleozoic tectonic history of the Chinese Altai, NW China: a review. Russian Geology and Geophysics 52 (12), 1619–1633.
Carroll, A.R., Graham, S.A., Chang, E.Z., McKnight, C., 2001. Sinian through Permian tectonostratigraphic evolution of the northwestern Tarim basin, China. Memoirs-Geological Society of America, 47–70.
Champion, D.C., Kositcin, N., Huston, D.L., Mathews, E., Brown, C., 2009. Geodynamic Synthesis of the Phanerozoic of Eastern Australia and Implications for Metallogeny. Geoscience Australia, p. 254.
Charvet, J., 2013. Late Paleozoic–Mesozoic tectonic evolution of SW Japan: a review – reappraisal of the accretionary orogeny and revalidation of the collisional model. Journal of Asian Earth Sciences 72, 88–101.
Charvet, J., Shu, L., Laurent-Charvet, S., Wang, B., Faure, M., Cluzel, D., Chen, Y., Jong, K., 2011. Palaeozoic tectonic evolution of the Tianshan belt, NW China. Science China Earth Sciences 54 (2), 166–184.
Chen, B., Jahn, B.M., Tian, W., 2009. Evolution of the Solonker suture zone: constraints from zircon U–Pb ages, Hf isotopic ratios and whole-rock Nd–Sr isotope compositions of subduction- and collision-related magmas and forearc sediments. Journal of Asian Earth Sciences 34 (3), 245–257.
Chen, D., Tucker, M., Zhu, J., Jiang, M., 2001. Carbonate sedimentation in a starved pull-apart basin, Middle to Late Devonian, southern Guilin, South China. Basin Research 13 (2), 141–167.
Chen, J.-F., Han, B.-F., Ji, J.-Q., Zhang, L., Xu, Z., He, G.-Q., Wang, T., 2010. Zircon U–Pb ages and tectonic implications of Paleozoic plutons in northern West Junggar, North Xinjiang, China. Lithos 115 (1–4), 137–152.
Chernicoff, C.J., Zappettini, E.O., Santos, J.O.S., McNaughton, N.J., Belousova, E., 2013. Combined U-Pb SHRIMP and Hf isotope study of the Late Paleozoic Yaminué Complex, Rio Negro Province, Argentina: implications for the origin and evolution of the Patagonia composite terrane. Geoscience Frontiers 4 (1), 37–56.
Chew, D.M., Schaltegger, U., Kosler, J., Whitehouse, M.J., Gutjahr, M., Spikings, R.A., Miskovic, A., 2007. U-Pb geochronologic evidence for the evolution of the Gondwanan margin of the north-central Andes. Geological Society of America Bulletin 119 (5–6), 697–711.
Choulet, F., Cluzel, D., Faure, M., Lin, W., Wang, B., Chen, Y., Wu, F.-Y., Ji, W., 2012a. New constraints on the pre-Permian continental crust growth of Central Asia (West Junggar, China) by U-Pb and Hf isotopic data from detrital zircon. Terra Nova 24 (3), 189–198.
Choulet, F., Faure, M., Cluzel, D., Chen, Y., Lin, W., Wang, B., 2012b. From oblique accretion to transpression in the evolution of the Altaid collage: new insights from West Junggar, northwestern China. Gondwana Research 21 (2–3), 530–547.
Cocks, L.R.M., Torsvik, T.H., 2005. Baltica from the late Precambrian to mid-Palaeozoic times: the gain and loss of a terrane's identity. Earth-Science Reviews 72 (1–2), 39–66.
Cocks, L.R.M., Torsvik, T.H., 2007. Siberia, the wandering northern terrane, and its changing geography through the Palaeozoic. Earth-Science Reviews 82 (1–2), 29–74.
Cocks, L.R.M., Torsvik, T.H., 2011. The Palaeozoic geography of Laurentia and western Laurussia: a stable craton with mobile margins. Earth-Science Reviews 106 (1–2), 1–51.
Cocks, L.R.M., Torsvik, T.H., 2013. The dynamic evolution of the Palaeozoic geography of eastern Asia. Earth-Science Reviews 117, 40–79.
Colpron, M., Nelson, J.L., 2009. A Palaeozoic Northwest Passage: incursion of Caledonian, Baltican and Siberian terranes into eastern Panthalassa, and the early evolution of the North American Cordillera. Geological Society, London, Special Publications 318 (1), 273–307.
Colpron, M., Nelson, J.L., 2011. A Palaeozoic NW Passage and the Timanian, Caledonian and Uralian connections of some exotic terranes in the North American Cordillera (Chapter 31). Geological Society, London Memoirs 35 (1), 463–484.
Conrad, C.P., Behn, M.D., 2010. Constraints on lithosphere net rotation and asthenospheric viscosity from global mantle flow models and seismic anisotropy. Geochemistry, Geophysics, Geosystems 11, Q05W05.
Cook, F.A., Vasudevan, K., 2006. Reprocessing and enhanced interpretation of the initial COCORP Southern Appalachians traverse. Tectonophysics 420 (1–2), 161–174.
Cope, T., Ritts, B.D., Darby, B.J., Fildani, A., Graham, S.A., 2005. Late paleozoic sedimentation on the northern margin of the North China block: implications for regional tectonics and climate change. International Geology Review 47 (3), 270–296.
Cowgill, E., Yin, A., Harrison, T.M., Xiao-Feng, W., 2003. Reconstruction of the Altyn Tagh fault based on U-Pb geochronology: role of back thrusts, mantle sutures, and heterogeneous crustal strength in forming the Tibetan Plateau. Journal of Geophysical Research 108 (B7), 2346.
Curtis, M.L., 2001. Tectonic history of the Ellsworth Mountains, West Antarctica: reconciling a Gondwana enigma. Geological Society of America Bulletin 113 (7), 939–958.
Dahlquist, J.A., Alasino, P.H., Eby, G.N., Galindo, C., Casquet, C., 2010. Fault controlled Carboniferous A-type magmatism in the proto-Andean foreland (Sierras Pampeanas, Argentina): geochemical constraints and petrogenesis. Lithos 115 (1–4), 65–81.
DeMets, C., Gordon, R.G., Argus, D.F., 2010. Geologically current plate motions. Geophysical Journal International 181, 1–80.
Demoux, A., Kroner, A., Hegner, E., Badarch, G., 2009. Devonian arc-related magmatism in the Tseel terrane of SW Mongolia: chronological and geochemical evidence. Journal of the Geological Society 166 (3), 459–471.
Dickinson, W.R., 2009. Anatomy and global context of the North American Cordillera. Backbone of the Americas: shallow subduction, plateau uplift, and ridge and terrane collision. Geological Society of America Memoirs 204, 1–29.
Ding, L., Yang, D., Cai, F.L., Pullen, A., Kapp, P., Gehrels, G.E., Zhang, L.Y., Zhang, Q.H., Lai, Q.Z., Yue, Y.H., Shi, R.D., 2013. Provenance analysis of the Mesozoic Hoh-Xil-Songpan-Ganzi turbidites in northern Tibet: implications for the tectonic evolution of the eastern Paleo-Tethys Ocean. Tectonics 32 (1), 34–48.
Domeier, M., Van der Voo, R., Torsvik, T.H., 2012. Paleomagnetism and Pangea: the road to reconciliation. Tectonophysics 514, 14–43.
Dong, Y., Zhang, G., Neubauer, F., Liu, X., Genser, J., Hauzenberger, C., 2011a. Tectonic evolution of the Qinling orogen, China: review and synthesis. Journal of Asian Earth Sciences 41 (3), 213–237.
Dong, Y., Zhang, G., Neubauer, F., Liu, X., Hauzenberger, C., Zhou, D., Li, W., 2011b. Syn- and post-collisional granitoids in the Central Tianshan orogen: geochemistry, geochronology and implications for tectonic evolution. Gondwana Research 20 (2–3), 568–581.
Donskaya, T.V., Gladkochub, D.P., Mazukabzov, A.M., Ivanov, A.V., 2013. Late Paleozoic – Mesozoic subduction-related magmatism at the southern margin of the Siberian continent and the 150 million-year history of the Mongol-Okhotsk Ocean. Journal of Asian Earth Sciences 62, 79–97.
Dostal, J., Vozár, J., Keppie, J., Hovorka, D., 2003. Permian volcanism in the Central Western Carpathians (Slovakia): Basin-and-Range type rifting in the southern Laurussian margin. International Journal of Earth Sciences 92 (1), 27–35.
Economos, R., Paterson, S., Said, L., Ducea, M., Anderson, J., Padilla, A., 2012. Gobi-Tianshan connections: field observations and isotopes from an early Permian arc complex in southern Mongolia. Geological Society of America Bulletin 124 (11–12), 1688–1701.
Elliot, D.H., Fanning, C.M., 2008. Detrital zircons from upper Permian and lower Triassic Victoria Group sandstones, Shackleton Glacier region, Antarctica: evidence for multiple sources along the Gondwana plate margin. Gondwana Research 13 (2), 259–274.
Faryad, S.W., 2011. Distribution and Geological Position of High-/Ultrahigh-pressure Units Within the European Variscan Belt, pp. 361–397.
Faryad, S.W., Kachlík, V., 2013. New evidence of blueschist facies rocks and their geotectonic implication for Variscan suture(s) in the Bohemian Massif. Journal of Metamorphic Geology 31 (1), 63–82.
Faure, M., Bé Mézème, E., Cocherie, A., Rossi, P., Chemenda, A., Boutelier, D., 2008. Devonian geodynamic evolution of the Variscan Belt, insights from the French Massif Central and Massif Armoricain. Tectonics 27, TC2005.
Faure, M., Sommers, C., Melleton, J., Cocherie, A., Lautout, O., 2010. The Léon Domain (French Massif Armoricain): a westward extension of the Mid-German Crystalline Rise? Structural and geochronological insights. International Journal of Earth Sciences 99 (1), 65–81.
Feng, J., Xiao, W., Windley, B., Han, C., Wan, B., Zhang, J.e., Ao, S., Zhang, Z., Lin, L., 2013. Field geology, geochronology and geochemistry of mafic–ultramafic rocks from Alxa, China: implications for Late Permian accretionary tectonics in the southern Altaids. Journal of Asian Earth Sciences 78, 114–142.
Fergusson, C.L., 2010. Plate-driven extension and convergence along the East Gondwana active margin: Late Silurian–Middle Devonian tectonics of the Lachlan Fold Belt, southeastern Australia. Australian Journal of Earth Sciences 57 (5), 627–649.
Franke, W., 2006. The Variscan orogen in Central Europe: construction and collapse. Geological Society London Memoirs 32 (1), 333–343.
Gaggero, L., Oggiano, G., Funedda, A., Buzzi, L., 2012. Rifting and arc-related Early Paleozoic volcanism along the North Gondwana margin: geochemical and geological evidence from Sardinia (Italy). The Journal of Geology 120 (3), 273–292.
Gao, J., Klemd, R., Qian, Q., Zhang, X., Li, J., Jiang, T., Yang, Y., 2011. The collision between the Yili and Tarim blocks of the Southwestern Altaids: geochemical and age constraints of a leucogranite dike crosscutting the HP–LT metamorphic belt in the Chinese Tianshan Orogen. Tectonophysics 499 (1–4), 118–131.

Gao, J., Long, L., Klemd, R., Qian, Q., Liu, D., Xiong, X., Su, W., Liu, W., Wang, Y., Yang, F., 2009. Tectonic evolution of the South Tianshan orogen and adjacent regions, NW China: geochemical and age constraints of granitoid rocks. International Journal of Earth Sciences 98 (6), 1221–1238.
Garzanti, E., Gaetani, M., 2002. Unroofing history of late paleozoic magmatic arcs within the "Turan Plate"(Tuarkyr, Turkmenistan). Sedimentary Geology 151 (1), 67–87.
Garzanti, E., Le Fort, P., Sciunnach, D., 1999. First report of Lower Permian basalts in South Tibet: tholeiitic magmatism during break-up and incipient opening of Neotethys. Journal of Asian Earth Sciences 17 (4), 533–546.
Ge, R., Zhu, W., Wu, H., Zheng, B., Zhu, X., He, J., 2012. The Paleozoic northern margin of the Tarim Craton: passive or active? Lithos 142–143, 1–15.
Gee, D.G., Bogolepova, O.K., Lorenz, H., 2006. The Timanide, Caledonide and Uralide orogens in the Eurasian high Arctic, and relationships to the palaeo-continents Laurentia, Baltica and Siberia. Geological Society, London Memoirs 32 (1), 507–520.
Geng, H., Sun, M., Yuan, C., Zhao, G., Xiao, W., 2011. Geochemical and geochronological study of early Carboniferous volcanic rocks from the West Junggar: petrogenesis and tectonic implications. Journal of Asian Earth Sciences 42 (5), 854–866.
Gilder, S., Zhao, X., Coe, R., Meng, Z., Courtillot, V., Besse, J., 1996. Paleomagnetism and tectonics of the southern Tarim basin, northwestern China. Journal of Geophysical Research: Solid Earth (1978–2012) 101 (B10), 22015–22031.
Glen, R.A., 2005. The Tasmanides of eastern Australia. Geological Society, London, Special Publications 246 (1), 23–96.
Glen, R.A., 2013. Refining accretionary orogen models for the Tasmanides of eastern Australia. Australian Journal of Earth Sciences 60 (3), 315–370.
Glorie, S., De Grave, J., Buslov, M.M., Zhimulev, F.I., Izmer, A., Vandoorne, W., Ryabinin, A., Van den haute, P., Vanhaecke, F., Elburg, M.A., 2011a. Formation and Palaeozoic evolution of the Gorny-Altai–Altai-Mongolia suture zone (South Siberia): zircon U/Pb constraints on the igneous record. Gondwana Research 20 (2–3), 465–484.
Glorie, S., De Grave, J., Buslov, M.M., Zhimulev, F.I., Stockli, D.F., Batalev, V.Y., Izmer, A., Van den haute, P., Vanhaecke, F., Elburg, M.A., 2011b. Tectonic history of the Kyrgyz South Tien Shan (Atbashi-Inylchek) suture zone: the role of inherited structures during deformation-propagation. Tectonics 30, TC6016.
Glorie, S., De Grave, J., Delvaux, D., Buslov, M.M., Zhimulev, F.I., Vanhaecke, F., Elburg, M.A., Van den haute, P., 2012. Tectonic history of the Irtysh shear zone (NE Kazakhstan): new constraints from zircon U/Pb dating, apatite fission track dating and palaeostress analysis. Journal of Asian Earth Sciences 45, 138–149.
Görz, I., Hielscher, P., 2010. An explicit plate kinematic model for the orogeny in the southern Uralides. Tectonophysics 493 (1–2), 1–26.
Gray, D.R., Foster, D.A., 2004. Tectonic evolution of the Lachlan Orogen, southeast Australia: historical review, data synthesis and modern perspectives. Australian Journal of Earth Sciences 51 (6), 773–817.
Grosse, P., Söllner, F., Báez, M.A., Toselli, A.J., Rossi, J.N., Jesus, D., 2009. Lower Carboniferous post-orogenic granites in central-eastern Sierra de Velasco, Sierras Pampeanas, Argentina: U–Pb monazite geochronology, geochemistry and Sr–Nd isotopes. International Journal of Earth Sciences 98 (5), 1001–1025.
Gurnis, M., Torsvik, T.H., 1994. Rapid drift of large continents during the late Precambrian and Paleozoic: paleomagnetic constraints and dynamic models. Geology 22, 1023–1026.
Gurnis, M., Turner, M., Zahirovic, S., DiCaprio, L., Spasojevic, S., Müller, R.D., Boyden, J., Seton, M., Manea, V.C., Bower, D.J., 2012. Plate tectonic reconstructions with continuously closing plates. Computers & Geosciences 38 (1), 35–42.
Gutiérrez-Alonso, G., Fernández-Suárez, J., Weil, A.B., Murphy, J.B., Nance, R.D., Corfú, F., Johnston, S.T., 2008. Self-subduction of the Pangaean global plate. Nature Geoscience 1 (8), 549–553.
Hacker, B.R., Wallis, S.R., Ratschbacher, L., Grove, M., Gehrels, G., 2006. High-temperature geochronology constraints on the tectonic history and architecture of the ultrahigh-pressure Dabie-Sulu Orogen. Tectonics 25, TC5006.
Han, B.-F., Guo, Z.-J., Zhang, Z.-C., Zhang, L., Chen, J.-F., Song, B., 2010. Age, geochemistry, and tectonic implications of a late Paleozoic stitching pluton in the North Tian Shan suture zone, western China. Geological Society of America Bulletin 122 (3–4), 627–640.
Han, B.-F., He, G.-Q., Wang, X.-C., Guo, Z.-J., 2011. Late Carboniferous collision between the Tarim and Kazakhstan–Yili terranes in the western segment of the South Tian Shan Orogen, Central Asia, and implications for the Northern Xinjiang, western China. Earth-Science Reviews 109 (3–4), 74–93.
Hanzl, P., Bat-Ulzii, D., Rejchrt, M., Kosler, J., Bolormaa, K., Hrdlickova, K., 2008. Geology and geochemistry of the Palaeozoic plutonic bodies of the Trans-Altay Gobi, SW Mongolia: implications for magmatic processes in an accreted volcanic-arc system. Journal of Geosciences 53 (2), 201–234.
Hatcher, R.D., 2010. The Appalachian orogen: a brief summary. From Rodinia to Pangea: The Lithotectonic Record of the Appalachian Region Geological Society of America Memoirs 206, 1–19.
Heatherington, A.L., Mueller, P.A., Wooden, J.L., 2010. Alleghanian plutonism in the Suwannee terrane, USA: implications for late Paleozoic tectonic models. Geological Society of America Memoirs 206, 607–620.
Helo, C., Hegner, E., Kröner, A., Badarch, G., Tomurtogoo, O., Windley, B.F., Dulski, P., 2006. Geochemical signature of Paleozoic accretionary complexes of the Central Asian Orogenic Belt in South Mongolia: constraints on arc environments and crustal growth. Chemical Geology 227 (3–4), 236–257.
Hervé, F., Calderón, M., Fanning, C.M., Pankhurst, R.J., Godoy, E., 2013. Provenance variations in the Late Paleozoic accretionary complex of central Chile as indicated by detrital zircons. Gondwana Research 23 (3), 1122–1135.
Hibbard, J.P., van Staal, C.R., Rankin, D.W., 2010. Comparative analysis of the geological evolution of the northern and southern Appalachian orogen: Late Ordovician-Permian. From Rodinia to Pangea: The Lithotectonic Record of the Appalachian Region Geological Society of America Memoirs 206, 51–69.
Hoepffner, C., Houari, M.R., Bouabdelli, M., 2006. Tectonics of the North African Variscides (Morocco, western Algeria): an outline. Comptes Rendus Geoscience 338 (1–2), 25–40.
Hu, X., Huang, Z., Wang, J., Yu, J., Xu, K., Jansa, L., Hu, W., 2012. Geology of the Fuding inlier in southeastern China: implication for late Paleozoic Cathaysian paleogeography. Gondwana Research 22 (2), 507–518.
Huang, B., Otofuji, Y.-i., Zhu, R., Shi, R., Wang, Y., 2001. Paleomagnetism of Carboniferous sediments in the Hexi corridor: its origin and tectonic implications. Earth and Planetary Science Letters 194 (1), 135–149.
Huang, K., Opdyke, N.D., Peng, X., Li, J., 1992. Paleomagnetic results from the Upper Permian of the eastern Qiangtang Terrane of Tibet and their tectonic implications. Earth and Planetary Science Letters 111 (1), 1–10.
Isozaki, Y., Aoki, K., Nakama, T., Yanai, S., 2010. New insight into a subduction-related orogen: a reappraisal of the geotectonic framework and evolution of the Japanese Islands. Gondwana Research 18 (1), 82–105.
Jahn, B.M., 2010. Accretionary orogen and evolution of the Japanese Islands: Implications from a Sr-Nd isotopic study of the Phanerozoic granitoids from SW Japan. American Journal of Science 310 (10), 1210–1249.
Jia, D., Wei, G., Chen, Z., Li, B., Zeng, Q., Yang, G., 2006. Longmen Shan fold-thrust belt and its relation to the western Sichuan Basin in central China: new insights from hydrocarbon exploration. AAPG Bulletin 90 (9), 1425–1447.
Jia, R.-Y., Jiang, Y.-H., Liu, Z., Zhao, P., Zhou, Q., 2013. Petrogenesis and tectonic implications of early Silurian high-K calc-alkaline granites and their potassic microgranular enclaves, western Kunlun orogen, NW Tibetan Plateau. International Geology Review 55 (8), 958–975.
Jian, P., Kröner, A., Windley, B.F., Shi, Y., Zhang, W., Zhang, L., Yang, W., 2012. Carboniferous and Cretaceous mafic–ultramafic massifs in Inner Mongolia (China): a SHRIMP zircon and geochemical study of the previously presumed integral "Hegenshan ophiolite". Lithos 142, 48–66.
Jian, P., Liu, D., Kröner, A., Zhang, Q., Wang, Y., Sun, X., Zhang, W., 2009a. Devonian to Permian plate tectonic cycle of the Paleo-Tethys Orogen in southwest China (I): geochemistry of ophiolites, arc/back-arc assemblages and within-plate igneous rocks. Lithos 113 (3–4), 748–766.
Jian, P., Liu, D., Kröner, A., Zhang, Q., Wang, Y., Sun, X., Zhang, W., 2009b. Devonian to Permian plate tectonic cycle of the Paleo-Tethys Orogen in southwest China (II): Insights from zircon ages of ophiolites, arc/back-arc assemblages and within-plate igneous rocks and generation of the Emeishan CFB province. Lithos 113 (3–4), 767–784.
Jiang, Y.-H., Jia, R.-Y., Liu, Z., Liao, S.-Y., Zhao, P., Zhou, Q., 2013. Origin of Middle Triassic high-K calc-alkaline granitoids and their potassic microgranular enclaves from the western Kunlun orogen, northwest China: a record of the closure of Paleo-Tethys. Lithos 156–159, 13–30.
Kato, T.T., Sharp, W.D., Godoy, E., 2008. Inception of a Devonian subduction zone along the southwestern Gondwana margin: $^{40}Ar$-$^{39}Ar$ dating of eclogite-amphibolite assemblages in blueschist boulders from the Coastal Range of Chile (41° S). Canadian Journal of Earth Sciences 45 (3), 337–351.
Keppie, J.D., Dostal, J., Murphy, J.B., Galaz-Escanilla, G., Ramos-Arias, M.A., Nance, R.D., 2012. High pressure rocks of the Acatlán Complex, southern Mexico: large-scale subducted Ordovician rifted passive margin extruded into the upper plate during the Devonian–Carboniferous. Tectonophysics 560–561, 1–21.
Keppie, J.D., Dostal, J., Murphy, J.B., Nance, R.D., 2008. Synthesis and tectonic interpretation of the westernmost Paleozoic Variscan orogen in southern Mexico: from rifted Rheic margin to active Pacific margin. Tectonophysics 461 (1–4), 277–290.
Keppie, J.D., Ramos, V.A., 1999. Odyssey of Terranes in the Iapetus and Rheic Oceans during the Paleozoic, vol. 336, pp. 267–276.
Khudoley, A.K., Guriev, G.A., 2003. Influence of syn-sedimentary faults on orogenic structure: examples from the Neoproterozoic–Mesozoic east Siberian passive margin. Tectonophysics 365 (1–4), 23–43.
Kirsch, M., Keppie, J.D., Murphy, J.B., Solari, L.A., 2012. Permian-Carboniferous arc magmatism and basin evolution along the western margin of Pangea: geochemical and geochronological evidence from the eastern Acatlan Complex, southern Mexico. Geological Society of America Bulletin 124 (9–10), 1607–1628.
Kleiman, L.E., Japas, M.S., 2009. The Choiyoi volcanic province at 34°S–36°S (San Rafael, Mendoza, Argentina): Implications for the Late Palaeozoic evolution of the southwestern margin of Gondwana. Tectonophysics 473 (3–4), 283–299.
Knittel, U., Hung, C.-H., Yang, T.F., Iizuka, Y., 2010. Permian arc magmatism in Mindoro, the Philippines: an early Indosinian event in the Palawan Continental Terrane. Tectonophysics 493 (1–2), 113–117.
Konopelko, D., Biske, G., Seltmann, R., Eklund, O., Belyatsky, B., 2007. Hercynian post-collisional A-type granites of the Kokshaal Range, Southern Tien Shan, Kyrgyzstan. Lithos 97 (1–2), 140–160.
Kravchinsky, V.A., Sorokin, A.A., Courtillot, V., 2002. Paleomagnetism of Paleozoic and Mesozoic sediments from the southern margin of Mongol-Okhotsk ocean, far eastern Russia. Journal of Geophysical Research 107 (B10), 2253.

Kroner, A., Lehmann, J., Schulmann, K., Demoux, A., Lexa, O., Tomurhuu, D., Stipska, P., Liu, D., Wingate, M.T.D., 2010. Lithostratigraphic and geochronological constraints on the evolution of the Central Asian Orogenic Belt in SW Mongolia: Early Paleozoic rifting followed by late Paleozoic accretion. American Journal of Science 310 (7), 523–574.
Kurihara, T., Tsukada, K., Otoh, S., Kashiwagi, K., Chuluun, M., Byambadash, D., Boijir, B., Gonchigdorj, S., Nuramkhan, M., Niwa, M., Tokiwa, T., Hikichi, G.y., Kozuka, T., 2009. Upper Silurian and Devonian pelagic deep-water radiolarian chert from the Khangai–Khentei belt of Central Mongolia: evidence for Middle Paleozoic subduction–accretion activity in the Central Asian Orogenic Belt. Journal of Asian Earth Sciences 34 (2), 209–225.
Lane, L.S., 2007. Devonian–Carboniferous paleogeography and orogenesis, northern Yukon and adjacent Arctic Alaska. Canadian Journal of Earth Sciences 44 (5), 679–694.
Laurent-Charvet, S., Charvet, J., Monié, P., Shu, L., 2003. Late Paleozoic strike-slip shear zones in eastern central Asia (NW China): new structural and geochronological data. Tectonics 22, 1009.
Leat, P.T., Storey, B.C., Pankhurst, R.J., 1993. Geochemistry of Palaeozoic-Mesozoic Pacific rim orogenic magmatism, Thurston Island area, West Antarctica. Antarctic Science 5, 281–296.
Lee, C.W., 1990. A review of platform sedimentation in the Early and Late Permian of Oman, with particular reference to the Oman Mountains. Geological Society, London, Special Publications 49 (1), 39–47.
Lepvrier, C., Van Vuong, N., Maluski, H., Truong Thi, P., Van Vu, T., 2008. Indosinian tectonics in Vietnam. Comptes Rendus Geoscience 340 (2–3), 94–111.
Levashova, N.M., Degtyarev, K.E., Bazhenov, M.L., 2012. Oroclinal bending of the Middle and Late Paleozoic volcanic belts in Kazakhstan: paleomagnetic evidence and geological implications. Geotectonics 46 (4), 285–302.
Li, S., Wang, T., Wilde, S.A., Tong, Y., Hong, D., Guo, Q., 2012a. Geochronology, petrogenesis and tectonic implications of Triassic granitoids from Beishan, NW China. Lithos 134–135, 123–145.
Li, X.-H., Li, Z.-X., He, B., Li, W.-X., Li, Q.-L., Gao, Y., Wang, X.-C., 2012b. The Early Permian active continental margin and crustal growth of the Cathaysia Block: In situ U–Pb, Lu–Hf and O isotope analyses of detrital zircons. Chemical Geology 328, 195–207.
Li, X.H., Li, Z.X., Li, W.X., Wang, Y., 2006. Initiation of the Indosinian Orogeny in South China: evidence for a Permian magmatic arc on Hainan Island. The Journal of Geology 114 (3), 341–353.
Li, Y., McWillams, M., Sharps, R., Cox, A., Li, Y., Li, Q., Gao, Z., Zhang, Z., Zhai, Y., 1990. A Devonian paleomagnetic pole from red beds of the Tarim Block, China. Journal of Geophysical Research 95 (B12), 19185.
Li, Y., McWilliams, M., Cox, A., Sharps, R., Li, Y., Gao, Z., Zhang, Z., Zhai, Y., 1988. Late Permian paleomagnetic pole from dikes of the Tarim craton, China. Geology 16 (3), 275–278.
Li, Y., Zhou, H., Brouwer, F.M., Xiao, W., Wijbrans, J.R., Zhao, J., Zhong, Z., Liu, H., 2013. Nature and timing of the Solonker suture of the Central Asian Orogenic Belt: insights from geochronology and geochemistry of basic intrusions in the Xilin Gol Complex, Inner Mongolia, China. International Journal of Earth Sciences, 1–20.
Li, Z.X., Li, X.H., Wartho, J.A., Clark, C., Li, W.X., Zhang, C.L., Bao, C., 2010. Magmatic and metamorphic events during the early Paleozoic Wuyi-Yunkai orogeny, southeastern South China: new age constraints and pressure-temperature conditions. Geological Society of America Bulletin 122 (5–6), 772–793.
Liu, J., Li, J., Chi, X., Qu, J., Hu, Z., Fang, S., Zhang, Z., 2013. A late-Carboniferous to early early-Permian subduction-accretion complex in Daqing pasture, southeastern Inner Mongolia: evidence of northward subduction beneath the Siberian paleoplate southern margin. Lithos 117, 285–296.
Liu, J., Tran, M.-D., Tang, Y., Nguyen, Q.-L., Tran, T.-H., Wu, W., Chen, J., Zhang, Z., Zhao, Z., 2012a. Permo-Triassic granitoids in the northern part of the Truong Son belt, NW Vietnam: geochronology, geochemistry and tectonic implications. Gondwana Research 22 (2), 628–644.
Liu, X., Li, S., Suo, Y., Liu, X., Dai, L., Santosh, M., 2012b. Structural analysis of the northern Tongbai Metamorphic Terranes, Central China: Implications for Paleozoic accretionary process on the southern margin of the North China Craton. Journal of Asian Earth Sciences 47, 143–154.
Liu, X.C., Jahn, B.M., Hu, J., Li, S.Z., Liu, X., Song, B., 2011. Metamorphic patterns and SHRIMP zircon ages of medium-to-high grade rocks from the Tongbai orogen, central China: implications for multiple accretion/collision processes prior to terminal continental collision. Journal of Metamorphic Geology 29 (9), 979–1002.
Long, L., Gao, J., Klemd, R., Beier, C., Qian, Q., Zhang, X., Wang, J., Jiang, T., 2011. Geochemical and geochronological studies of granitoid rocks from the Western Tianshan Orogen: implications for continental growth in the southwestern Central Asian Orogenic Belt. Lithos 126 (3–4), 321–340.
Lorenz, H., Männik, P., Gee, D., Proskurnin, V., 2008. Geology of the Severnaya Zemlya Archipelago and the North Kara Terrane in the Russian high Arctic. International Journal of Earth Sciences 97 (3), 519–547.
Ma, X., Shu, L., Meert, J.G., 2014a. Early Permian slab breakoff in the Chinese Tianshan belt inferred from the post-collisional granitoids. Gondwana Research 25 (2), 797–819.
Ma, X., Shu, L., Meert, J.G., Li, J., 2014b. The Paleozoic evolution of Central Tianshan: geochemical and geochronological evidence. Gondwana Research 25 (2), 797–819.
Mao, Q., Xiao, W., Windley, B.F., Han, C., Qu, J., Ao, S., Zhang, J.E., Guo, Q., 2011. The Liuyuan complex in the Beishan, NW China: a Carboniferous–Permian ophiolitic fore-arc sliver in the southern Altaids. Geological Magazine 149 (3), 483–506.
Martina, F., Viramonte, J.M., Astini, R.A., Pimentel, M.M., Dantas, E., 2011. Mississippian volcanism in the south-central Andes: new U–Pb SHRIMP zircon geochronology and whole-rock geochemistry. Gondwana Research 19 (2), 524–534.
Martínez Catalán, J.R., Arenas, R., García, F.D., Cuadra, P.G., Gómez-Barreiro, J., Abati, J., Castiñeiras, P., Fernández-Suárez, J., Martínez, S.S., Andonaegui, P., 2007. Space and time in the tectonic evolution of the northwestern Iberian Massif: Implications for the Variscan belt. Geological Society of America Memoirs 200, 403–423.
Martínez Dopico, C.I., López de Luchi, M.G., Rapalini, A.E., Kleinhanns, I.C., 2011. Crustal segments in the North Patagonian Massif, Patagonia: an integrated perspective based on Sm–Nd isotope systematics. Journal of South American Earth Sciences 31 (2–3), 324–341.
Martínez, J.C., Dristas, J.A., Massonne, H.-J., 2012. Palaeozoic accretion of the microcontinent Chilenia, North Patagonian Andes: high-pressure metamorphism and subsequent thermal relaxation. International Geology Review 54 (4), 472–490.
Massonne, H.-J., Calderón, M., 2008. PT evolution of metapelites from the Guarguaraz Complex, Argentina: evidence for Devonian crustal thickening close to the western Gondwana margin. Revista geológica de Chile 35 (2), 215–231.
Matte, P., 2001. The Variscan collage and orogeny (480–290 Ma) and the tectonic definition of the Armorica microplate: a review. Terra Nova 13 (2), 122–128.
Mattern, F., Schneider, W., 2000. Suturing of the Proto-and Paleo-Tethys oceans in the western Kunlun (Xinjiang, China). Journal of Asian Earth Sciences 18 (6), 637–650.
Maury, R.C., Béchennec, F., Cotten, J., Caroff, M., Cordey, F., Marcoux, J., 2003. Middle Permian plume-related magmatism of the Hawasina Nappes and the Arabian Platform: implications on the evolution of the Neotethyan margin in Oman. Tectonics 22, 1073.
McCann, T., Pascal, C., Timmerman, M.J., Krzywiec, P., Lopez-Gomez, J., Wetzel, L., Krawczyk, C.M., Rieke, H., Lamarche, J., 2006. Post-Variscan (end Carboniferous-Early Permian) basin evolution in Western and Central Europe. Geological Society London Memoirs 32 (1), 355–388.
McFadden, P., Ma, X., McElhinny, M., Zhang, Z.K., 1988. Permo-Triassic magnetostratigraphy in China: northern Tarim. Earth and Planetary Science Letters 87 (1), 152–160.
Meert, J.G., Van der Voo, R., Powell, C.M.A., Li, Z.X., McElhinny, M.W., Chen, Z., Symons, D.T.A., 1993. A plate-tectonic speed limit? Nature 363, 216–217.
Miao, L., Fan, W., Liu, D., Zhang, F., Shi, Y., Guo, F., 2008. Geochronology and geochemistry of the Hegenshan ophiolitic complex: Implications for late-stage tectonic evolution of the Inner Mongolia-Daxinganling Orogenic Belt, China. Journal of Asian Earth Sciences 32 (5–6), 348–370.
Miao, L., Zhang, F., Fan, W.M., Liu, D., 2007. Phanerozoic evolution of the Inner Mongolia Daxinganling orogenic belt in North China: constraints from geochronology of ophiolites and associated formations. Geological Society, London, Special Publications 280 (1), 223–237.
Michard, A., Soulaimani, A., Hoepffner, C., Ouanaimi, H., Baidder, L., Rjimati, E.C., Saddiqi, O., 2010. The South-Western Branch of the Variscan Belt: evidence from Morocco. Tectonophysics 492 (1–4), 1–24.
Millar, I.L., Pankhurst, R.J., Fanning, C.M., 2002. Basement chronology of the Antarctic Peninsula: recurrent magmatism and anatexis in the Palaeozoic Gondwana Margin. Journal of the Geological Society 159 (2), 145–157.
Miller, E.L., Gehrels, G.E., Pease, V., Sokolov, S., 2010. Stratigraphy and U-Pb detrital zircon geochronology of Wrangel Island, Russia: Implications for Arctic paleogeography. AAPG Bulletin 94 (5), 665–692.
Miller, E.L., Kuznetsov, N., Soboleva, A., Udoratina, O., Grove, M.J., Gehrels, G., 2011. Baltica in the Cordillera? Geology 39 (8), 791–794.
Miskovic, A., Spikings, R.A., Chew, D.M., Kosler, J., Ulianov, A., Schaltegger, U., 2009. Tectonomagmatic evolution of Western Amazonia: geochemical characterization and zircon U-Pb geochronologic constraints from the Peruvian Eastern Cordilleran granitoids. Geological Society of America Bulletin 121 (9–10), 1298–1324.
Moix, P., Beccaletto, L., Kozur, H.W., Hochard, C., Rosselet, F., Stampfli, G.M., 2008. A new classification of the Turkish terranes and sutures and its implication for the paleotectonic history of the region. Tectonophysics 451 (1–4), 7–39.
Moore, T.E., Wallace, W., Bird, K., Karl, S., Mull, C.G., Dillon, J., 1994. Geology of Northern Alaska. The Geology of Alaska: Boulder, Colorado, Geological Society of America, Geology of North America, vol. 1, pp. 49–140.
Mortimer, N., Gans, P., Calvert, A., Walker, N., 1999a. Geology and thermochronometry of the east edge of the Median Batholith (Median Tectonic Zone): a new perspective on Permian to Cretaceous crustal growth of New Zealand. Island Arc 8 (3), 404–425.
Mortimer, N., Tulloch, A., Spark, R., Walker, N., Ladley, E., Allibone, A., Kimbrough, D., 1999b. Overview of the Median Batholith, New Zealand: a new interpretation of the geology of the Median Tectonic Zone and adjacent rocks. Journal of African Earth Sciences 29 (1), 257–268.
Mueller, P.A., Heatherington, A.L., Foster, D.A., Thomas, W.A., Wooden, J.L., 2014. The Suwannee suture: significance for Gondwana-Laurentia terrane transfer and formation of Pangaea. Gondwana Research (in press).
Murphy, J.B., Gutierrez-Alonso, G., Nance, R.D., Fernandez-Suarez, J., Keppie, J.D., Quesada, C., Dostal, J., Braid, J.A., 2009. Rheic Ocean mafic complexes: overview and synthesis. Geological Society, London, Special Publications 327 (1), 343–369.
Murphy, J.B., Keppie, J.D., 2005. The acadian orogeny in the Northern Appalachians. International Geology Review 47 (7), 663–687.

Muttoni, G., Gaetani, M., Kent, D.V., Sciunnach, D., Angiolini, L., Berra, F., Garzanti, E., Mattei, M., Zanchi, A., 2009a. Opening of the Neo-Tethys Ocean and the Pangea B to Pangea A transformation during the Permian. GeoArabia 14 (4), 17–48.
Muttoni, G., Mattei, M., Balini, M., Zanchi, A., Gaetani, M., Berra, F., 2009b. The drift history of Iran from the Ordovician to the Triassic. Geological Society, London, Special Publications 312 (1), 7–29.
Nakano, N., Osanai, Y., Sajeev, K., Hayasaka, Y., Miyamoto, T., Minh, N.T., Owada, M., Windley, B., 2010. Triassic eclogite from northern Vietnam: inferences and geological significance. Journal of Metamorphic Geology 28 (1), 59–76.
Nance, R.D., Keppie, J.D., Miller, B.V., Murphy, J.B., Dostal, J., 2009. Palaeozoic palaeogeography of Mexico: constraints from detrital zircon age data. Geological Society, London, Special Publications 327 (1), 239–269.
Nance, R.D., Linnemann, U., 2008. The rheic ocean: origin, evolution, and significance. GSA Today 18 (12), 4–12.
Natal'in, B.A., Şengör, A.M.C., 2005. Late Palaeozoic to Triassic evolution of the Turan and Scythian platforms: the pre-history of the Palaeo-Tethyan closure. Tectonophysics 404 (3–4), 175–202.
Nebel, O., Münker, C., Nebel-Jacobsen, Y.J., Kleine, T., Mezger, K., Mortimer, N., 2007. Hf–Nd–Pb isotope evidence from Permian arc rocks for the long-term presence of the Indian–Pacific mantle boundary in the SW Pacific. Earth and Planetary Science Letters 254 (3–4), 377–392.
Nokleberg, W.J., Parfenov, L.M., Monger, J.W., Norton, I.O., Chanďuk, A.I., Stone, D.B., Scotese, C.R., Scholl, D.W., Fujita, K., 2000. Phanerozoic Tectonic Evolution of the Circum-North Pacific. U.S. Geological Survey Professional Paper 1626.
O'Connell, R.J., Gable, C.W., Hager, B.H., 1991. Toroidal-poloidal partioning of lithospheric plate motions. In: Glacial Isostasy, Sea-level and Mantle Rheology. NATO ASI Series, vol. 334, pp. 535–551.
Oh, C.W., 2006. A new concept on tectonic correlation between Korea, China and Japan: histories from the late Proterozoic to Cretaceous. Gondwana Research 9 (1–2), 47–61.
Okay, A.I., Satir, M., Siebel, W., 2006. Pre-Alpide Palaeozoic and Mesozoic orogenic events in the Eastern Mediterranean region. Geological Society London Memoirs 32 (1), 389–405.
Okay, N., Zack, T., Okay, A.I., Barth, M., 2011. Sinistral transport along the Trans-European Suture Zone: detrital zircon–rutile geochronology and sandstone petrography from the Carboniferous flysch of the Pontides. Geological Magazine 148 (03), 380–403.
Pankhurst, R., Weaver, S., Bradshaw, J., Storey, B., Ireland, T., 1998. Geochronology and geochemistry of pre-Jurassic superterranes in Marie Byrd Land, Antarctica. Journal of Geophysical Research: Solid Earth (1978–2012) 103 (B2), 2529–2547.
Pankhurst, R.J., Rapela, C.W., Fanning, C.M., Márquez, M., 2006. Gondwanide continental collision and the origin of Patagonia. Earth-Science Reviews 76 (3–4), 235–257.
Pe-Piper, G., Kamo, S.L., McCall, C., 2010. The German Bank pluton, offshore SW Nova Scotia: age, petrology, and regional significance for Alleghanian plutonism. Geological Society of America Bulletin 122 (5–6), 690–700.
Pease, V., 2011. Chapter 20 Eurasian orogens and Arctic tectonics: an overview. Geological Society London Memoirs 35 (1), 311–324.
Pease, V., Scott, R.A., 2009. Crustal affinities in the Arctic Uralides, northern Russia: significance of detrital zircon ages from Neoproterozoic and Palaeozoic sediments in Novaya Zemlya and Taimyr. Journal of the Geological Society 166 (3), 517–527.
Pereira, M.F., Chichorro, M., Johnston, S.T., Gutiérrez-Alonso, G., Silva, J.B., Linnemann, U., Hofmann, M., Drost, K., 2012. The missing Rheic Ocean magmatic arcs: provenance analysis of Late Paleozoic sedimentary clastic rocks of SW Iberia. Gondwana Research 22 (3–4), 882–891.
Peters, T.J., Ayers, J.C., Gao, S., Liu, X.-M., 2013. The origin and response of zircon in eclogite to metamorphism during the multi-stage evolution of the Huwan Shear Zone, China: Insights from Lu–Hf and U–Pb isotopic and trace element geochemistry. Gondwana Research 23 (2), 726–747.
Pharaoh, T.C., Winchester, J.A., Verniers, J., Lassen, A., Seghedi, A., 2006. The Western accretionary margin of the East European Craton: an overview. Geological Society London Memoirs 32 (1), 291–311.
Pillevuit, A., Marcoux, J., Stampfli, G., Baud, A., 1997. The Oman Exotics: a key to the understanding of the Neotethyan geodynamic evolution. Geodinamica Acta 10 (5), 209–238.
Puchkov, V.N., 2009a. The diachronous (step-wise) arc–continent collision in the Urals. Tectonophysics 479 (1–2), 175–184.
Puchkov, V.N., 2009b. The evolution of the Uralian orogen. Geological Society, London, Special Publications 327 (1), 161–195.
Ramos, V., Jordan, T., Allmendinger, R.W., Mpodozis, C., Kay, S.M., Cortés, J., Palma, M., 1986. Paleozoic terranes of the central Argentine-Chilean Andes. Tectonics 5 (6), 855–880.
Ramos, V.A., 2008. Patagonia: a paleozoic continent adrift? Journal of South American Earth Sciences 26 (3), 235–251.
Ran, B., Wang, C., Zhao, X., Li, Y., He, M., Zhu, L., Coe, R.S., 2012. New paleomagnetic results of the early Permian in the Xainza area, Tibetan Plateau and their paleogeographical implications. Gondwana Research 22 (2), 447–460.
Rapalini, A.E., 2005. The accretionary history of southern South America from the latest Proterozoic to the Late Palaeozoic: some palaeomagnetic constraints. Geological Society, London, Special Publications 246 (1), 305–328.
Rapalini, A.E., de Luchi, M.L., Tohver, E., Cawood, P.A., 2013. The South American ancestry of the North Patagonian Massif: geochronological evidence for an autochthonous origin? Terra Nova 25 (4), 337–342.
Rapalini, A.E., López de Luchi, M.G., Martínez Dopico, C., Lince Klinger, F.G., Giménez, M.E., Martínez, P., 2010. Did Patagonia collide with Gondwana in the Late Paleozoic? Some insights from a multidisciplinary study of magmatic units of the North Patagonian Massif. Geologica Acta 8 (4), 349–371.
Ratschbacher, L., Hacker, B.R., Calvert, A., Webb, L.E., Grimmer, J.C., McWilliams, M.O., Ireland, T., Dong, S., Hu, J., 2003. Tectonics of the Qinling (Central China): tectonostratigraphy, geochronology, and deformation history. Tectonophysics 366 (1–2), 1–53.
Ren, R., Han, B.-F., Ji, J.-Q., Zhang, L., Xu, Z., Su, L., 2011. U–Pb age of detrital zircons from the Tekes River, Xinjiang, China, and implications for tectonomagmatic evolution of the South Tian Shan Orogen. Gondwana Research 19 (2), 460–470.
Ricard, Y., Doglioni, C., Sabadini, R., 1991. Differential rotation between lithosphere and mantle: a consequence of lateral mantle viscosity variations. Journal of Geophysical Research: Solid Earth 96, 8407–8415.
Ridd, M.F., Barber, A.J., Crow, M.J., 2011. The Geology of Thailand. Geological Society.
Riley, T.R., Flowerdew, M.J., Whitehouse, M.J., 2012. U-Pb ion-microprobe zircon geochronology from the basement inliers of eastern Graham Land, Antarctic Peninsula. Journal of the Geological Society 169 (4), 381–393.
Rippington, S., Cunningham, D., England, R., 2008. Structure and petrology of the Altan Uul Ophiolite: new evidence for a Late Carboniferous suture in the Gobi Altai, southern Mongolia. Journal of the Geological Society 165 (3), 711–723.
Rippington, S., Cunningham, D., England, R., Hendriks, B., 2013. The crustal assembly of southern Mongolia: new structural, lithological and geochronological data from the Nemegt and Altan ranges. Gondwana Research 23 (4), 1535–1553.
Safonova, I.Y., Simonov, V.A., Kurganskaya, E.V., Obut, O.T., Romer, R.L., Seltmann, R., 2012. Late Paleozoic oceanic basalts hosted by the Char suture-shear zone, East Kazakhstan: geological position, geochemistry, petrogenesis and tectonic setting. Journal of Asian Earth Sciences 49, 20–39.
Saintot, A., Stephenson, R.A., Stovba, S., Brunet, M.F., Yegorova, T., Starostenko, V., 2006. The evolution of the southern margin of Eastern Europe (Eastern European and Scythian platforms) from the Latest Precambrian- Early Palaeozoic to the Early Cretaceous. Geological Society London Memoirs 32 (1), 481–505.
Schulmann, K., Konopásek, J., Janoušek, V., Lexa, O., Lardeaux, J.-M., Edel, J.-B., Štípská, P., Ulrich, S., 2009. An Andean type Palaeozoic convergence in the Bohemian Massif. Comptes Rendus Geoscience 341 (2–3), 266–286.
Schwab, M., Ratschbacher, L., Siebel, W., McWilliams, M., Minaev, V., Lutkov, V., Chen, F., Stanek, K., Nelson, B., Frisch, W., Wooden, J.L., 2004. Assembly of the Pamirs: age and origin of magmatic belts from the southern Tien Shan to the southern Pamirs and their relation to Tibet. Tectonics 23, TC4002.
Scott, J., Muhling, J., Fletcher, I., Billia, M., Palin, J.M., Elliot, T., Günter, C., 2011. The relationship of Palaeozoic metamorphism and S-type magmatism on the paleo-Pacific Gondwana margin. Lithos 127 (3–4), 522–534.
Seltmann, R., Konopelko, D., Biske, G., Divaev, F., Sergeev, S., 2011. Hercynian post-collisional magmatism in the context of Paleozoic magmatic evolution of the Tien Shan orogenic belt. Journal of Asian Earth Sciences 42 (5), 821–838.
Seton, M., Müller, R., Zahirovic, S., Gaina, C., Torsvik, T., Shephard, G., Talsma, A., Gurnis, M., Turner, M., Maus, S., 2012. Global continental and ocean basin reconstructions since 200 Ma. Earth-Science Reviews 113 (3), 212–270.
Shail, R.K., Leveridge, B.E., 2009. The Rhenohercynian passive margin of SW England: development, inversion and extensional reactivation. Comptes Rendus Geoscience 341 (2–3), 140–155.
Sharps, R., McWilliams, M., Li, Y., Cox, A., Zhang, Z., Zhai, Y., Gao, Z., Li, Y., Li, Q., 1989. Lower Permian paleomagnetism of the Tarim block, northwestern China. Earth and Planetary Science Letters 92 (3), 275–291.
Shellnutt, J.G., Bhat, G.M., Brookfield, M.E., Jahn, B.M., 2011. No link between the Panjal Traps (Kashmir) and the Late Permian mass extinctions. Geophysical Research Letters 38, L19308.
Shen, J.-W., Webb, G.E., Jell, J.S., 2008. Platform margins, reef facies, and microbial carbonates; a comparison of Devonian reef complexes in the Canning Basin, Western Australia, and the Guilin region, South China. Earth-Science Reviews 88 (1–2), 33–59.
Siddoway, C.S., Fanning, C.M., 2009. Paleozoic tectonism on the East Gondwana margin: evidence from SHRIMP U–Pb zircon geochronology of a migmatite–-granite complex in West Antarctica. Tectonophysics 477 (3–4), 262–277.
Sone, M., Metcalfe, I., 2008. Parallel Tethyan sutures in mainland Southeast Asia: new insights for Palaeo-Tethys closure and implications for the Indosinian orogeny. Comptes Rendus Geoscience 340 (2–3), 166–179.
Song, D., Xiao, W., Han, C., Li, J., Qu, J., Guo, Q., Lin, L., Wang, Z., 2013a. Progressive accretionary tectonics of the Beishan orogenic collage, southern Altaids: Insights from zircon U–Pb and Hf isotopic data of high-grade complexes. Precambrian Research 227, 368–388.
Song, D., Xiao, W., Han, C., Tian, Z., 2013b. Geochronological and geochemical study of gneiss–schist complexes and associated granitoids, Beishan Orogen, southern Altaids. International Geology Review 55 (14), 1705–1727.
Song, S., Niu, Y., Su, L., Xia, X., 2013c. Tectonics of the North Qilian orogen, NW China. Gondwana Research 23 (4), 1378–1401.
Spandler, C., Worden, K., Arculus, R., Eggins, S., 2005. Igneous rocks of the Brook Street Terrane, New Zealand: implications for Permian tectonics of eastern Gondwana and magma genesis in modern intra-oceanic volcanic arcs. New Zealand Journal of Geology and Geophysics 48 (1), 167–183.
Stampfli, G., Borel, G., 2002. A plate tectonic model for the Paleozoic and Mesozoic constrained by dynamic plate boundaries and restored synthetic oceanic isochrons. Earth and Planetary Science Letters 196 (1), 17–33.

Stampfli, G., Marcoux, J., Baud, A., 1991. Tethyan margins in space and time. Palaeogeography, Palaeoclimatology, Palaeoecology 87 (1), 373–409.
Stampfli, G.M., 2000. Tethyan oceans. Geological Society, London, Special Publications 173 (1), 1–23.
Stampfli, G.M., Hochard, C., Vérard, C., Wilhem, C., vonRaumer, J., 2013. The formation of Pangea. Tectonophysics 593, 1–19.
Stampfli, G.M., von Raumer, J.F., Borel, G.D., 2002. Paleozoic evolution of pre-Variscan terranes: from Gondwana to the Variscan collision. Special Papers – Geological Society of America, 263–280.
Stephenson, R.A., Yegorova, T., Brunet, M.F., Stovba, S., Wilson, M., Starostenko, V., Saintot, A., Kusznir, N., 2006. Late Palaeozoic intra- and pericratonic basins on the East European Craton and its margins. Geological Society London Memoirs 32 (1), 463–479.
Tait, J., 1999. New Early Devonian paleomagnetic data from NW France: paleogeography and implications for the Armorican microplate hypothesis. Journal of Geophysical Research 104 (B2), 2831–2839.
Tait, J., Bachtadse, V., Dinarès-Turell, J., 2000. Paleomagnetism of Siluro-Devonian sequences, NE Spain. Journal of Geophysical Research 105 (B10), 23595–23603.
Tait, J., Bachtadse, V., Soffel, H., 1996. Eastern Variscan fold belt: paleomagnetic evidence for oroclinal bending. Geology 24 (10), 871–874.
Taylor, J.P., Webb, L.E., Johnson, C.L., Heumann, M.J., 2013. The lost South Gobi microcontinent: protolith studies of metamorphic tectonites and implications for the evolution of continental crust in southeastern Mongolia. Geosciences 3 (3), 543–584.
Thomas, W.A., 2004. Genetic relationship of rift-stage crustal structure, terrane accretion, and foreland tectonics along the southern Appalachian-Ouachita orogen. Journal of Geodynamics 37 (3–5), 549–563.
Tian, Z., Xiao, W., Shan, Y., Windley, B., Han, C., Zhang, J.e., Song, D., 2013. Mega-fold interference patterns in the Beishan orogen (NW China) created by change in plate configuration during Permo-Triassic termination of the Altaids. Journal of Structural Geology 52, 119–135.
Tomurtogoo, O., Windley, B.F., Kroner, A., Badarch, G., Liu, D.Y., 2005. Zircon age and occurrence of the Adaatsag ophiolite and Muron shear zone, central Mongolia: constraints on the evolution of the Mongol-Okhotsk ocean, suture and orogen. Journal of the Geological Society 162 (1), 125–134.
Torsvik, T., Smethurst, M., Burke, K., Steinberger, B., 2008a. Long term stability in deep mantle structure: evidence from the ~300 Ma Skagerrak-Centered Large Igneous Province (the SCLIP). Earth and Planetary Science Letters 267 (3–4), 444–452.
Torsvik, T.H., Andersen, T.B., 2002. The Taimyr fold belt, Arctic Siberia: timing of prefold remagnetisation and regional tectonics. Tectonophysics 352 (3), 335–348.
Torsvik, T.H., Burke, K., Steinberger, B., Webb, S.J., Ashwal, L.D., 2010a. Diamonds sampled by plumes from the core-mantle boundary. Nature 466 (7304), 352–355.
Torsvik, T.H., Cocks, L.R.M., 2004. Earth geography from 400 to 250 Ma: a palaeomagnetic, faunal and facies review. Journal of the Geological Society 161 (4), 555–572.
Torsvik, T.H., Cocks, L.R.M., 2009. The Lower Palaeozoic palaeogeographical evolution of the northeastern and eastern peri-Gondwanan margin from Turkey to New Zealand. Geological Society, London, Special Publications 325 (1), 3–21.
Torsvik, T.H., Cocks, L.R.M., 2011. The Palaeozoic palaeogeography of central Gondwana. Geological Society, London, Special Publications 357 (1), 137–166.
Torsvik, T.H., Cocks, L.R.M., 2013. Gondwana from top to base in space and time. Gondwana Research 24 (3–4), 999–1030.
Torsvik, T.H., Rehnström, E.F., 2003. The Tornquist Sea and Baltica–Avalonia docking. Tectonophysics 362 (1–4), 67–82.
Torsvik, T.H., Steinberger, B., Cocks, L.R.M., Burke, K., 2008b. Longitude: linking Earth's ancient surface to its deep interior. Earth and Planetary Science Letters 276 (3–4), 273–282.
Torsvik, T.H., Steinberger, B., Gurnis, M., Gaina, C., 2010b. Plate tectonics and net lithosphere rotation over the past 150My. Earth and Planetary Science Letters 291 (1), 106–112.
Torsvik, T.H., Van der Voo, R., Doubrovine, P.V., Burke, K., Steinberger, B., Ashwal, L.D., Trønnes, R.G., Webb, S.J., Bull, A.L., 2014. Deep mantle structure as a reference frame for movements in and on the Earth. Proceedings of the National Academy of Sciences (in revision).
Torsvik, T.H., Van der Voo, R., Preeden, U., Mac Niocaill, C., Steinberger, B., Doubrovine, P.V., van Hinsbergen, D.J.J., Domeier, M., Gaina, C., Tohver, E., Meert, J.G., McCausland, P.J.A., Cocks, L.R.M., 2012. Phanerozoic polar wander, palaeogeography and dynamics. Earth-Science Reviews 114 (3–4), 325–368.
Tulloch, A.J., Ramezani, J., Kimbrough, D.L., Faure, K., Allibone, A.H., 2009. U-Pb geochronology of mid-Paleozoic plutonism in western New Zealand: Implications for S-type granite generation and growth of the east Gondwana margin. Geological Society of America Bulletin 121 (9–10), 1236–1261.
van Staal, C.R., Whalen, J.B., Valverde-Vaquero, P., Zagorevski, A., Rogers, N., 2009. Pre-Carboniferous, episodic accretion-related, orogenesis along the Laurentian margin of the northern Appalachians. Geological Society, London, Special Publications 327 (1), 271–316.
Van Vuong, N., Hansen, B.T., Wemmer, K., Lepvrier, C., Van Tich, V., Thang, T.T., 2012. U/Pb and Sm/Nd dating on ophiolitic rocks of the Song Ma suture zone (northern Vietnam): evidence for upper paleozoic paleotethyan lithospheric remnants. Journal of Geodynamics 69, 140–147.
von Gosen, W., 2003. Thrust tectonics in the North patagonian massif (Argentina): Implications for a patagonia plate. Tectonics 22 (1) (n/a-n/a).
von Raumer, J.F., Bussy, F., Schaltegger, U., Schulz, B., Stampfli, G.M., 2013. Pre-mesozoic Alpine basements–Their place in the european paleozoic framework. Geological Society of America Bulletin 125 (1–2), 89–108.
von Raumer, J.F., Stampfli, G.M., 2008. The birth of the Rheic Ocean—Early Palaeozoic subsidence patterns and subsequent tectonic plate scenarios. Tectonophysics 461 (1), 9–20.
Vyssotski, A.V., Vyssotski, V.N., Nezhdanov, A.A., 2006. Evolution of the West Siberian Basin. Marine and Petroleum Geology 23 (1), 93–126.
Wainwright, A.J., Tosdal, R.M., Forster, C.N., Kirwin, D.J., Lewis, P.D., Wooden, J.L., 2011. Devonian and Carboniferous arcs of the Oyu Tolgoi porphyry Cu-Au district, South Gobi region, Mongolia. Geological Society of America Bulletin 123 (1–2), 306–328.
Wakita, K., 2013. Geology and tectonics of Japanese islands: a review – the key to understanding the geology of Asia. Journal of Asian Earth Sciences 72, 75–87.
Wang, B., Shu, L., Faure, M., Jahn, B.-m., Cluzel, D., Charvet, J., Chung, S.-l., Meffre, S., 2011. Paleozoic tectonics of the southern Chinese Tianshan: insights from structural, chronological and geochemical studies of the Heiyingshan ophiolitic mélange (NW China). Tectonophysics 497 (1–4), 85–104.
Wang, C.Y., Zhang, Q., Qian, Q., Zhou, M.F., 2005. Geochemistry of the Early Paleozoic Baiyin volcanic rocks (NW China): implications for the tectonic evolution of the North Qilian orogenic belt. The Journal of Geology 113 (1), 83–94.
Wang, D., Zheng, J., Ma, Q., Griffin, W.L., Zhao, H., Wong, J., 2013a. Early Paleozoic crustal anatexis in the intraplate Wuyi–Yunkai orogen, South China. Lithos 175–176, 124–145.
Wang, T., Jahn, B.-M., Kovach, V.P., Tong, Y., Hong, D.-W., Han, B.-F., 2009. Nd–Sr isotopic mapping of the Chinese Altai and implications for continental growth in the Central Asian Orogenic Belt. Lithos 110 (1–4), 359–372.
Wang, X., Wang, T., Zhang, C., 2013b. Neoproterozoic, Paleozoic, and Mesozoic granitoid magmatism in the Qinling Orogen, China: constraints on orogenic process. Journal of Asian Earth Sciences 72, 129–151.
Wang, Y., Fan, W., Zhang, G., Zhang, Y., 2013c. Phanerozoic tectonics of the South China Block: key observations and controversies. Gondwana Research 23 (4), 1273–1305.
Weber, B., Scherer, E.E., Martens, U.K., Mezger, K., 2012. Where did the lower Paleozoic rocks of Yucatan come from? A U–Pb, Lu–Hf, and Sm–Nd isotope study. Chemical Geology 312–313, 1–17.
Wegener, A., 1912. Die entstehung der kontinente. Geologische Rundschau 3 (4), 276–292.
Wendt, J., Kaufmann, B., Belka, Z., Farsan, N., Karimi Bavandpur, A., 2005. Devonian/Lower Carboniferous stratigraphy, facies patterns and palaeogeography of Iran. Part II. Northern and central Iran. Acta Geologica Polonica 55 (1), 31–97.
Wilhem, C., Windley, B.F., Stampfli, G.M., 2012. The Altaids of Central Asia: a tectonic and evolutionary innovative review. Earth-Science Reviews 113 (3–4), 303–341.
Willman, C., VandenBerg, A., Morand, V., 2002. Evolution of the southeastern Lachlan fold belt in Victoria. Australian Journal of Earth Sciences 49 (2), 271–289.
Willner, A.P., 2005. Time markers for the evolution and exhumation history of a Late Palaeozoic paired metamorphic Belt in North-Central Chile (34 -35 30'S). Journal of Petrology 46 (9), 1835–1858.
Willner, A.P., Gerdes, A., Massonne, H.-J., Schmidt, A., Sudo, M., Thomson, S.N., Vujovich, G., 2011. The geodynamics of collision of a microplate (Chilenia) in Devonian times deduced by the pressure–temperature–time evolution within part of a collisional belt (Guarguaraz Complex, W-Argentina). Contributions to Mineralogy and Petrology 162 (2), 303–327.
Wilson, M., Neumann, E.R., Davies, G.R., Timmerman, M.J., Heeremans, M., Larsen, B.T., 2004. Permo-Carboniferous magmatism and rifting in Europe: introduction. Geological Society, London, Special Publications 223 (1), 1–10.
Windley, B.F., Alexeiev, D., Xiao, W., Kroner, A., Badarch, G., 2007. Tectonic models for accretion of the Central Asian Orogenic Belt. Journal of the Geological Society 164 (1), 31–47.
Woodcock, N.H., Soper, N.J., Strachan, R.A., 2007. A Rheic cause for the Acadian deformation in Europe. Journal of the Geological Society 164 (5), 1023–1036.
Wu, Y.-B., Zheng, Y.-F., 2013. Tectonic evolution of a composite collision orogen: an overview on the Qinling–Tongbai–Hong'an–Dabie–Sulu orogenic belt in central China. Gondwana Research 23 (4), 1402–1428.
Xiao, W., Windley, B., Liu, D.Y., Jian, P., Liu, C., Yuan, C., Sun, M., 2005. Accretionary tectonics of the Western Kunlun Orogen, China: a Paleozoic–Early Mesozoic, long-lived active continental margin with implications for the growth of Southern Eurasia. The Journal of Geology 113 (6), 687–705.
Xiao, W., Windley, B.F., Allen, M.B., Han, C., 2013. Paleozoic multiple accretionary and collisional tectonics of the Chinese Tianshan orogenic collage. Gondwana Research 23 (4), 1316–1341.
Xiao, W., Windley, B.F., Badarch, G., Sun, S., Li, J., Qin, K., Wang, Z., 2004. Palaeozoic accretionary and convergent tectonics of the southern Altaids: implications for the growth of Central Asia. Journal of the Geological Society 161 (3), 339–342.
Xiao, W., Windley, B.F., Hao, J., Zhai, M., 2003. Accretion leading to collision and the Permian Solonker suture, Inner Mongolia, China: termination of the central Asian orogenic belt. Tectonics 22, 1069.
Xiao, W., Windley, B.F., Yong, Y., Yan, Z., Yuan, C., Liu, C., Li, J., 2009a. Early Paleozoic to Devonian multiple-accretionary model for the Qilian Shan, NW China. Journal of Asian Earth Sciences 35 (3–4), 323–333.
Xiao, W.J., Mao, Q.G., Windley, B.F., Han, C.M., Qu, J.F., Zhang, J.E., Ao, S.J., Guo, Q.Q., Cleven, N.R., Lin, S.F., Shan, Y.H., Li, J.L., 2010. Paleozoic multiple accretionary and collisional processes of the Beishan orogenic collage. American Journal of Science 310 (10), 1553–1594.

Xiao, W.J., Windley, B.F., Chen, H.L., Zhang, G.C., Li, J.L., 2002. Carboniferous-Triassic subduction and accretion in the western Kunlun, China: implications for the collisional and accretionary tectonics of the northern Tibetan Plateau. Geology 30 (4), 295–298.

Xiao, W.J., Windley, B.F., Huang, B.C., Han, C.M., Yuan, C., Chen, H.L., Sun, M., Sun, S., Li, J.L., 2009b. End-Permian to mid-Triassic termination of the accretionary processes of the southern Altaids: implications for the geodynamic evolution, Phanerozoic continental growth, and metallogeny of Central Asia. International Journal of Earth Sciences 98 (6), 1189–1217.

Xu, X., Harbert, W., Dril, S., Kravchinksy, V., 1997. New paleomagnetic data from the Mongol–Okhotsk collision zone, Chita region, south-central Russia: implications for Paleozoic paleogeography of the Mongol–Okhotsk ocean. Tectonophysics 269 (1–2), 113–129.

Xu, Z., Han, B.-F., Ren, R., Zhou, Y.-Z., Su, L., 2013. Palaeozoic multiphase magmatism at Barleik Mountain, southern West Junggar, Northwest China: implications for tectonic evolution of the West Junggar. International Geology Review 55 (5), 633–656.

Xun, Z., Allen, M.B., Whitham, A.G., Price, S.P., 1996. Rift-related Devonian sedimentation and basin development in South China. Journal of Southeast Asian Earth Sciences 14 (1), 37–52.

Yan, Z., Wang, Z., Yan, Q., Wang, T., Guo, X., 2012. Geochemical constraints on the provenance and depositional setting of the Devonian Liuling Group, East Qinling Mountains, Central China: implications for the tectonic evolution of the Qinling Orogenic Belt. Journal of Sedimentary Research 82 (1), 9–20.

Yang, G., Li, Y., Gu, P., Yang, B., Tong, L., Zhang, H., 2012. Geochronological and geochemical study of the Darbut Ophiolitic Complex in the West Junggar (NW China): implications for petrogenesis and tectonic evolution. Gondwana Research 21 (4), 1037–1049.

Yarmolyuk, V.V., Kovalenko, V.I., Sal'nikova, E.B., Kovach, V.P., Kozlovsky, A.M., Kotov, A.B., Lebedev, V.I., 2008. Geochronology of igneous rocks and formation of the Late Paleozoic south Mongolian active margin of the Siberian continent. Stratigraphy and Geological Correlation 16 (2), 162–181.

Ye, H.-M., Li, X.-H., Li, Z.-X., Zhang, C.-L., 2008. Age and origin of high Ba–Sr appinite–granites at the northwestern margin of the Tibet Plateau: implications for early Paleozoic tectonic evolution of the Western Kunlun orogenic belt. Gondwana Research 13 (1), 126–138.

Žák, J., Kratinová, Z., Trubač, J., Janoušek, V., Sláma, J., Mrlina, J., 2011. Structure, emplacement, and tectonic setting of Late Devonian granitoid plutons in the Teplá–Barrandian unit, Bohemian Massif. International Journal of Earth Sciences 100 (7), 1477–1495.

Zhang, R.Y., Lo, C.H., Chung, S.L., Grove, M., Omori, S., Iizuka, Y., Liou, J.G., Tri, T.V., 2013a. Origin and tectonic implication of ophiolite and eclogite in the Song Ma suture zone between the South China and Indochina Blocks. Journal of Metamorphic Geology 31 (1), 49–62.

Zhang, S.-H., Zhao, Y., Kröner, A., Liu, X.-M., Xie, L.-W., Chen, F.-K., 2009a. Early Permian plutons from the northern North China Block: constraints on continental arc evolution and convergent margin magmatism related to the Central Asian Orogenic Belt. International Journal of Earth Sciences 98 (6), 1441–1467.

Zhang, S.-H., Zhao, Y., Song, B., Hu, J.-M., Liu, S.-W., Yang, Y.-H., Chen, F.-K., Liu, X.-M., Liu, J., 2009b. Contrasting Late Carboniferous and Late Permian–Middle Triassic intrusive suites from the northern margin of the North China craton: geochronology, petrogenesis, and tectonic implications. Geological Society of America Bulletin 121 (1–2), 181–200.

Zhang, S.-H., Zhao, Y., Song, B., Yang, Y.-H., 2007a. Zircon SHRIMP U–Pb and in-situ Lu–Hf isotope analyses of a tuff from Western Beijing: evidence for missing Late Paleozoic arc volcano eruptions at the northern margin of the North China block. Gondwana Research 12 (1–2), 157–165.

Zhang, S.H., Zhao, Y., Song, B., Yang, Z.Y., Hu, J.M., Wu, H., 2007b. Carboniferous granitic plutons from the northern margin of the North China block: implications for a late Palaeozoic active continental margin. Journal of the Geological Society 164 (2), 451–463.

Zhang, W., Pease, V., Wu, T., Zheng, R., Feng, J., He, Y., Luo, H., Xu, C., 2012a. Discovery of an adakite-like pluton near Dongqiyishan (Beishan, NW China) — its age and tectonic significance. Lithos 142–143, 148–160.

Zhang, X., Wilde, S.A., Zhang, H., Zhai, M., 2011a. Early Permian high-K calc-alkaline volcanic rocks from NW Inner Mongolia, North China: geochemistry, origin and tectonic implications. Journal of the Geological Society 168 (2), 525–543.

Zhang, Y.-c., Shen, S.-z., Shi, G.R., Wang, Y., Yuan, D.-x., Zhang, Y.-j., 2012b. Tectonic evolution of the Qiangtang Block, northern Tibet during the Late Cisuralian (Late Early Permian): evidence from fusuline fossil records. Palaeogeography, Palaeoclimatology, Palaeoecology 350–352, 139–148.

Zhang, Y.-c., Shi, G.R., Shen, S.-z., 2013b. A review of Permian stratigraphy, palaeobiogeography and palaeogeography of the Qinghai–Tibet Plateau. Gondwana Research 24 (1), 55–76.

Zhang, Y., Dostal, J., Zhao, Z., Liu, C., Guo, Z., 2011b. Geochronology, geochemistry and petrogenesis of mafic and ultramafic rocks from Southern Beishan area, NW China: Implications for crust–mantle interaction. Gondwana Research 20 (4), 816–830.

Zhao, P., Chen, Y., Xu, B., Faure, M., Shi, G., Choulet, F., 2013. Did the Paleo-Asian Ocean between North China Block and Mongolia Block exist during the late Paleozoic? First paleomagnetic evidence from central-eastern Inner Mongolia, China. Journal of Geophysical Research: Solid Earth 118, 1873–1894.

Zhao, X., Coe, R., Gilder, S., Frost, G., 1996. Palaeomagnetic constraints on the palaeogeography of China: Implications for Gondwanaland*. Australian Journal of Earth Sciences 43 (6), 643–672.

Zheng, R., Wu, T., Zhang, W., Xu, C., Meng, Q., 2013a. Late Paleozoic subduction system in the southern Central Asian Orogenic Belt: evidences from geochronology and geochemistry of the Xiaohuangshan ophiolite in the Beishan orogenic belt. Journal of Asian Earth Sciences 62, 463–475.

Zheng, R., Wu, T., Zhang, W., Xu, C., Meng, Q., Zhang, Z., 2013b. Late Paleozoic subduction system in the northern margin of the Alxa block, Altaids: geochronological and geochemical evidences from ophiolites. Gondwana Research 25, 842–858.

Zhu, D.C., Mo, X.X., Zhao, Z.D., Niu, Y., Wang, L.Q., Chu, Q.H., Pan, G.T., Xu, J.F., Zhou, C.Y., 2010. Presence of Permian extension- and arc-type magmatism in southern Tibet: paleogeographic implications. Geological Society of America Bulletin 122 (7–8), 979–993.

Zwing, A., Bachtadse, V., 2000. Paleoposition of the northern margin of Armorica in Late Devonian times: paleomagnetic and rock magnetic results from the Frankenstein Intrusive Complex (Mid-German Crystalline Rise). Journal of Geophysical Research: Solid Earth (1978–2012) 105 (B9), 21445–21456.

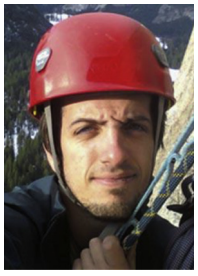

**Mathew Domeier** is a postdoctoral researcher at the Centre for Earth Evolution and Dynamics (CEED) at the University of Oslo, with research interests in tectonics, paleogeography and paleomagnetism.

**Trond Torsvik** is a geophysicist and director of the Centre for Earth Evolution and Dynamics (CEED) at the University of Oslo, and with particular interests in paleomagnetism, plate reconstructions and mantle dynamics.